SHIELDING OF AN AC EXTRA HIGH VOLTAGE (EHV) TRANSMISSION SYSTEMS AGAINST LIGHTNING STROKES

A Thesis

Presented to

The Faculty of Graduate Studies

University of Manitoba

In Partial Fulfillment

of the Requirements for the Degree

Master of Science

Electrical Engineering Department

Aly Osman

September 1980

SHIELDING OF AN AC EXTRA HIGH VOLTAGE (EHV) TRANSMISSION SYSTEMS AGAINST LIGHTNING STROKES

BY

ALY OSMAN

A thesis submitted to the Faculty of Graduate Studies of
the University of Manitoba in partial fulfillment of the requirements
of the degree of

MASTER OF SCIENCE

ABSTRACT

Most outages of Extra High Voltage Power transmission systems are caused by lightning surges. To minimize such disturbances and thus enhance the system's reliability, it is necessary to analyze the causes of shielding failure of the transmission system.

It is impractical to provide a sufficiently high insulation level to withstand these surges. Furthermore, the methods of shielding used in the past are ineffective in improving the performance of modern systems.

In view of these inherent difficulties, a promising solution has been eliminating the exposure arcs of the phase conductors by shielding wires, which are generally required on E.H.V. lines. This thesis presents an effective shielding scheme for the centre and outer phase conductors. The optimum height of the shielding wires, the concept of negative shielding angles and the effects of grounding, all of which are necessary for effectively shielded transmission lines, are investigated, and the results are presented in useful curves.

ACKNOWLEDGEMENTS

This work would be incomplete without the expression of my deepest gratitude to my supervisor, Professor M.Z. Tarnawecky. His guidance and counsel throughout have been invaluable. A very special word of thanks to manuscript editor, Mrs. Pat Ohlendorf, for her guidance and assistance. Appreciation is also expressed to Mrs. Paula Weber for her expert typing of the manuscript. Finally, I am very grateful to Khadiga Osman, my wife, for her encouragement and support.

TABLE OF CONTENTS

LIST OF ILLUSTRATIONS

CHAPTER I

INTRODUCTION

1.1 BRIEF HISTORICAL REVIEW

Since Benjamin Franklin's experiments for the first practical protection device against lightning, the lightning rod, time and effort have been devoted to modelling the actual lightning performance, establishing its basic parameters, and applying them to the protection of tall structures and power transmission systems. In 1941 Wagner and McCann[1] conducted model investigations of the effects of shielding, and recommended shielding angles of thirty to forty degrees, based on this work.

1.2 SHIELDING BY GROUND WIRE - AIEE METHOD

In 1950, the Lightning and Insulator Subcommittee of the AIEE Transmission and Distribution Committee presented a report entitled "A Method of Estimating Lightning Performance of Transmission Lines".[2] This paper summarized the work of many authors and presented a comprehensive review of the factors affecting the line performance. The effects of shielding angle, height, and spacing presented in this paper are based on the model studies by Wagner and Clayton[3] with the results shown in Figure 1. In the 1950's and 1960's, power consumption increased very rapidly, leading to the development of ever-higher transmission voltages and thus taller structure and greater average heights of transmission lines. As large numbers of 345 KV. lines were

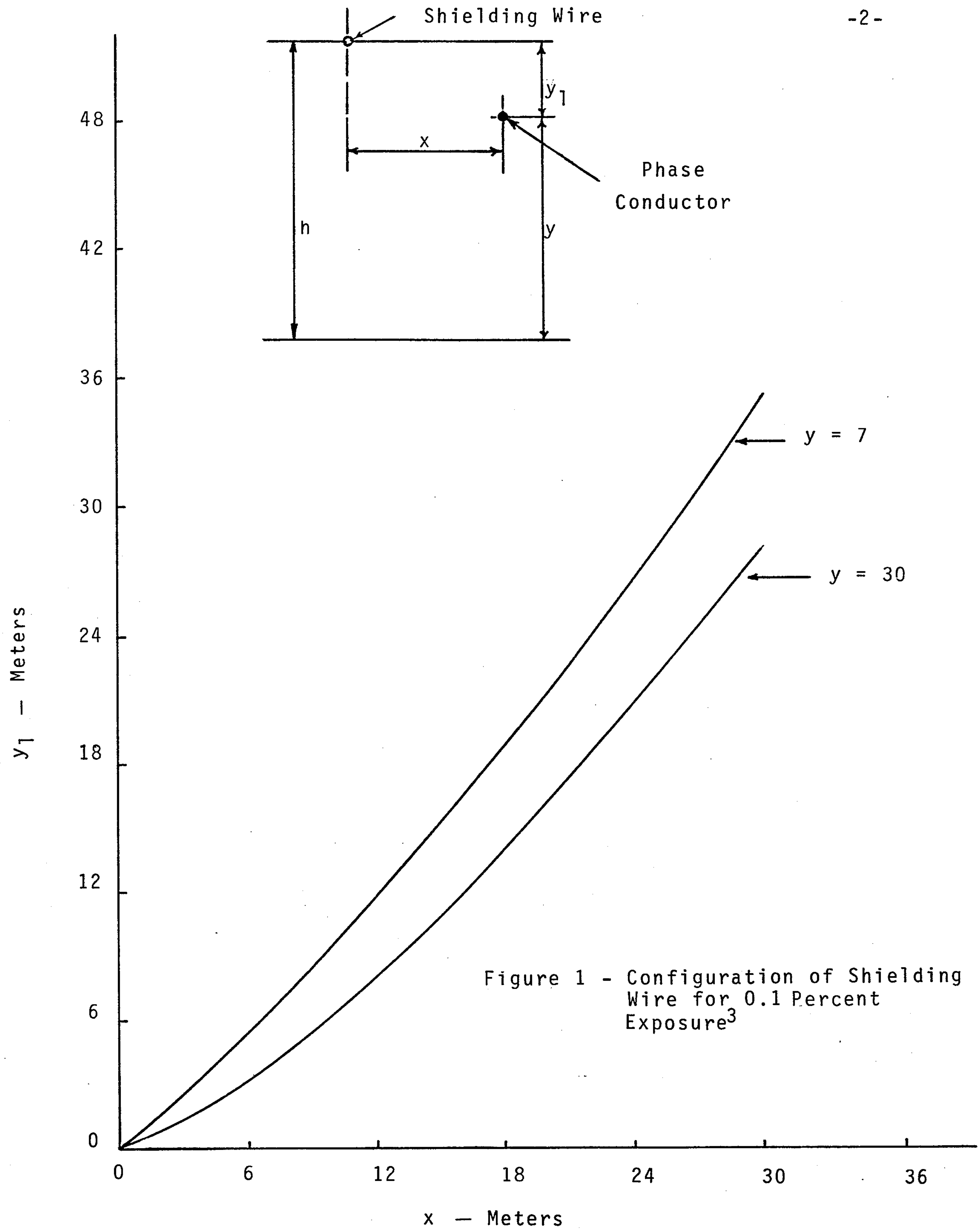

Figure 1 - Configuration of Shielding Wire for 0.1 Percent Exposure[3]

built, it became increasingly apparent that the AIEE method was inadequate. For example, the 345 KV. Lines of Ohaio Valley Electric Corporation experienced over seven outages per one hundred miles per year. The use of the AIEE method resulted in only 0.5 outages per one hundred miles per year.

After rigorous investigations in the field of lightning mechanisms, Young and Clayton[4] concluded that the last step of the leader, during which the return stroke begins, is of great importance. It was assumed that conditions are such that there is little or no tendency for the stroke to hit any given point until the last step, when the nearest ground will be struck. The length of this last step, denoted by r_s, and called the "strike distance", thus forms the basis for geometrical analysis of the lightning performance. In this study it is also assumed that all strokes are vertical, and with a given number of strokes per unit area and unit time, the number of strokes per unit length and unit time hitting the line is

$$n = \int_{r_s \min.}^{r_s \max.} N_0 \quad x \; f_{r_s}(r_s) \quad dr_s \qquad (1)$$

where:

n = number of strokes per unit length and unit time,

N_0 = number of strokes per unit area and unit time,

x = swath, as a function of r_s and h,

r_s min. = minimum strike distance,

$r_{s\ max.}$ = maximum strike distance, and

$f_{r_s}(r_s)$ = frequency function of r_s.

Figure 2 shows the parameters of Equation 1. Equation 1 can be applied for the case of a shielded line, except that the swath is as shown in Figure 3, and thus the application of shielding wire reduces the phase conductor swath. The solution of Equation 1 requires the determination of $f_{r_s}(r_s)$, the strike distance distribution function. However, Wagner[7,8] arrived at the following relation

$$f_{r_s}(r_s)\,dr_s = f_I(I)\,dI, \qquad (2)$$

which relates the strike distance distribution function to the known frequency function of the occurrence of the stroke current I. Thus, Equation 1 can be written as

$$n = \int_{I \text{ at } r_{s\ max.}}^{I \text{ at } r_{s\ max.}} N_0 \times f_I(I)\,dI \qquad (3)$$

This study will focus on the following shielding criteria:

1) shielding requirements for the centre phase conductor of a flat configuration transmission line,

2) shielding requirements for the outer phase conductors, with emphasis on the approach angle of the lightning strokes,

3) the achievement of effective shielding through the elimination of the phase conductor exposure arcs, utilizing the negative

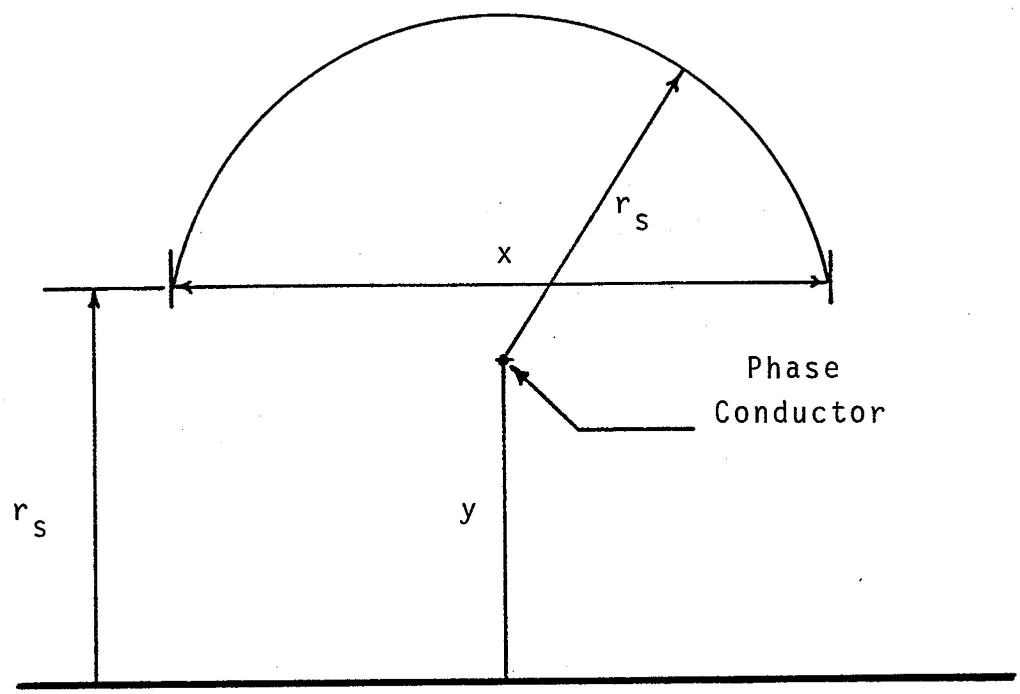

Figure 2 - Configuration of the Exposure of a Conductor Above Ground[4]

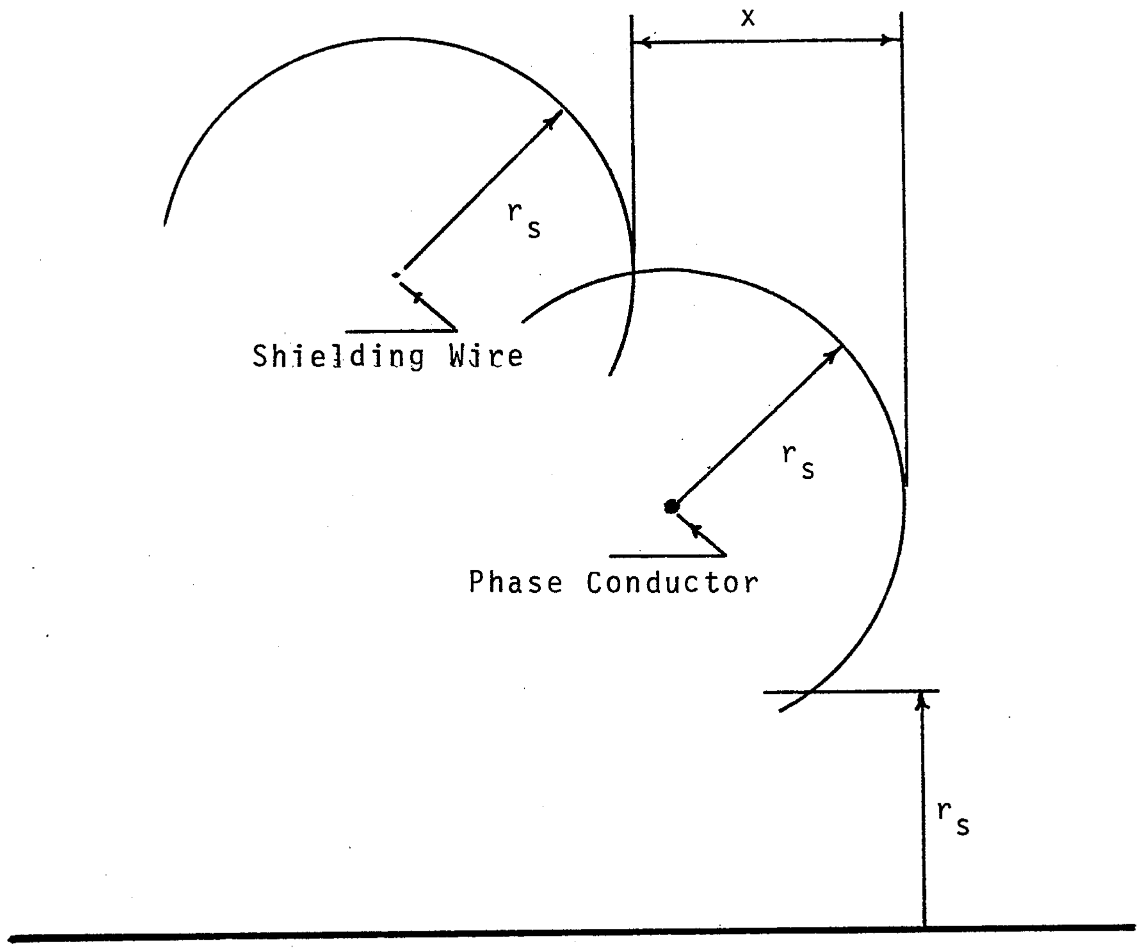

Figure 3 - Illustration of the Shielding Effect of a Shielding Wire[4]

shielding angle concept and

4) a brief investigation of lightning mechanisms.

1.3 THE LIGHTNING STROKE MECHANISM[5,6,9,10]

The lightning stroke consists of two stages: The leader process, during which charge is distributed around a narrow (millimeters) channel, and the return stroke process, where the charge laid out by the leader is collected by a larger (centimeters), highly-ionized channel that conducts the charge to ground. Prior to the development of the leader, charge must collect in some localized region in a cloud, and fields must build up to levels sufficient to initiate breakdown. The phenomenon of charge separation and buildup of charges in localized regions in the cloud has been studied by many investigators. Among the processes thought to play a part in the charge separation are charge formation, collision and breakup of raindrops, freezing, melting and refreezing of water within the cloud, and contact between water (rain) and ice (snow) in regions where the temperature is near freezing (0 C^{o}).[3] It is generally agreed that updrafts and wind patterns within the cloud account for the large-scale collection of charge in local regions within the cloud. A general picture of charge distribution in the cloud is shown in Figure 4.

In the study of transmission system protection, the most important considerations lie within the leader and return streamer.[7] B.F.J. Schonland,[8,9,10] clearly showed the two-stage process of the stroke. The leader is characterized as in

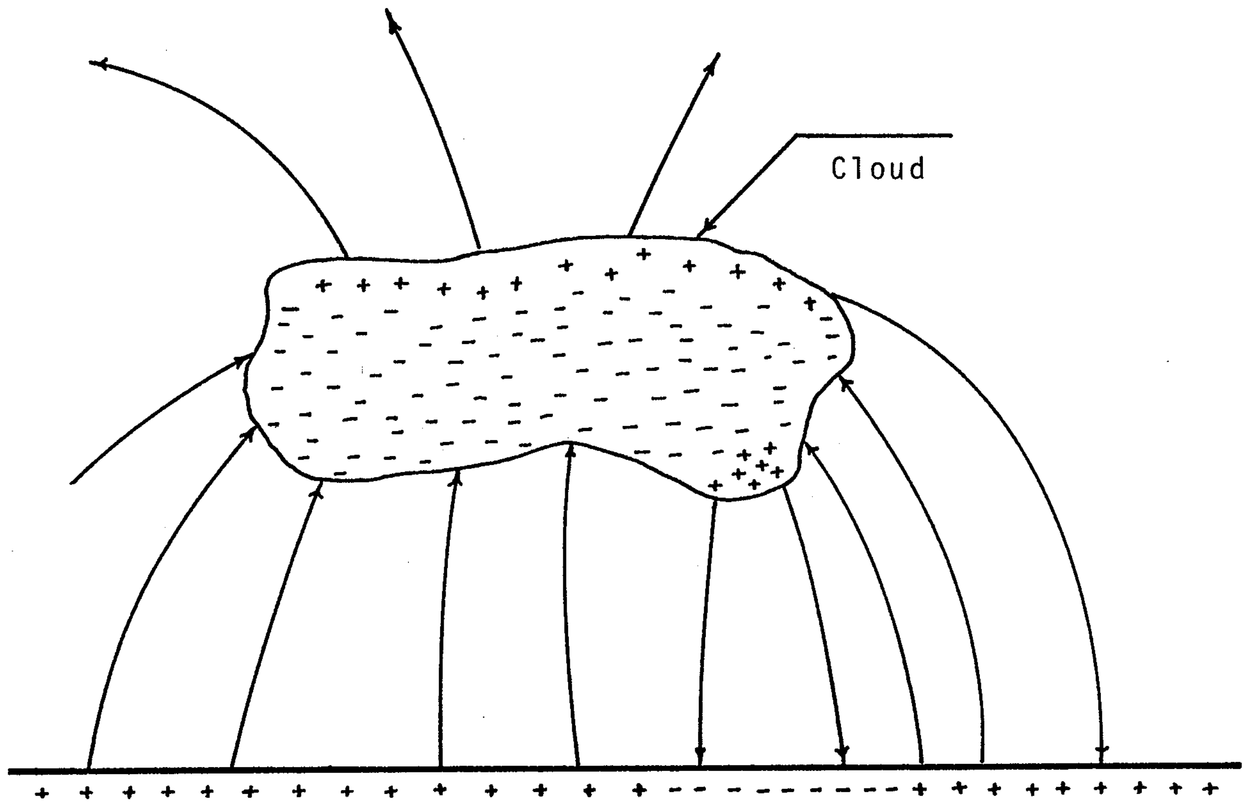

Figure 4 - Illustration of Cloud and Ground Charge Distribution[9].

Figure 5, by a progressive lengthening of a narrow conductor towards ground. Within each step, the channel lengthens at a velocity of the order of 0.2C, where C is the velocity of light[6]. However, at the end of each step there is a pause of the order of a hundred microseconds, so that the average velocity of progression may be as little as 0.0001 C.[6] The leader is preceded by a pilot streamer. After the pilot streamer has travelled about fifty meters, a conducting channel, the leader, develops rapidly within the extended pilot, and the process continues.

It should be noted that 90 to 95 percent of the strokes are negative[3]. The occasional positive strokes that exist are believed to be very high-current strokes, with strike distances so large that they do not constitute a serious transmission line shielding problem. At a certain point above ground, the field intensity becomes sufficiently great that the return streamer starts from earth.

The distance from the tip of the leader to earth at this point is the strike distance to ground, and is assumed to be the distance which would be struck by a point to plane voltage equal to that of the leader channel.[4] A model for the leader at this point, just prior to initiation of the return streamer, will now be presented.

1.4 THE LEADER MODEL

The leader, as it progresses, is a very small- (millimeters) radius channel, dropping in steps of about fifty to one hundred and fifty meters per step.[12] If it is assumed that the bulk of

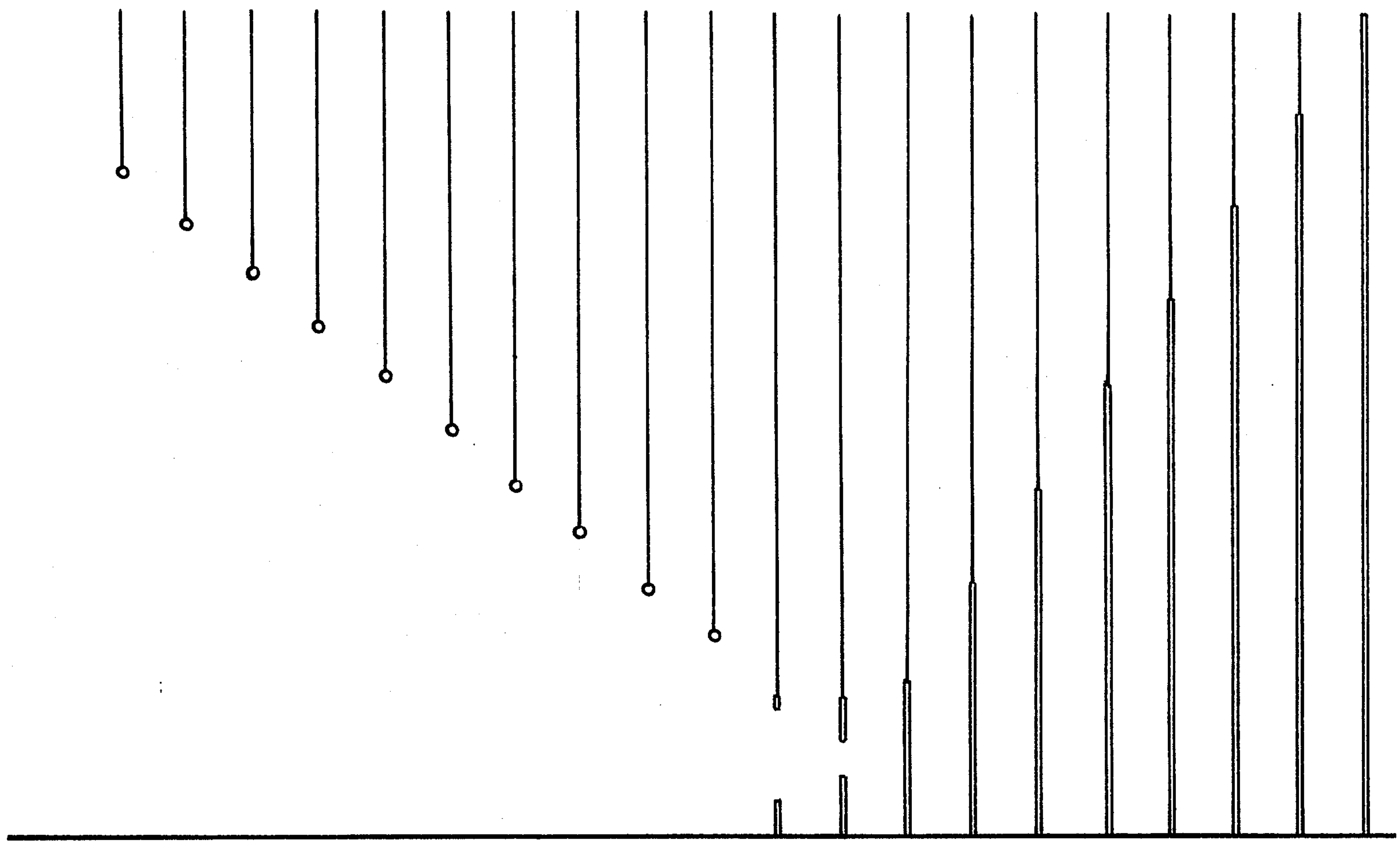

Figure 5 - The Two Basic Stages of the Lightning Stroke.[5]

the charge Q, in a cloud charge centre is passed along the leader, the process can be described as shown in Figure 6. It is clear that as the leader lengthens, the charge per unit length, q, decreases, and since the capacitance to ground increases, the leader voltage drops as it progresses.

The system can be assumed to be a cylindrical capacitor with a uniform charge distribution. This approximation can be justified as follows:

"The potential just outside the surface of a long, narrow vertical rod above the ground will be the same as for a filament of the same length except very near the ends."[13] Thus, referring to Figure 7, the voltage at the conductor surface (radius b) may be calculated as follows: The potential at point P due to the element charge qdx is

$$dv = \frac{qdx}{4\pi\varepsilon_o} \left(\frac{1}{R_1} - \frac{1}{R_2}\right)$$

$$= \frac{qdx}{4\pi\varepsilon_o} \left[\frac{1}{\sqrt{(y-x)^2 + b^2}} - \frac{1}{\sqrt{(y+x)^2 + b^2}}\right] \quad (4)$$

Thus $$V_{(r_o)} = \frac{q}{4\pi\varepsilon_o} \int_s^h \left[\frac{dx}{\sqrt{(y-x)^2 + b^2}} - \frac{dx}{\sqrt{(y+x)^2 + b^2}}\right]$$

$$V_{(r_o)} = \frac{q}{4\pi\varepsilon_o} \ln\left[\left(\frac{y-s+\sqrt{(y-s)^2 + b^2}}{y-h+\sqrt{(y-h)^2 + b^2}} \cdot \frac{y+s+\sqrt{(y+s)^2 + b^2}}{y+h+\sqrt{(y+h)^2 + b^2}}\right)\right] \quad (5)$$

This result is verified in Reference 13.

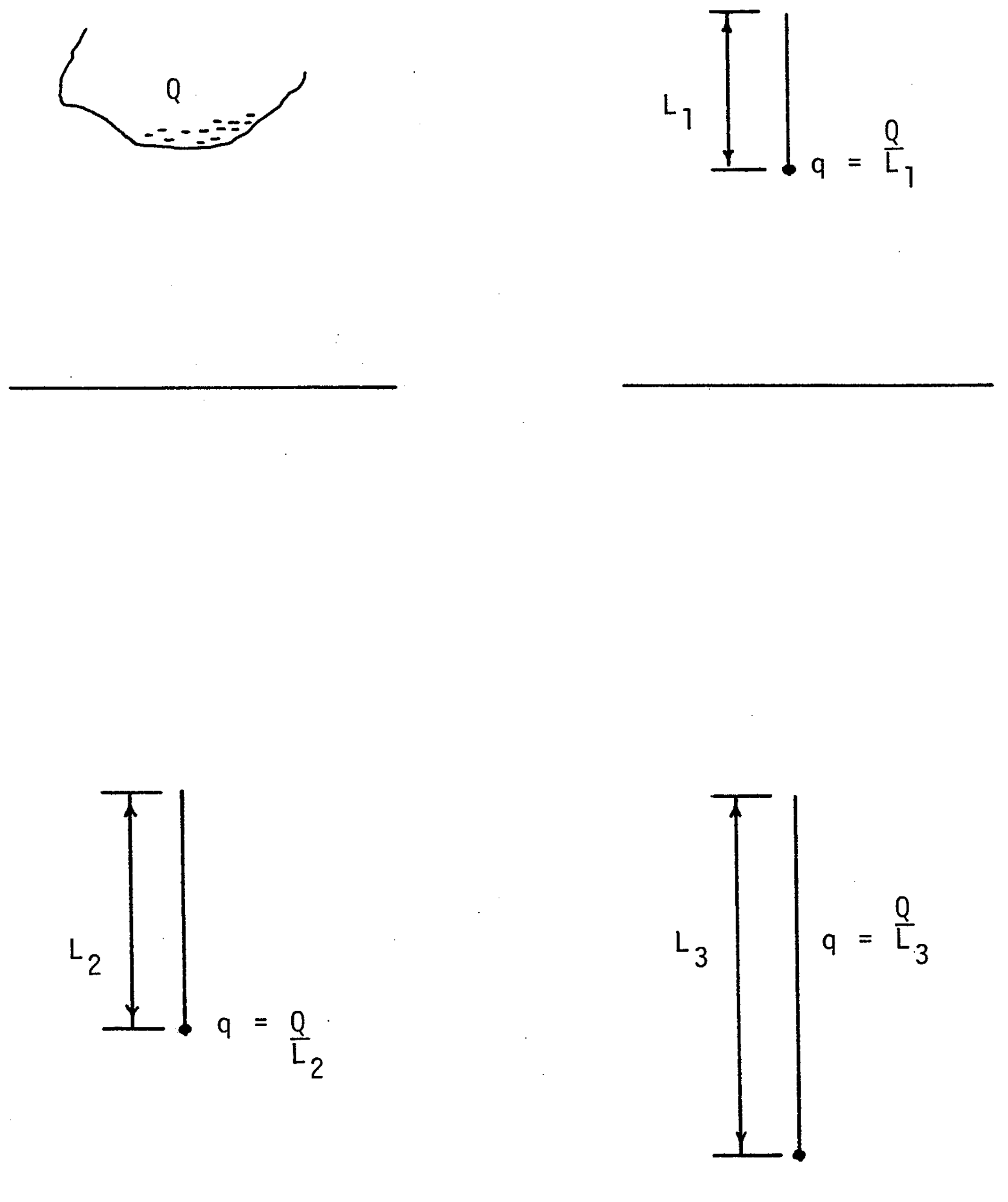

Figure 6 - Progression of the Leader Channel[12]

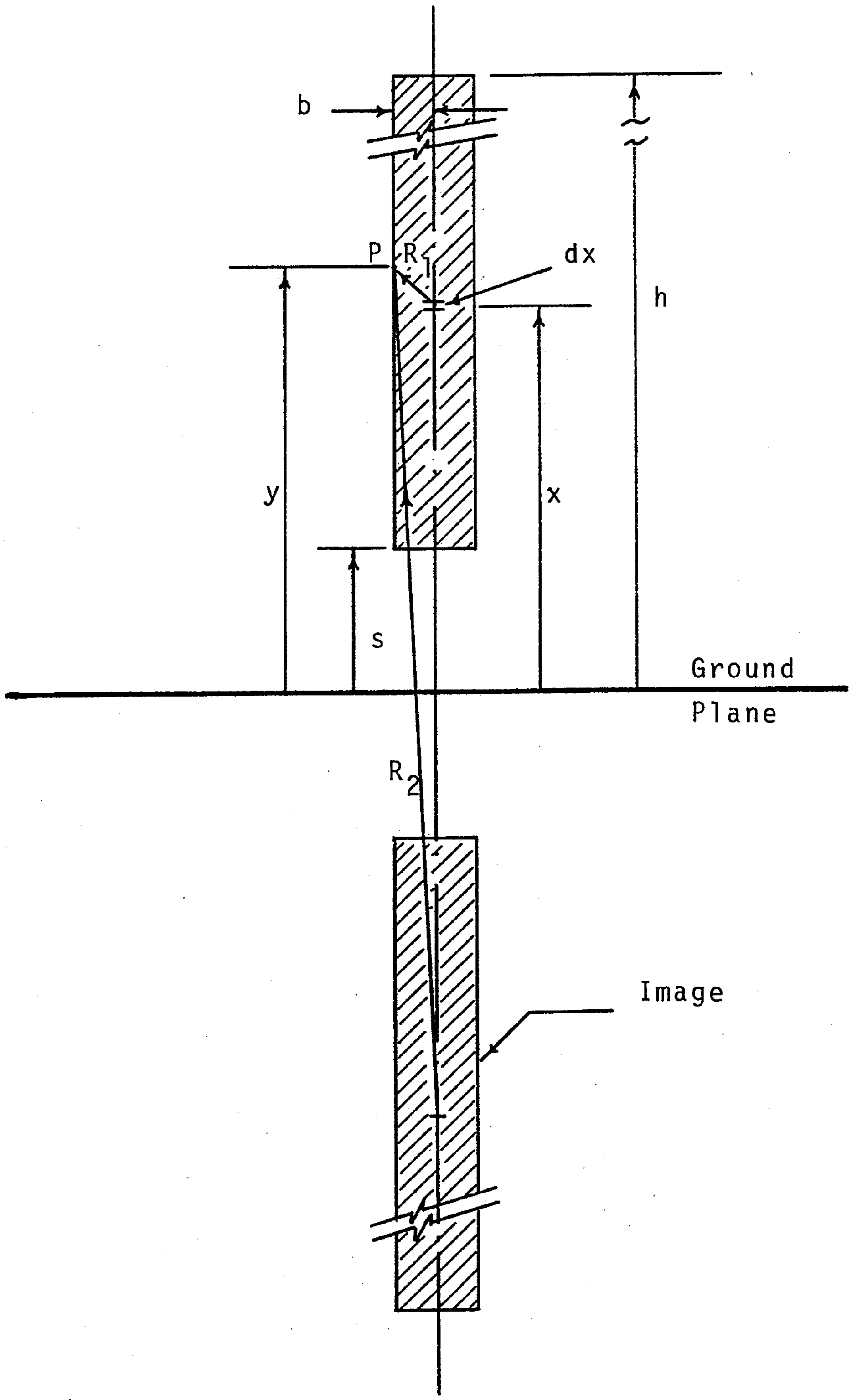

Figure 7 - A Vertical Rod with Uniform Charge Distribution.[13]

Equation 5 is

$$V(r_o) = \frac{q}{4\pi\varepsilon o} \ln\left[\frac{(y-s)+\sqrt{((y-s)^2+b^2)}}{(y-h)+\sqrt{((y-h)^2+b^2)}} \cdot \frac{(y+s)+\sqrt{((y+s)^2+b^2)}}{(y+h)+\sqrt{((y+h)^2+b^2)}}\right] \quad (5)$$

using the following values for the leader channel:

$h = 2{,}000$ meters

$s = 50$ meters

$b = 1$ meter

This yields

$y-s > 1$

$h-y > 1$

Thus

$$V(r_o) = \frac{q}{4\pi\varepsilon_o} \ln\left[\frac{(y-s)\left[1+\sqrt{1+\frac{b^2}{(y-s)^2}}\right](y+s)\left[1+\sqrt{1+\frac{b^2}{(y+s)^2}}\right]}{\left[(y-h)+(h-y)\sqrt{1+\frac{b^2}{(h-y)^2}}\right](y+h)\left[1+\sqrt{1+\frac{b^2}{(y+h)^2}}\right]}\right]$$

$$V(r_o) = \frac{q}{4\pi\varepsilon o} \ln\left[\frac{2(y-s)(y+s)}{(y+h)\left[(y-h)+(h-y)\sqrt{1+\frac{b^2}{(h-y)^2}}\right]}\right] \quad (6)$$

Again for $\frac{b}{h-y} < 1$, and by using binomial expansion for

$$(h-y)\sqrt{1+\frac{b^2}{(h-y)^2}}$$

this gives $(h-y)\sqrt{1+\frac{b^2}{(h-y)^2}} = h-y+\frac{1}{2}\left[b^2/h-y\right]$

Therefore $(y-h)+(h-y)\sqrt{1+\frac{b^2}{(h-y)^2}} \cong \frac{b^2}{2(h-y)}$ (7)

Substituting Equation 7 in Equation 6,

$$V_{(b)} = \frac{q}{4 \pi \varepsilon_o} \ln \left[\frac{4 (y-s) (y+s) (h-y)}{b^2 (y+h)} \right] \quad (8)$$

and for the channel leader values indicated

h = 2,000 s = 50 and b = 1 meters

Thus

$$V_{(b)} = \frac{q}{4 \pi \varepsilon_o} \ln \left[\frac{4 (y-50) (y+50) (2{,}000-y)}{(y+2{,}000)} \right] \quad (9)$$

where

$$50 < y < 2{,}000$$

subject to the limitations

$$y - 50 > 1$$

$$2{,}000 - y > 1$$

A plot of Equation 9 for $60 < y < 1990$ is shown in Figure 8. Except near the ends, the voltage is approximately constant. Therefore, a constant linear charge distribution for the leader channel is justified.

Assuming this to be the case, the capacitance per unit length is

$$C_s = \frac{q}{V(b)} = \frac{4 \pi \varepsilon_o}{\ln \left[\frac{4 (y-s) (y+s) (h-y)}{b^2 (y+h)} \right]} \quad (10)$$

$$C_s = \frac{2 \pi \varepsilon_o}{\frac{1}{2} \ln \left[\frac{4(y-s) (y+s) (h-y)}{b^2 (y+h)} \right]}$$

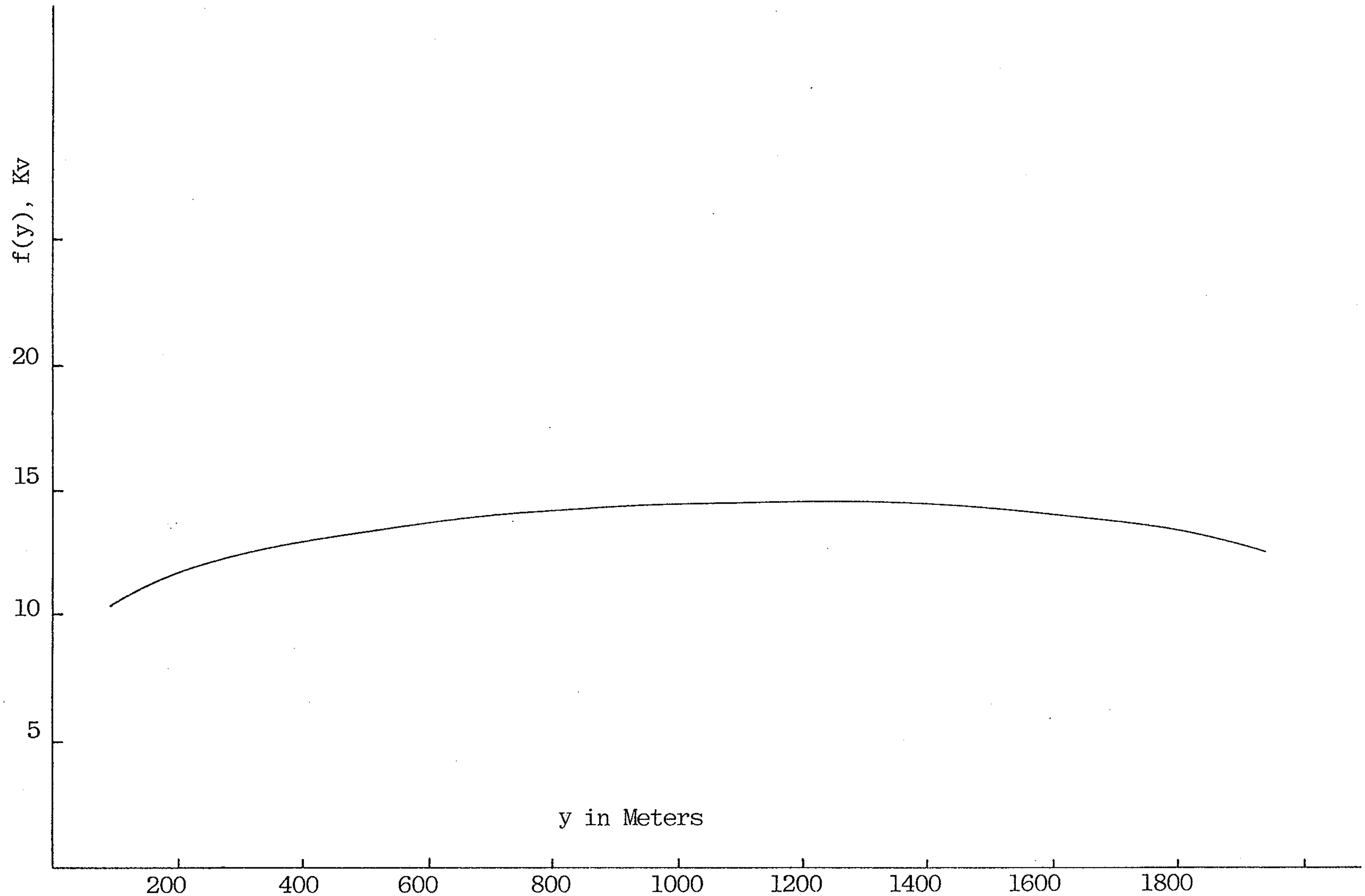

Figure 8 - A Quantity Proportional to Voltage at Surface of Rod as a Function of Vertical Distance.

$$C_s = \frac{2\pi\varepsilon_o}{\ln\left[\frac{2}{b}\sqrt{\frac{(y-s)(y+s)(h-y)}{(y+h)}}\right]} \quad (11)$$

For $y = \frac{h+s}{2}$ and considering $h > s$ thus Equation 11 gives

$$C_s = \frac{2\pi\varepsilon_o}{\ln\left[\frac{h/\sqrt{3}}{b}\right]} \quad (12)$$

From Equation 12 the leader channel can be represented by a cylindrical "cable" of outer radius R, and inner radius b, where

$$R = h/\sqrt{3} \quad (13)$$

Now, for the case of a vertical rod of radius b, height above ground r_s, Length L, and uniform charge distribution, Figure 9, for such situation, the voltage and thus capacitance per unit length, C_s, is almost constant if $L > r_s > b$. This is actually the case for the leader channel.

That is,

$$C_s = \frac{2\pi\varepsilon_o}{\ln L/\sqrt{3}\,b} \quad (14)$$

For a cylindrical system in air, Figure 10, the capacitance per unit length is

$$C = \frac{2\pi\varepsilon_o}{\ln(R/b)} \quad (15)$$

where R and b are the outer and inner radii, respectively. The voltage will be constant, for a uniform charge distribution.

If a cylindrical model for the leader is considered as shown in Figure 10, then

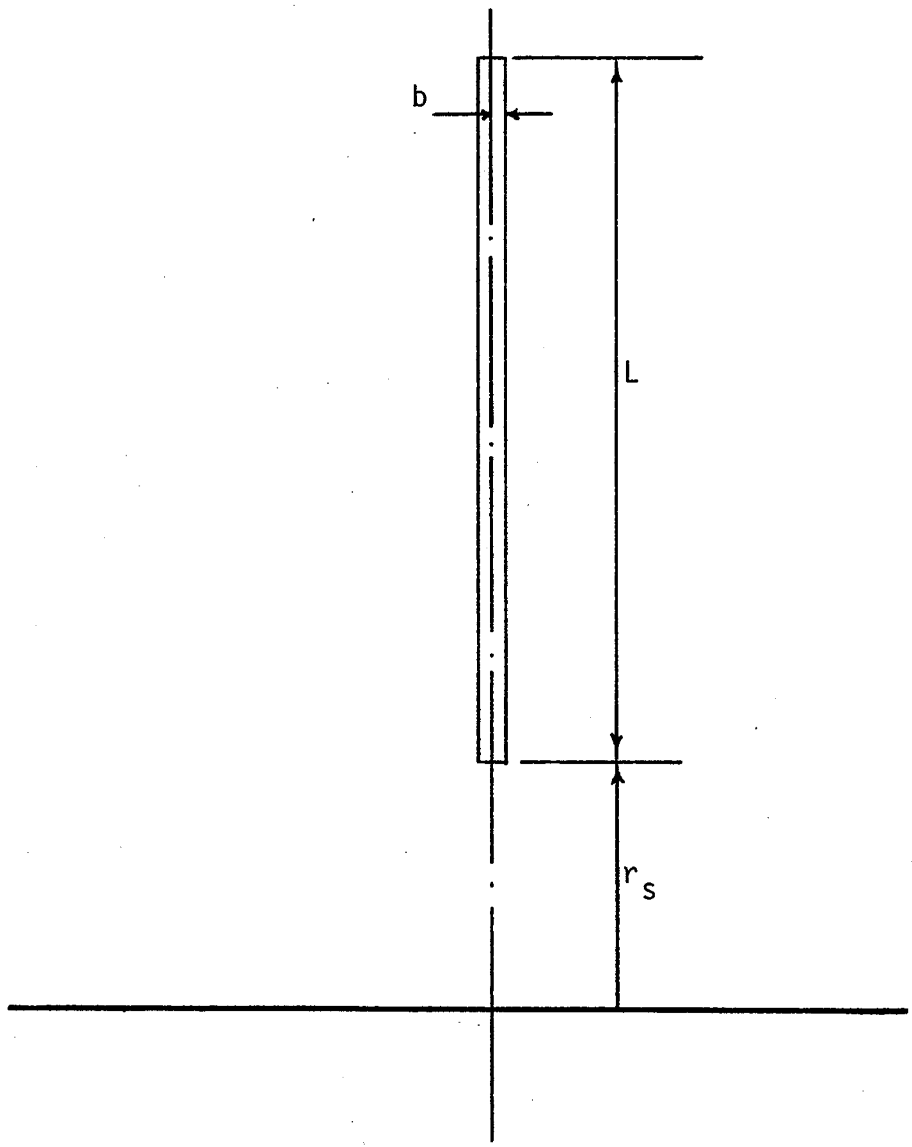

Figure 9 -A Long, Narrow Rod Above Ground.[13]

$$C_s = \frac{2 \pi \varepsilon_0}{\ln(\frac{R}{b})} \qquad (16)$$

where $$R = \frac{L}{\sqrt{3}} \qquad (17)$$

Once L is determined, R and thus b can be determined as follows: Let Eo be the breakdown gradient for air. Then, referring to Figure 10, for a cylindrical system

$$V(r) = V_s \quad \ln(R/r) / \ln(R/b) \qquad (18)$$

and

$$E_{(r)} = \frac{-\partial V}{\partial r} = \frac{+V_s}{r \ln(R/b)} \quad , \text{V/m} \qquad (19)$$

setting $E_{(r)}$ = Eo at r = b,

Hence

$$E_0 = \frac{V_s}{b \ln(R/b)} \quad , \text{V/m} \qquad (20)$$

Therefore $$\frac{V_s}{E_0} = b \ln(R/b) \qquad (21)$$

Assuming E_0 to be the short gap breakdown strength of air

$$E_0 = 30 \text{ KV/Cm}$$
$$= 3 \times 10^6 \text{ v/met.}$$

then $$b \ln(\frac{R}{b}) = \frac{V_s}{3 \times 10^6} \qquad (22)$$

Knowing the values of V_s and E_0 and using Equations 17 and 21, the values of R and b can be determined.

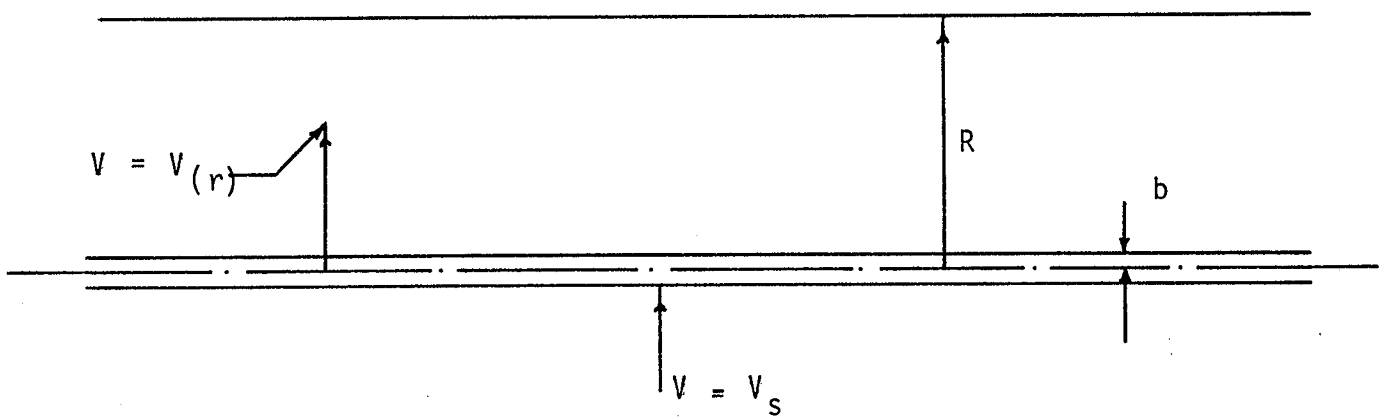

Figure 10 - Cylindrical Model Assumed for Leader.

A major consideration is the variation of $\ln\left(\frac{R}{b}\right)$. Since it is logarithmic, the variation will be relatively small. In addition, it is expected that L, and thus R, rises with the voltage. In fact, the leader voltage is assumed proportional to R. Then

$$V_s = KR. \tag{23}$$

From Equations 21 and 22, this gives

$$b \ln\left(\frac{R}{b}\right) = \frac{V_s}{3 \times 10^6} = \frac{KR}{3 \times 10^6}$$

That is,

$$\ln\left(\frac{R}{b}\right) = \frac{KR}{b \times 3 \times 10^6} = \frac{K\,(R/b)}{3 \times 10^6}$$

$$\ln\left(\frac{R}{b}\right) = \frac{K}{3 \times 10^6}\left(\frac{R}{b}\right) \tag{24}$$

From Equation 24 it can be seen that $\ln\left(\frac{R}{b}\right)$ is relatively constant for all strokes. Thus the cylindrical model for the leader is complete.

The height of the channel is of interest, since it is necessary in the determination of R. Schonland has studied strokes of mean height of 2,000 meters.[12] This figure is consistent with Hagenguth's[11] study, which indicates that most cloud heights fall within the range of 2,000 to 7,000 feet (600 - 2,100 meters).

1.5 THE RETURN STROKE

The return stroke begins when an ionized channel rises from the ground to meet the developed leader.[5,7] As indicated in

Figure 5, after the streamer is well developed, and rising, it appears as a wave of current of approximately constant velocity, of the order of ten to forty percent of the speed of light.[10] The current wave travels up the narrow, highly-ionized leader channel, rapidly expanding and further ionizing it, until, in a few microseconds, the current reaches a maximum. As an approximation, the current at a particular point along the channel is assumed to be as shown in Figure 11. This figure is based on the fact that if there is no time lag for the release of the charge, and if the velocity of the return streamer is constant, the current wave would have a rectangular wave. However, to approximate the effect of time lag, the current wave can be assumed to rise to a crest in 2 to 4 microseconds.

Although this introductory chapter is not of direct application to transmission line shielding, it has been presented to clarify the lightning stroke phenomena. The following chapter will focus on the shielding of transmission systems.

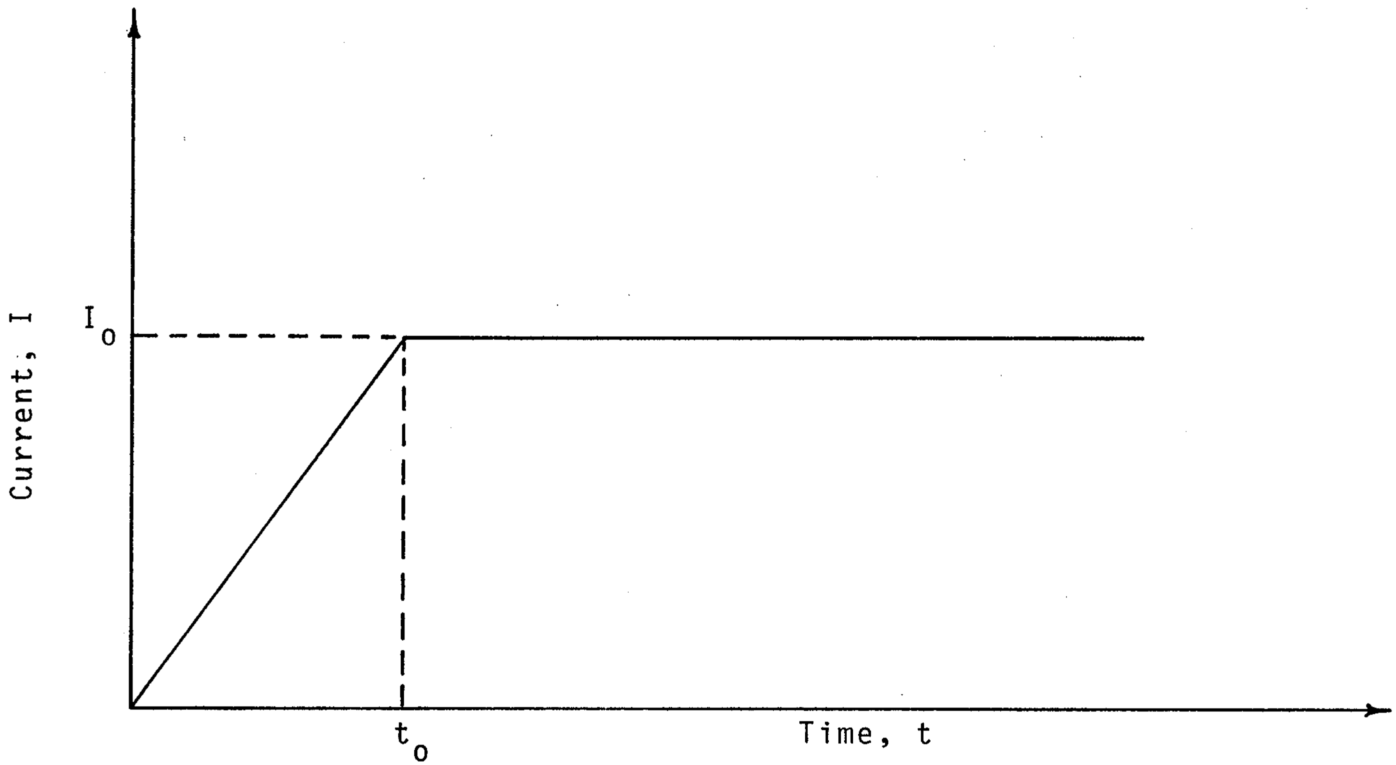

Figure 11 - Approximation to the Current at a Given Point.[10]

CHAPTER II

THE GEOMETRY OF TRANSMISSION LINE SHIELDING

One of the considerations in designing effectively shielded transmission lines is the location of the shielding wires with respect to the phase conductors. The shielding wires should be located so that all lightning strokes terminate on the towers or on the shielding wires. Common practice has been to design lines with shielding angles ranging from 20 to 45 degrees.[4] Again, emphasis will be placed on the stroke approach angle, the shielding requirements as applied to the outer phase conductors, and the shielding requirements as applied to the centre phase conductor. The basis for achieving effectively shielded transmission systems is the elimination of the exposure arcs of the phase conductors.[14,15]

2.1 THE STROKE APPROACH ANGLE

Equation 1 indicates the number of strokes per unit length and unit time, that is

$$n = \int_{r_s\ min}^{r_s\ max.} No \times f_{r_s}(r_s)\, dr_s \qquad \text{from (1)}$$

This equation is modified to account for the stroke current limitations, that is,

$$n = \int_{I\ at\ r_s\ min.}^{I\ at\ r_s\ max.} No \times f_I(I)\, dI \qquad \text{from (2)}$$

Neither Equation 1 nor Equation 2 has taken into consideration the stroke approach angle as shown in Figures 12 and 13, and since not all stroke leaders approach the earth (or line) from a vertical direction, an angular distribution of stroke directions is assumed to be of the form

$$f_\Phi = f_\Phi(\Phi) \tag{25}$$

= frequency function of the approach angle of the lightning stroke[14,15] (Figures 12 and 13). It is also assumed that Φ is limited to the range

$$-\frac{\pi}{2} \leqslant \Phi \leqslant \frac{\pi}{2} \tag{26}$$

Now, if Φ_2 and Φ_1 represent the lower and upper limits of Φ respectively, then for a given arrangement and given strike distance r_s, the number of strokes n_2 per unit length and unit time that strike an exposed region $r_s\,d\theta$ between r_s and (r_s+dr_s) as shown in Figure 13 is

$$n_2 = N_o\, r_s\, f_{r_s}(r_s) \int_{\Phi_2(\theta)}^{\Phi_1(\theta)} g(\theta, \Phi)\, f_\Phi(\Phi)\, d\Phi\, d\theta\, dr_s \tag{27}$$

As indicated by Equation 27, Φ_1 and Φ_2 may be a function of θ, with limiting range

$$\theta_2 \leqslant \theta \leqslant \theta_1 \tag{28}$$

Thus the total number of strokes having r_s within the limits $r_{s\,min.} \leqslant r_s \leqslant r_{s\,max.}$ hitting the exposed region is

$$n = N_o \int_{r_{s\,min.}}^{r_{s\,max.}} r_s\, f_s(r_s) \int_{\theta_2}^{\theta_1}\int_{\Phi_2(\theta)}^{\Phi_1(\theta)} g(\theta, \Phi)\, f_\Phi(\Phi)\, d\Phi\, d\theta\, dr_s \tag{29}$$

The functions of Equation 29 will be explained in the following pages.

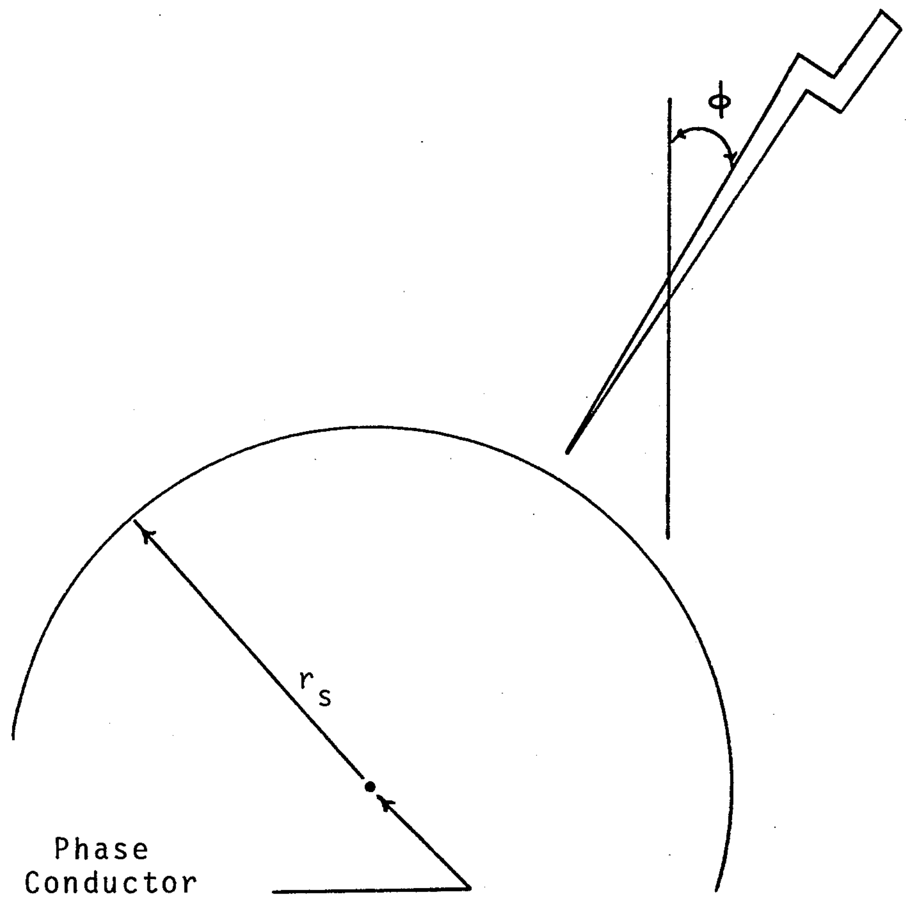

Figure 12 - Illustration of the Approach Angle of a Lightning Stroke.[14]

Equation 29, which relates the number of strokes to different parameters, will now be explained. The number of strokes per unit length per unit time is, as in Equation 29,

$$n = No \int_{r_{s\,min.}}^{r_{s\,max.}} r_s \, f_{r_s}(r_s) \int_{\Theta_2}^{\Theta_1} \int_{\Phi_2(\Theta)}^{\Phi_1(\Theta)} g(\Theta, \Phi) \, f_\Phi(\Phi) \, d\Phi \, d\Theta \, dr_s \qquad (29)$$

where:

n = the number of shielding failures per unit length and unit time,

N_o = the number of strokes per unit area and unit time,

r_s = the strike distance,

$f_{r_s}(r_s)$ = the frequency function of the occurrence of a stroke for a given r_s,

$f_\Phi(\Phi)$ = the frequency function of the occurrence of a stroke with a given approach angle Φ ,

$g(\Theta, \Phi)$ = a function relating stroke with approach angle Φ to an element area $r_s d\Theta$ at an angle Θ ,

Θ_1 = the upper angle limit for an exposed arc,

Θ_2 = the lower angle limit for an exposed arc,

Φ_1 = the upper limit of the approach angle for a given geometry (this may be a function of Θ), and

Φ_2 = the lower limit of the approach angle for a given geometry (this may be also a function of Θ).

The applicable variables for a line and shielding wire geometry are illustrated in Figure 13.

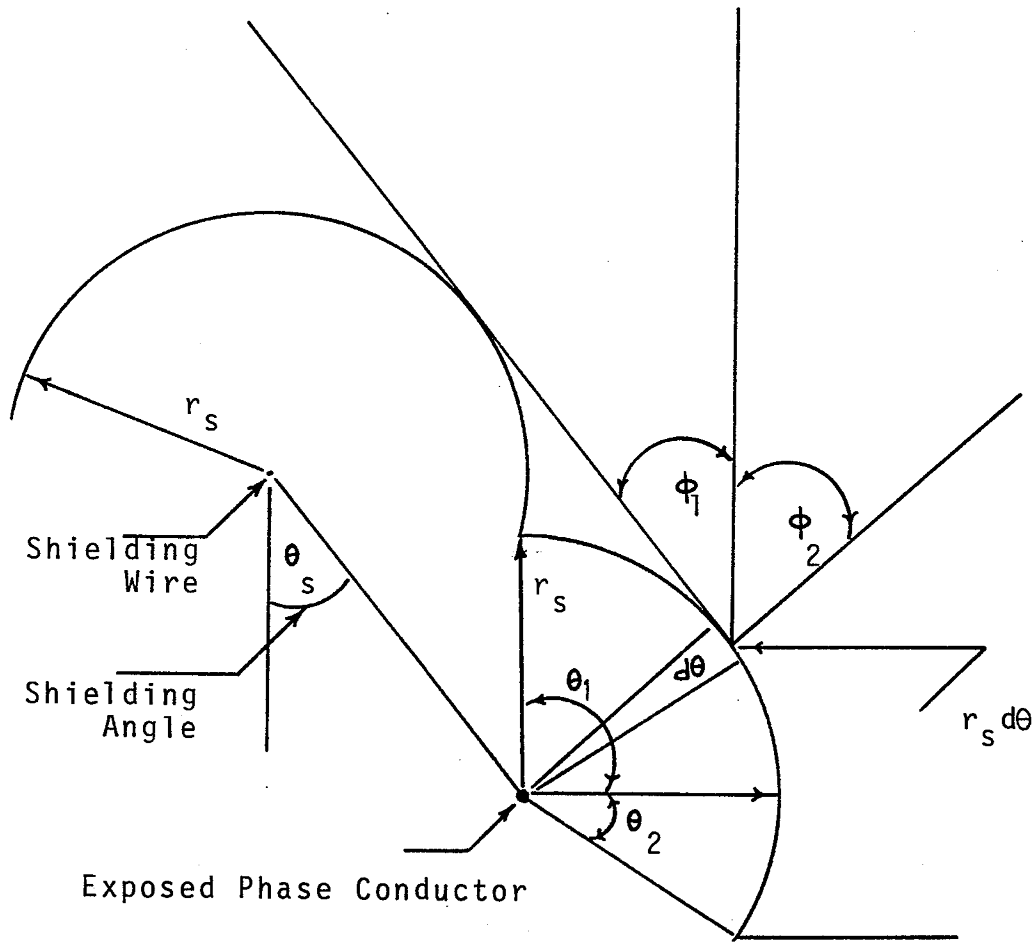

Figure 13 - Illustration of Elemental Exposed Region[14]

2.2 THE ANGULAR DISTRIBUTION FUNCTION $f_\Phi(\Phi)$[14,15]

There are insufficient data to determine an empirical frequency distribution of the angle of approach, ϕ, of a lightning stroke.

Several assumptions are necessary. It is assumed that Φ, as measured in a plane perpendicular to the ground wire and conductor, is limited by

$$-\frac{\pi}{2} \leqslant \Phi \leqslant \frac{\pi}{2} \qquad (26)$$

where Φ is measured zero for a vertical stroke. Thus the probability of finding a stroke angle between Φ_1 and Φ_2 can be assumed to be

$$P = \int_{-\frac{\pi}{2}}^{\frac{\pi}{2}} f_\Phi(\Phi)\, d\Phi = 1 \qquad (30)$$

where $f_\Phi(\Phi)$ is the frequency distribution function of the occurrence of the stroke angle between Φ_1 and Φ_2.

Since the shielding geometry will be expressed in terms of trigonometric form, and for convenience $f_\Phi(\Phi)$ can be approximated as

$$f_\Phi(\Phi) = K_m \operatorname{Cos}^m(\Phi) \qquad (31)$$

Thus, applying Equation 30, gives

$$\int_{-\frac{\pi}{2}}^{\frac{\pi}{2}} K_m \operatorname{Cos}^m(\Phi)\, d\phi = 1 \qquad (32)$$

A study by Whitehead and Armstrong[14] indicated that the value of m can be taken as $1 \leqslant m \leqslant 2$, with values near 2 more probable. Thus, for m equal to o, 1 and 2, yields

$$K_o = \frac{1}{\pi}$$

$$K_1 = \frac{1}{2} \qquad (33)$$

$$K_2 = \frac{2}{\pi}$$

Hence, the frequency distribution function of the occurrence of the stroke angle Φ, between Φ_1 and Φ_2, with the exponent m equal 2, is

$$\frac{2}{\pi}\int_{-\frac{\pi}{2}}^{\frac{\pi}{2}} f_\phi(\phi)\, d\phi = \frac{2}{\pi}\int_{-\frac{\pi}{2}}^{\frac{\pi}{2}} \cos^2\phi \; d\phi \tag{34}$$

with $-\frac{\pi}{2} \leqslant \Phi \leqslant \frac{\pi}{2}$

2.3 THE DETERMINATION OF THE FUNCTION $g(\theta, \Phi)$[14,15]

Let

N_Φ = the effective number of strokes per unit area and time, measured from a plane perpendicular to Φ, for strokes approaching at angle Φ. Referring to Figure 14 and assuming

N_o = the number of strokes per unit area as measured from the horizontal plane,

then $$N_o X_1 = N_\Phi X_2 \tag{35}$$

and $$N_\Phi = N_o \frac{X_1}{X_2} = \frac{N_o}{\cos\Phi} \tag{36}$$

Now, consider the number of strokes per unit length of line and unit time, dn, to be approaching at angle Φ with variation $d\Phi$, and striking the elemental arc, $r_s d\theta$, at angle θ as in Figure 15. Then,

$$dn = N_\Phi f_\Phi(\Phi)\, d\Phi \; dA \tag{37}$$

where dA is the elemental exposed area per unit length of line perpendicular to strokes with approach angle Φ. So from

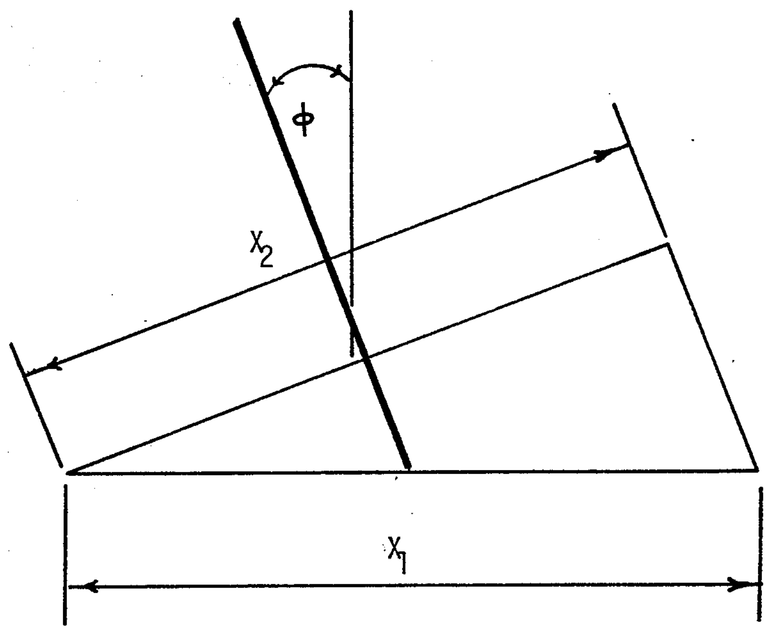

Figure 14 - Stroke Density Viewed at Angle (Φ)[15]

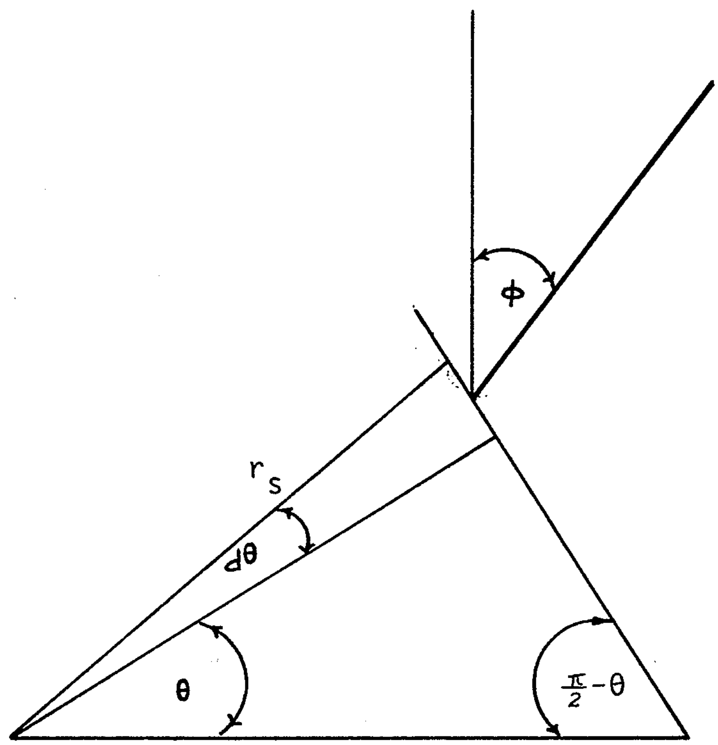

Figure 15 - Elemental Exposed Arc r_s $d\Theta$[15]

Figure 16

$$dA = r_s \, d\theta \quad \sin(\theta - \Phi) \tag{38}$$

Thus,

$$dn = N_\Phi \, f_\Phi(\Phi) \, d\Phi \, r_s \sin(\theta - \Phi) \, d\theta \tag{39}$$

$$= N_o r_s \frac{\sin(\theta - \Phi)}{\cos\Phi} f_\Phi(\Phi) \, d\Phi \, d\theta \tag{40}$$

Hence in Equation 29

$$g(\theta, \Phi) = \frac{\sin(\theta - \Phi)}{\cos\Phi}$$

$$= \frac{\sin\theta \cos\Phi - \cos\theta \sin\Phi}{\cos\Phi}$$

$$g(\theta, \Phi) = \sin\theta - \cos\theta \tan\Phi \tag{41}$$

Thus Equation 29 becomes

$$n = N_o \int_{r_s \min.}^{r_s \max.} r_s \, f_{r_s}(r_s) \int_{\theta_2}^{\theta_1} \int_{\Phi_2(\theta)}^{\Phi_1(\theta)} \left[\sin\theta - \cos\theta \tan\Phi\right] f_\Phi(\Phi) \, d\Phi \, d\theta \, dr_s \tag{42}$$

2.4 THE CHANGE OF VARIABLE TO REPLACE THE FUNCTION $f_{r_s}(r_s)$ [14,15]

The function $f_{r_s}(r_s)$ can be expressed in the form of stroke current, that is,

$$f_{r_s}(dr_s) = f_I(I) \, dI$$

where $f_I(I)$ = frequency function of the occurrence of the strokes with a given current I.

Thus Equation 29 becomes

$$n = N_o \int_{I_2}^{I_1} r_s(I) \, f_I(I) \int_{\theta_2}^{\theta_1} \int_{\Phi_2(\theta)}^{\Phi_1(\theta)} (\sin\theta - \cos\theta \tan\Phi) f_\Phi(\Phi) \, d\Phi \, d\theta \, dI \tag{43}$$

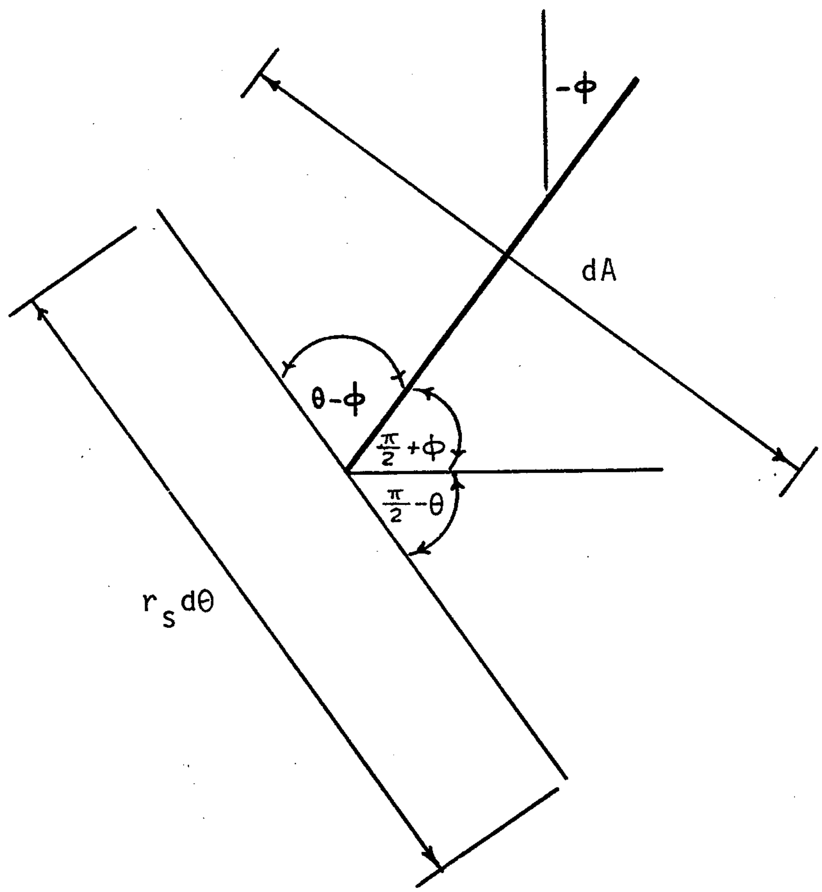

Figure 16 - Elemental Arc Area Presented to Incoming Stroke.[15]

where

I_1 = the maximum value of I, corresponding to $r_{s\ max.}$, and

I_2 = the minimum value of I, corresponding to $r_{s\ min}$.

Comparing Equation 3 with Equation 43 gives the equivalent swath X for a given r_s and given stroke current I. The equivalent swath X is then

$$X = r_s \int_{\theta_2}^{\theta_1} \int_{\phi_2(\theta)}^{\phi_1(\theta)} (\sin\theta - \operatorname{Cos}\theta \tan\Phi) f_\Phi(\Phi)\, d\Phi\, d\theta \quad (44)$$

To indicate the relationship between the strike distance r_s and the stroke current, it has been found, based on studies of the breakdown of long gaps, that the relation between the breakdown voltage V_g and the gap length L_g is

$$L_g = 1.4\ (V_g)^{1.2} \text{ meters} \quad (45)$$

where V is in (MV). Assuming the same relation to hold for the last step of the stroke leader, the strike distance r_s is then

$$r_s = 1.4\ (V_s)^{1.2} \text{ meters} \quad (46)$$

Again, studies[14] of the relation between the return stroke velocity V_1, the stroke current I_s, and the stroke voltage V_s showed that

$$V_s = 0{\cdot}426\ \frac{Is}{V_1} \text{ megavolts and} \quad (47)$$

$$V_1 = 0.11\ (I_s)^{0.375} \text{ per unit} \quad (48)$$

where

V_s is the leader stroke voltage,

I_s is the stroke current, and

$V_1 = \frac{V}{C}$ is the return stroke velocity expressed in per unit of the light velocity. Combining the above equations results in

$$r_s = 1.4 \left[0.426 \frac{I_s}{0.11\ I_s^{0.375}} \right]^{1.2} \quad \text{meters and}$$

$$r_s = 7.1(I_s)^{0.75} \quad \text{meters} \tag{49}$$

This function is shown in Figure 17.

2.5 THE LIMITS OF INTEGRATION OF THE STROKE CURRENT I

When lightning strikes a transmission line - two current waves travel down the line, as in Figure 18. If the line surge impedance is Z ohms, then the voltage wave is

$$V_L = \frac{I}{2}\ Z \tag{50}$$

This wave travels with the current. When it reaches a tower, the voltage, V_L, is impressed across the line insulator. Thus, if the insulator has the capacity to withstand a voltage denoted BIL (Basic Insulation Level) without failure, then only the current

$$I_2 = I_s > 2\ \frac{BIL}{Z} \tag{51}$$

will have sufficient capacity to cause damage to the insulators. This establishes the lower or the critical limits of the current, that is $I_2 = I_s = \frac{BIL}{Z/2}$ (52)

2.6 DETERMINING THE UPPER LIMIT OF CURRENT I.[15]

The tower geometry can determine the upper limit of the current. That is, the incoming stroke could strike either the earth or other nearby ground objects such as trees.

The leader to ground strike distance may be different from the leader to conductor strike distance. Whitehead and

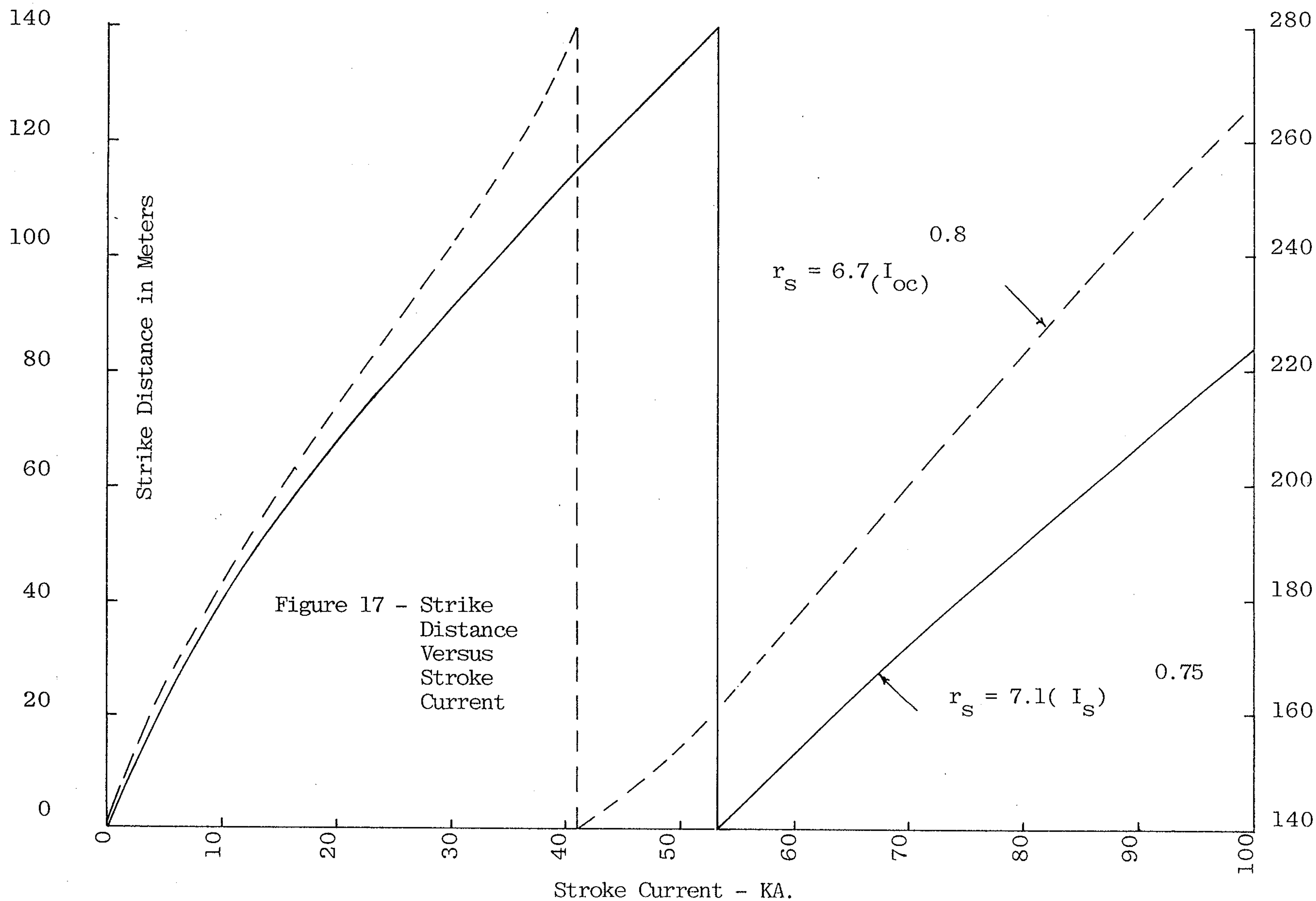

Figure 17 - Strike Distance Versus Stroke Current

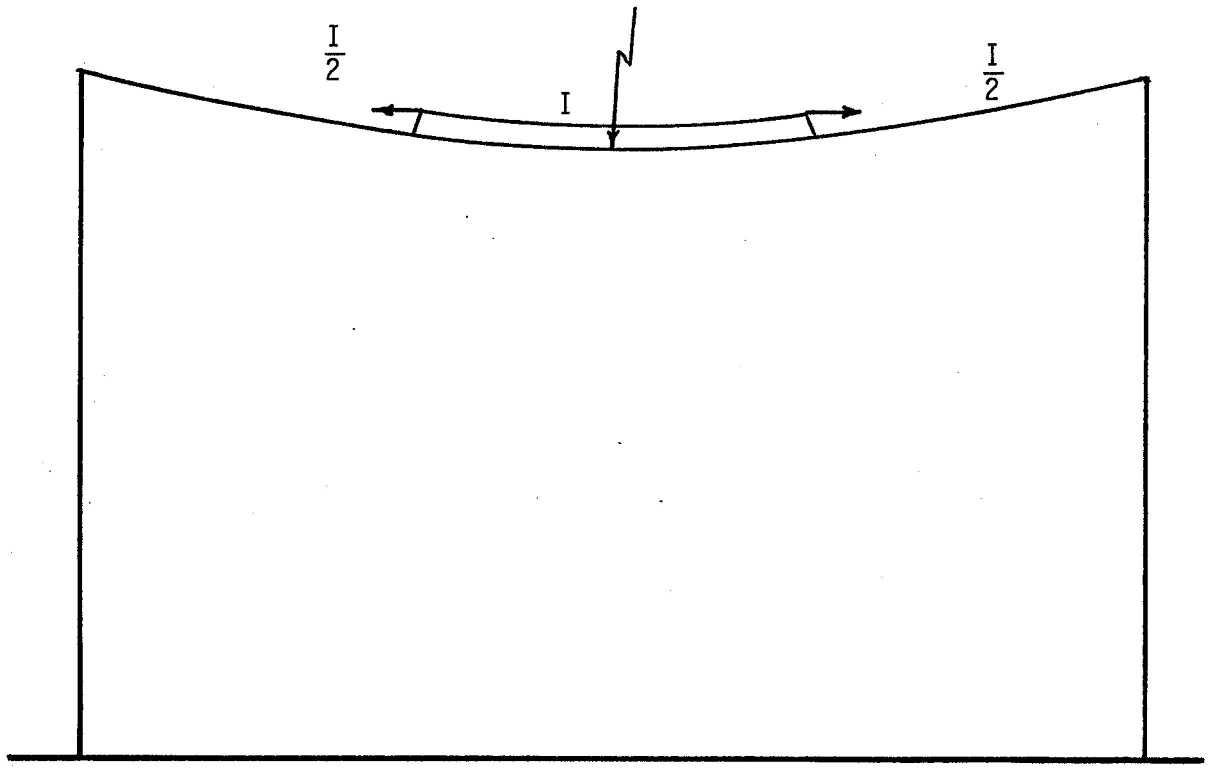

Figure 18 - Illustration of Travelling Current Wave[14]

Armstrong[13] suggest using the relation

$$r_{s_g} = K_{s_g} \, r_s \tag{53}$$

where

r_{s_g} = the point to plane strike distance (stroke to ground),

r_s = the point to line strike distance, and

Ks_g = a factor relating r_{s_g} to r_s

$$= 0.85 \tag{54}$$

Knowing the relation between r_{g_s} and r_s, as in Equation 53, recalling the relationship between the stroke current and the strike distance to phase conductors as indicated by Equation 49.

$$r_s = 7.1(I_s)^{0.75} \text{ meters} \tag{49}$$

and using the distribution function of the stroke current as shown in Figure 20, it is clear that the higher the current, the larger is the strike distance to phase conductors. This implies that under certain conditions the phase conductors strike distance is large enough, so that beyond which no strokes can reach the phase conductors as shown in Figure 19. With a higher stroke current, which is limited to a low probability of occurrence,[2] then the practical choice of the current I_1, will be limited.

2.7 THE LIMITS OF INTEGRATION OF THE ANGLE (Θ)[15]

The angles Θ_1 and Θ_2 are limited by the geometric configuration of the transmission line. It is convenient to

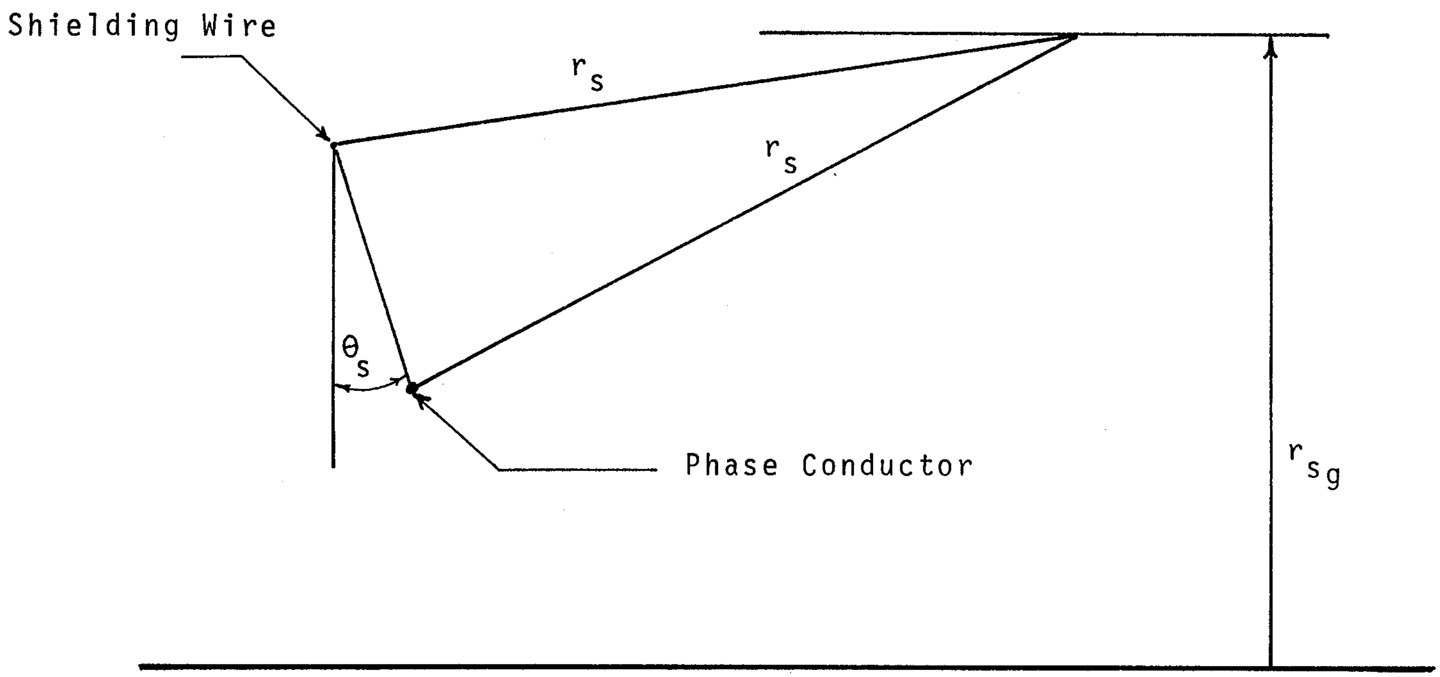

Figure 19 - Geometric Limitation on Strike Distance.

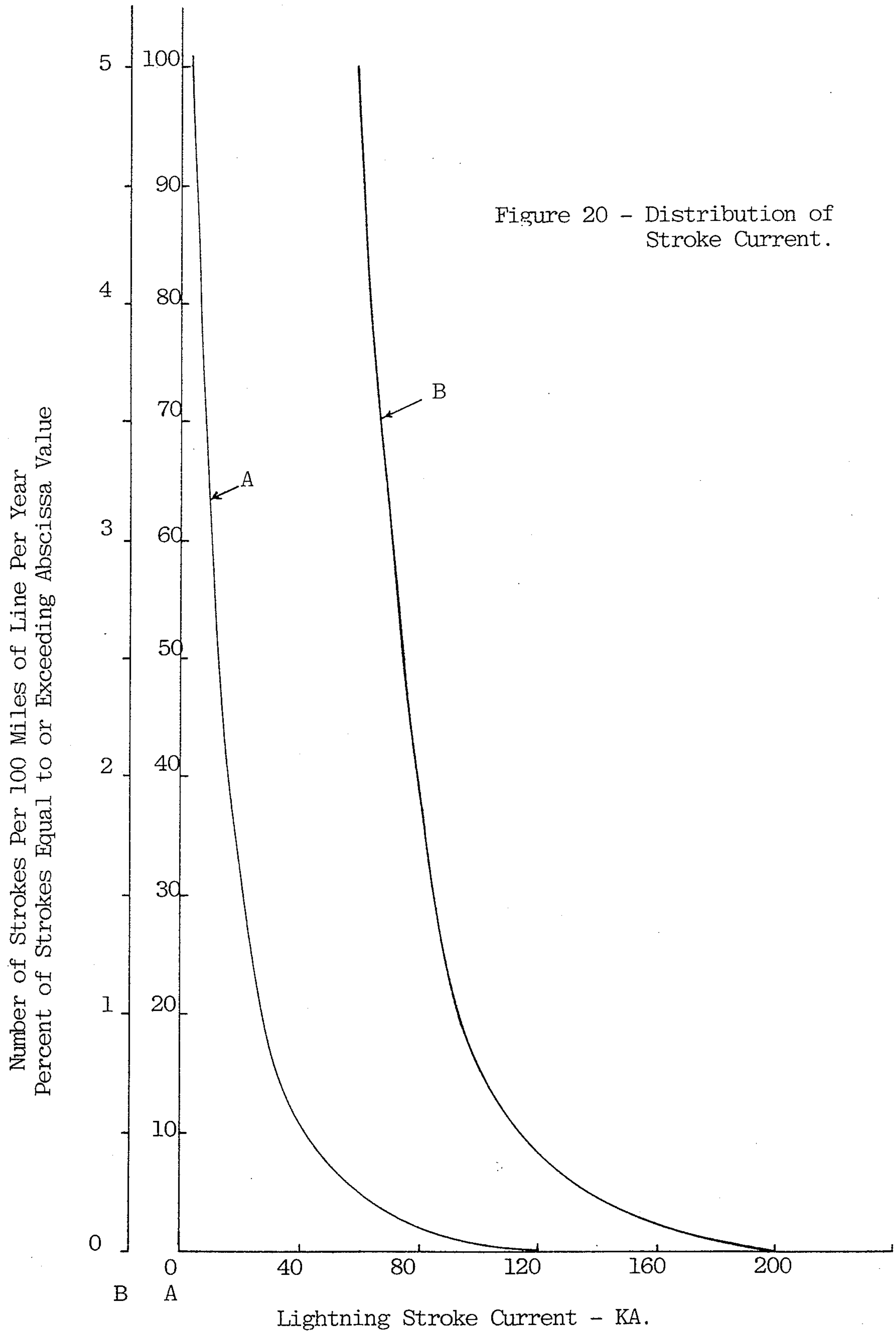

Figure 20 - Distribution of Stroke Current.

define the parameters that constitute the physical configuration of the tower:

Θ_s = the shielding angle,

a = the conductor to shielding wire spacing,

$$B = \mathrm{Sin}^{-1} \frac{a}{2\ r_s} \tag{55}$$

$\bar{h}$ = average shielding wire height, and

$\bar{y}$ = average phase conductor height

As shown in Figure 21, clearly the upper limit Θ_1 is

$$\Theta_1 = \Theta_s + B \tag{56}$$

As indicated in the figure, the lower limit, Θ_2, is defined, implicity, by

$$\sin(-\Theta_2) = -\sin\Theta_2 = \frac{\bar{y} - r_{sg}}{r_s}$$

$$\Theta_2 = \sin^{-1}\left(\frac{r_{sg} - \bar{y}}{r_s}\right) \tag{57}$$

For low values of current and strike distance, the line of a distance r_{s_g} from the earth may not intersect the arc a distance r_s from the conductor, or may intersect it at

$$\Theta_2 = \frac{-\pi}{2} \tag{58}$$

which is the lower limit of Θ_2.

2.8 THE LIMITS OF INTEGRATION OF THE STROKE APPROACH ANGLE(Φ)[14,15,18]

Recalling that Φ_1 and Φ_2 are the stroke approach angle limits for a stroke hitting an elemental arc located at angle Θ, thus from Figure 22a, the lower limit is

$$\Phi_2 = \frac{-\pi}{2} \tag{59}$$

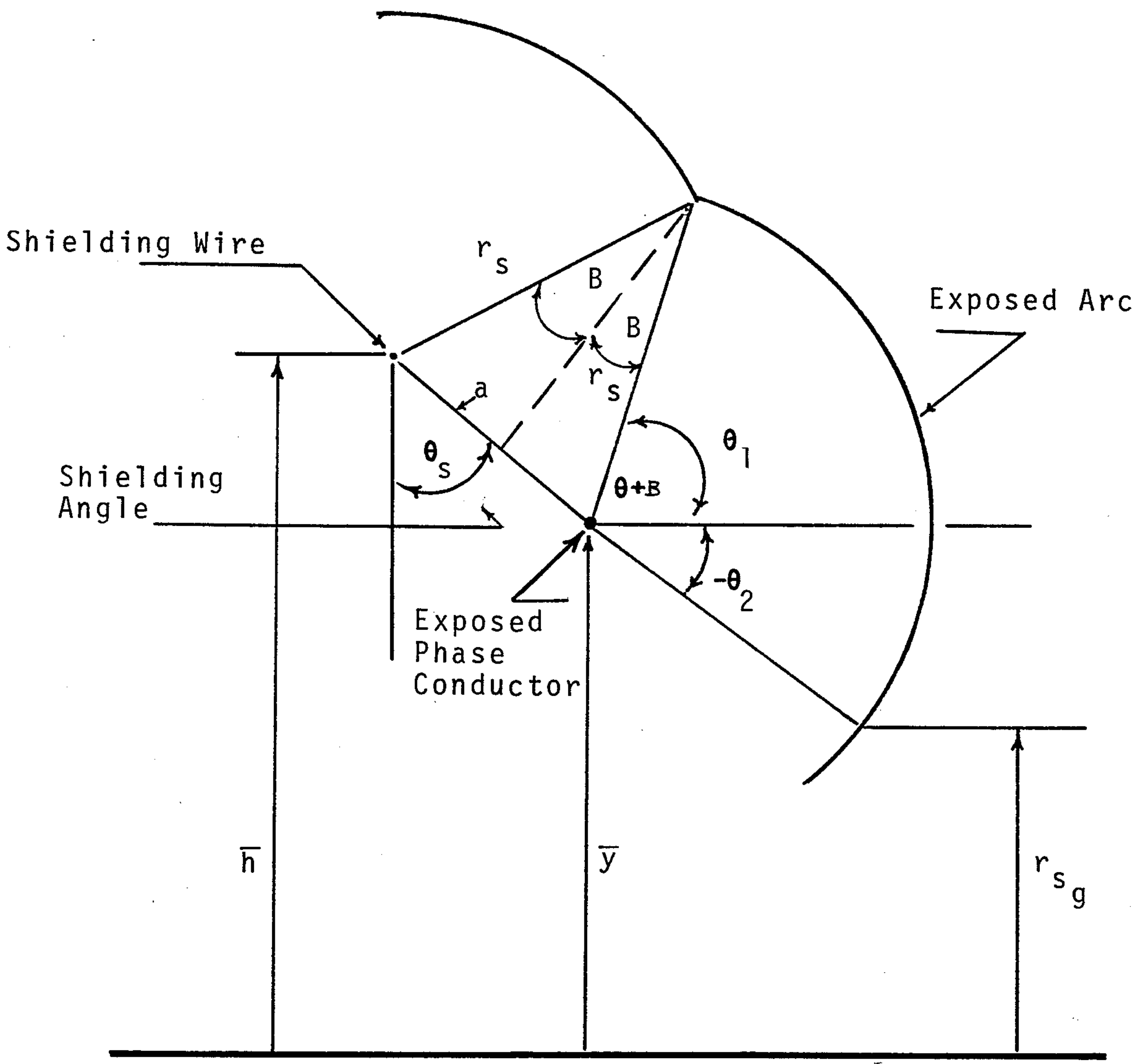

Figure 21 - A Conductor With Exposed Arc Between Θ_1 and Θ_2[18]

where $\frac{-\pi}{2} \leqslant \theta \leqslant \theta_s$ (60)

This limit applies for Figure 22b. The upper limit can be determined from Figure 22a, for $\theta_s > \theta$, as

$$\theta_1 = \theta \tag{61}$$

For $\theta > \theta_s$, as shown in Figure 22b, and referring to Figure 23, it is necessary to express the limit implicitly. Thus,

$$\frac{\bar{a}}{\bar{b}} = \tan\Phi = \frac{\sin\Phi}{\cos\Phi} = \frac{2r_s \sin B \sin\theta_s + r_s \cos\theta - r_s \cos\Phi}{2r_s \sin B \operatorname{Cos}\theta_s + r_s \sin\Phi - r_s \sin\theta} \tag{62}$$

Thus

$$2 \sin B \operatorname{Cos}\theta_s \sin\Phi + \sin^2\Phi - \sin\theta \sin\Phi =$$

$$2 \sin B \sin\theta_s \operatorname{Cos}\Phi + \operatorname{Cos}\theta \operatorname{Cos}\Phi - \operatorname{Cos}^2\Phi$$

whence $\operatorname{Cos}(\Phi - \theta) - 2 \sin B \sin(\Phi - \theta_s) = 1$ (63)

where $\frac{-\pi}{2} \leqslant \theta_s \leqslant \theta \leqslant \theta_s + B$ (64)

Thus, to summarize, eliminating the phase conductors exposure arcs is the basic criterion for achieving effectively shielded transmission systems, and the last stage of the lightning stroke process has been considered of great importance in their design.

Whitehead[18,19] has concluded that the basic lightning stroke mechanisms leading to the transmission line insulation flashover are:

a) Stroke to tower or shielding wire, with resultant voltage across the insulator strings. This is called the "Backflashover Mechanism"[18].

b) Stroke directly to the phase conductors, with resultant

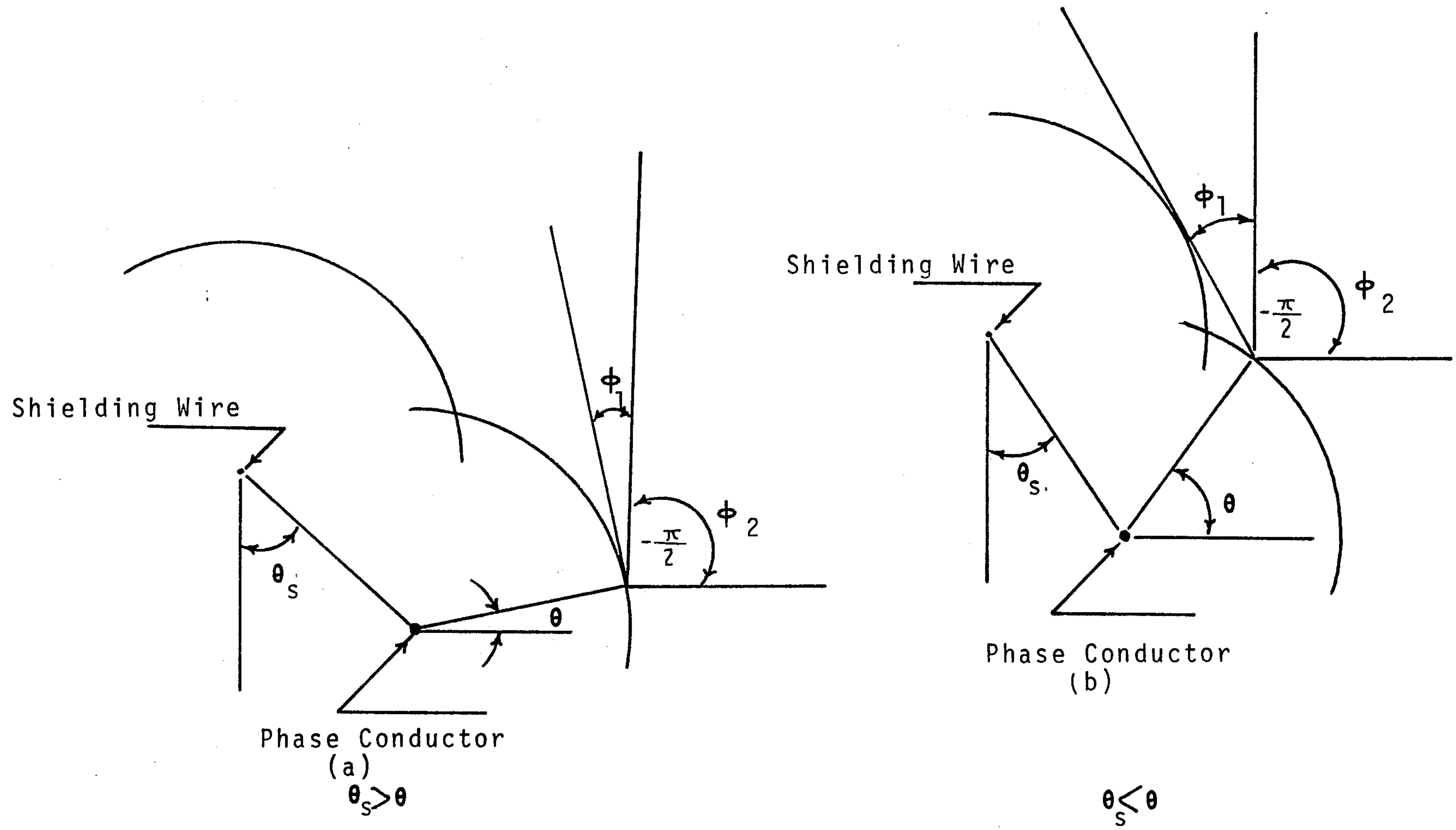

Figure 22 - Common Limitations on the Approach Angle.[18]

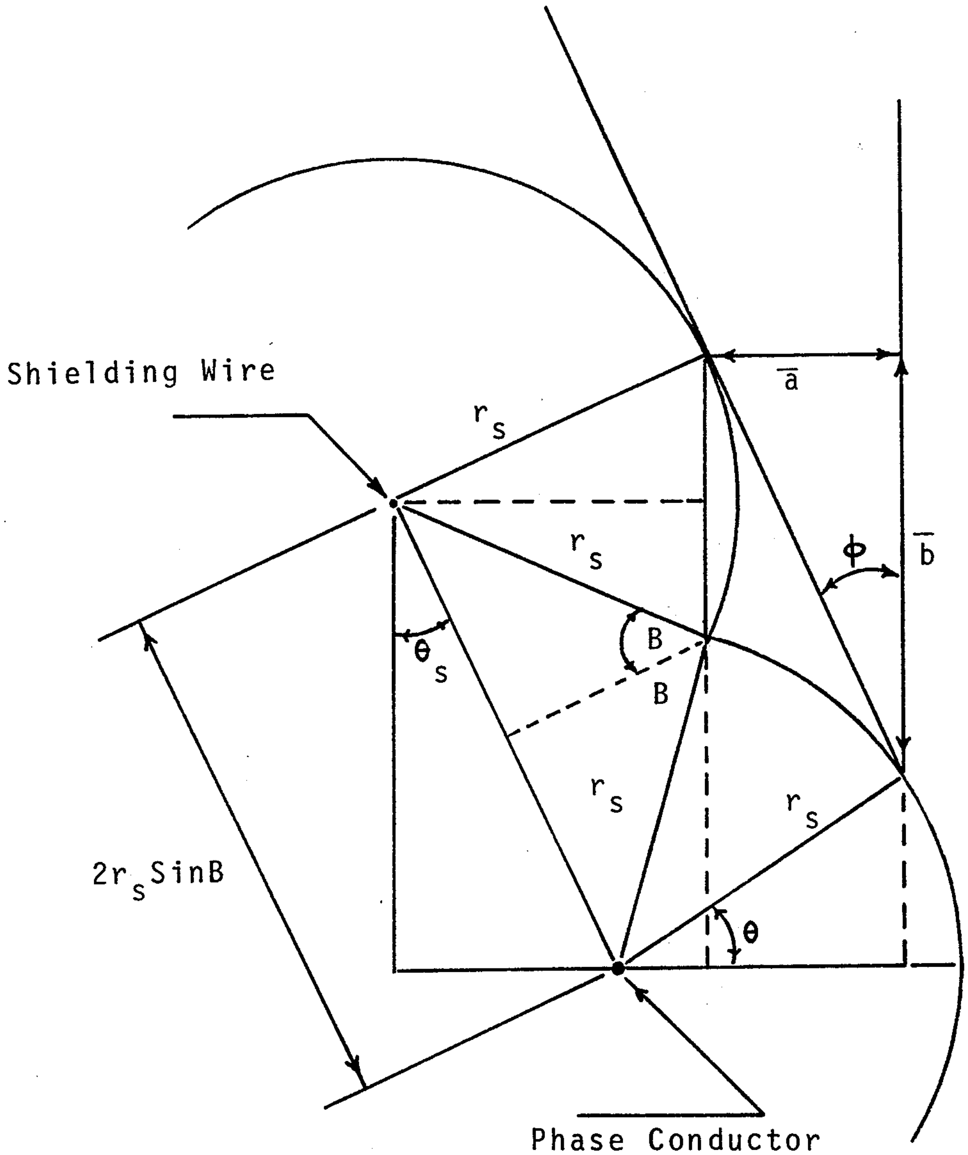

Figure 23 - Geometry for Determining the Angle(ϕ)[18]

voltage across the insulator strings. This is called "Shielding Failure Mechanism".[18]

c) Stroke to earth near the line with resultant electromagnetically induced voltage across the insulator strings. This is called "Induced Voltage Mechanism".[18] It has been generally accepted that the induced voltage mechanism is an insignificant factor in the lightning performance of E.H.V. lines. Accordingly, the basic factor to be considered is the direct stroke to the phase conductors. Figure 24 shows the different stroke flashover mechanisms.

2.9 THE TRANSMISSION LINE ANALYTICAL MODEL

The analytical model[18,19] is based on a combination of geometrical and electrical quantities and has been called the "Electro-Geometrical Model", the basic relations and assumptions that have been considered in developing the aforementioned model are:

a) It has been concluded that as the stroke leader approaches the earth or an earthed target,[4] it is relatively unaffected by these targets, which may serve as stroke termini until a specific target acquires a voltage gradient of 10 KV per centimeter[15] and is within a certain distance r_s defined as the strike distance.

b) The relation between the stroke current and the strike distance is given by Equation 49 as $r_s = 7.1(I_s)^{0.75}$ (49)
Recently, Gilman and Whitehead[18] have arrived at a more conservative relation between the stroke current and the strike distance:

$$r_s = 6.7\,(I_{OC})^{0.8} \text{ meters} \tag{65}$$

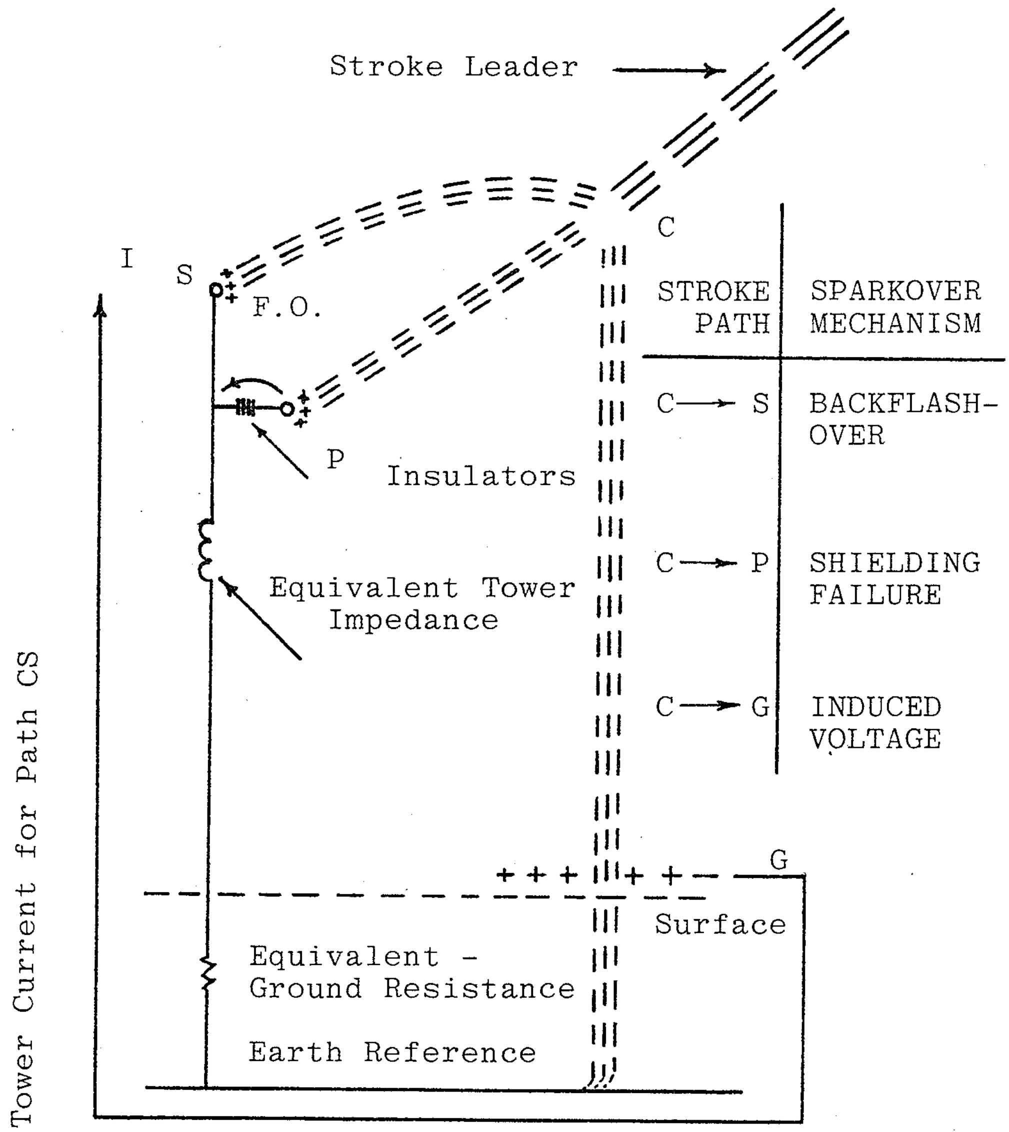

Figure 24 - Mechanisms of Lightning Stroke Flashover [18].

Where I_{OC} is the critical prospective stroke current to zero resistance ground in KA, and r_s is the strike distance in meters. Equation 65 is also shown in Figure 17.

c) It has been assumed that the lightning strokes lower 90 to 95 percent negative charges.

d) The critical stroke current to the phase conductors is given by Equation 52. That is,

$$I_s = \frac{BIL}{Z/2} \tag{52}$$

where

Z = the surge impedance of the phase conductor with ground return. Its value can be calculated as follows:

$$Z = 60 \ln \frac{2\,\bar{y}}{r} \quad \text{Ohms} \tag{66}$$

where

r = the outside radius of the phase conductor, if single, or the geometric mean radius of the phase conductor in the case of bundled conductor; and

$\bar{y}$ = the average height of the phase conductor = the phase conductor height at the tower minus two-thirds of the maximum sag of the phase conductor.

e) The critical prospective lightning current to zero ground resistance is related to the critical lightning current to the phase conductors by the following relationship

$$I_{OC} = 1.1 \quad I_s \tag{67}$$

2.9.1 THE EFFECTS OF SAG ON CONDUCTOR HEIGHT

For effectively shielded transmission lines, several factors should be considered.

1. Sag and Average Height

All overhead lines sag to some extent. In fact, "rule of thumb"[14] formulae are of the order of

$$S_{max} = 0.03\ L, \tag{68}$$

where S_{max} = maximum sag, and

L = span length

The sagging line is expressed by the catenary equation. Referring to Figure 25

$$y = C \cosh \frac{x}{C} \tag{69}$$

Therefore

$$S = S_{max} - C\left(\cosh \frac{x}{C} - 1\right) \tag{70}$$

and at the tower s = o and $x = \frac{L}{2}$. This results in

$$S_{max} = C\left(\cosh \frac{L}{2C} - 1\right) \tag{71}$$

From the "rule of thumb" formula

$$S_{max} = 0.03\ L, \text{yields} \tag{72}$$

$\frac{L}{2C} = 0.1$; that is, $\frac{L}{2C}$ is small.

However, from Equation 70

$$\overline{S} = \frac{1}{L/2} \int_0^{\frac{L}{2}} \left[S_{max} - C\left(\cosh \frac{x}{C} - 1\right)\right] dx \tag{73}$$

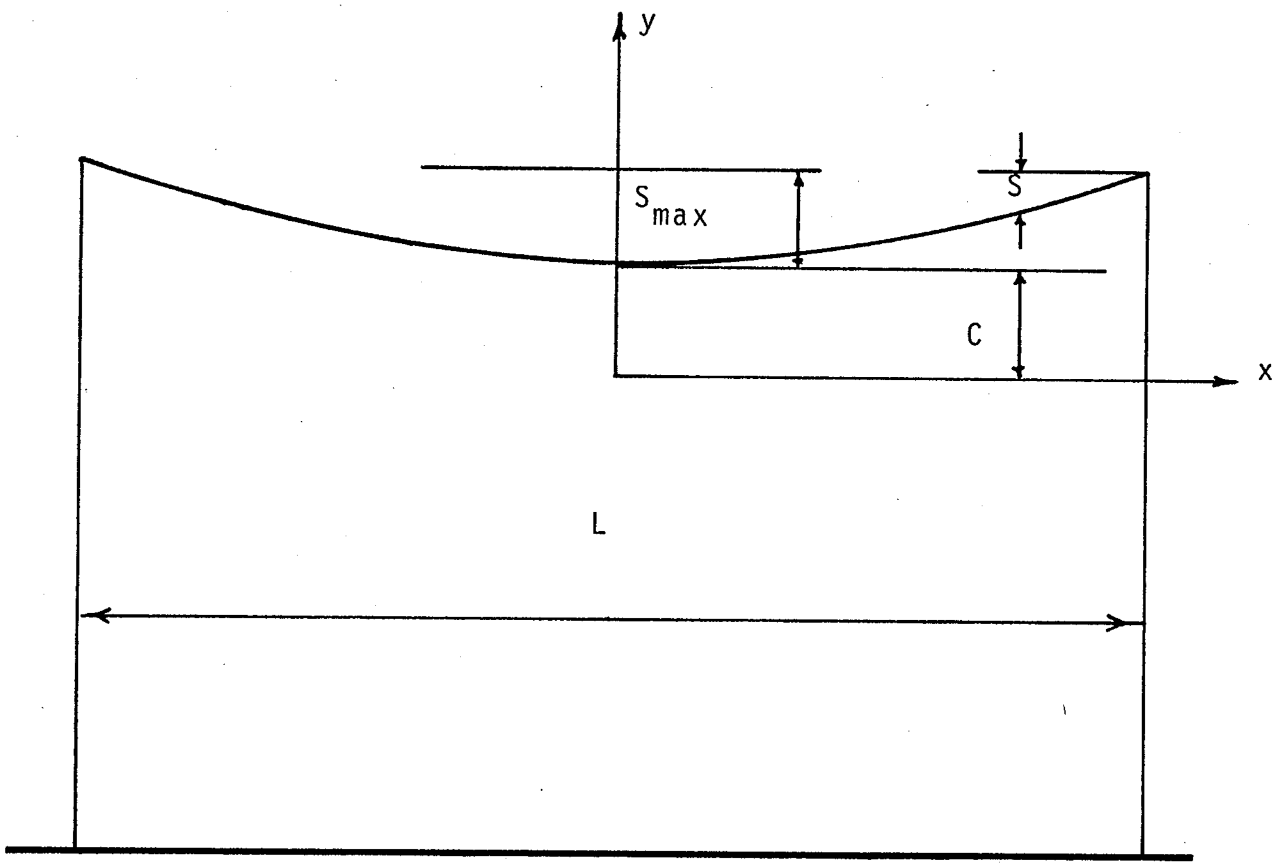

Figure 25 - Catenary Sag.

$$\overline{S} = S_{max} - C \left[\frac{2C}{L}\sinh \frac{L}{2C} - 1\right]$$

and

$$\frac{\overline{S}}{S_{max}} = 1 - \frac{\left[\frac{2C}{L} \sinh \frac{L}{2C} - 1\right]}{\left[\cosh \frac{L}{2C} - 1\right]} \tag{74}$$

by taking the limit of $\frac{\overline{S}}{S_{max}}$, for $\frac{L}{2C} \longrightarrow 0$

therefore,

$$\lim_{\frac{L}{2C} \to 0} \left(\frac{\overline{S}}{S_{max}} \right) = 2/3. \tag{75}$$

Accordingly, for a real transmission line it is assumed that the average height of the conductor is reduced by two thirds of the maximum sag.

Now the following symbols will be defined:

Sg = maximum Sag of the shielding wire,

Sc = maximum Sag of the phase conductor,

H_t = Shielding wire height at tower,

y_t = Conductor height at tower,

a = Shielding wire to phase conductor spacing, and

θ_s = Shielding angle.

Therefore, the average heights of the shielding wire and the phase conductor (Figure 26) are:

$$\overline{h} = H_t - 2/3\ Sg \tag{76}$$

$$\overline{y} = h_t - 2/3\ Sc \tag{77}$$

2.9.2 THE EFFECTS OF TERRAIN

Terrain[18,19] affects the average height of the phase conductor,

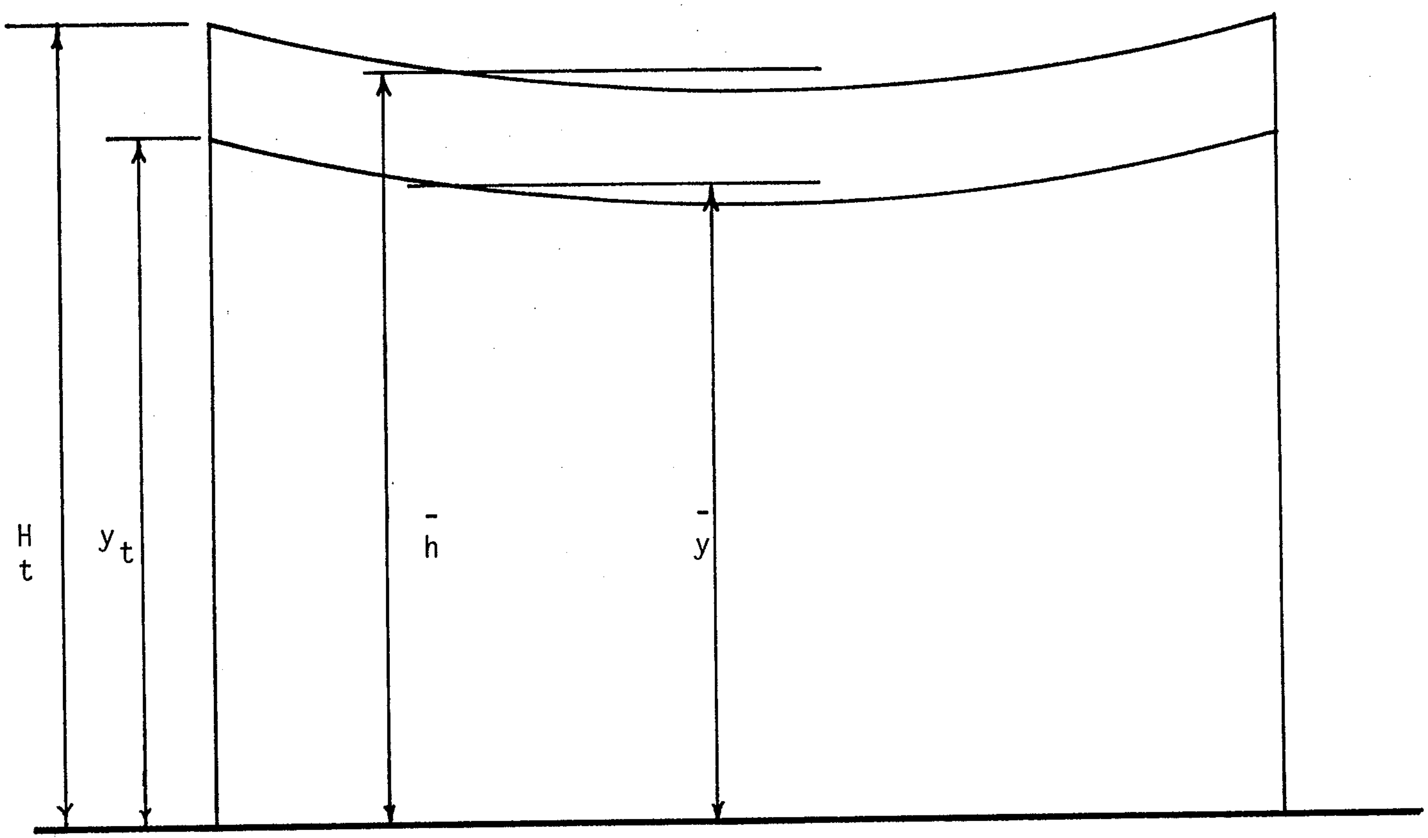

Figure 26 - Geometry of the Average Height of the Shielding Wires and the Phase Conductors.[14]

$\overline{y}$, as shown in Figure 27. The figure indicates that for hilly or mountainous country, where towers are placed at high points, $\overline{y}$ may be considerably greater than the phase conductor height at the tower h_t. It has been suggested that for rolling terrain "earth sag" be assumed equal to the conductor sag, and that for mountainous terrain the average conductor height be equal to about twice the height of the conductor at the tower y_t. It should be noted that in this study "rolling" terrain is defined as quite hilly (thirty feet up and down at each tower).

Thus, flat terrain will be assumed, since the effects of rolling terrain are beyond the scope of this study, which covers the shielding requirements of a three phase flat configuration on flat terrain.

2.10 THE SHIELDING OF THE CENTRE PHASE CONDUCTOR

Figures 28 and 29 show ineffectively and effectively shielded transmission lines. "In cases where the stroke current is low, the geometry shown in Fig. 28 may allow the stroke to sneak by the shielding wires and hit the centre phase conductor"[18] Accordingly, a proposed procedure as shown in Fig. 29 will be introduced.

2.10.1 THE SHIELDING REQUIREMENTS OF THE CENTRE PHASE CONDUCTOR[19]

Referring to Figure 29, the equation of the exposure arc centered at C_2 (o , o), with radius r_s, is

$$r_s^2 = x^2 + y^2 \tag{78}$$

The equation of the exposure arc centered at

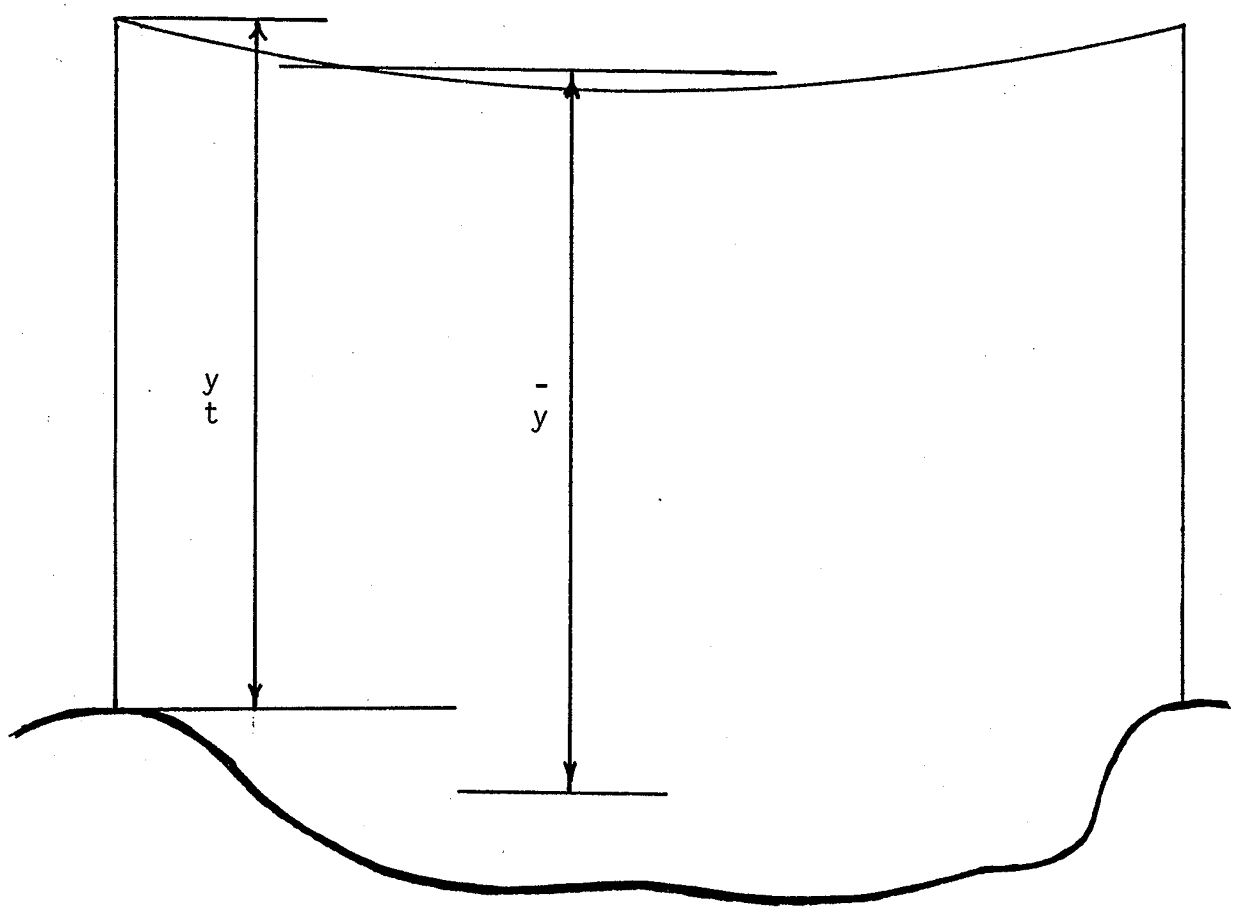

Figure 27 - Effect of Rolling Terrain and Sag on the Average Height.

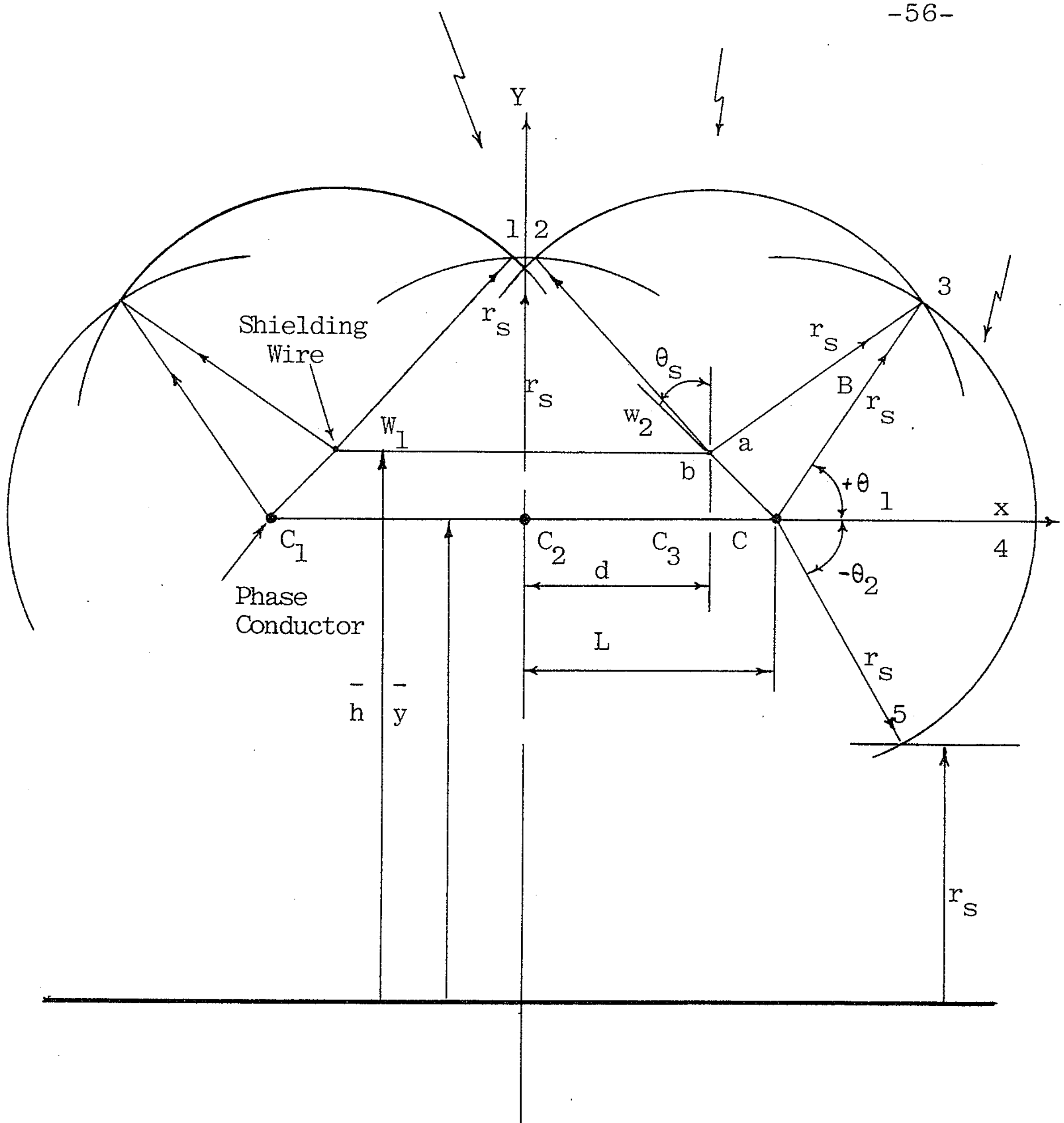

Figure 28 - Geometry of Ineffective Shielding.[18]

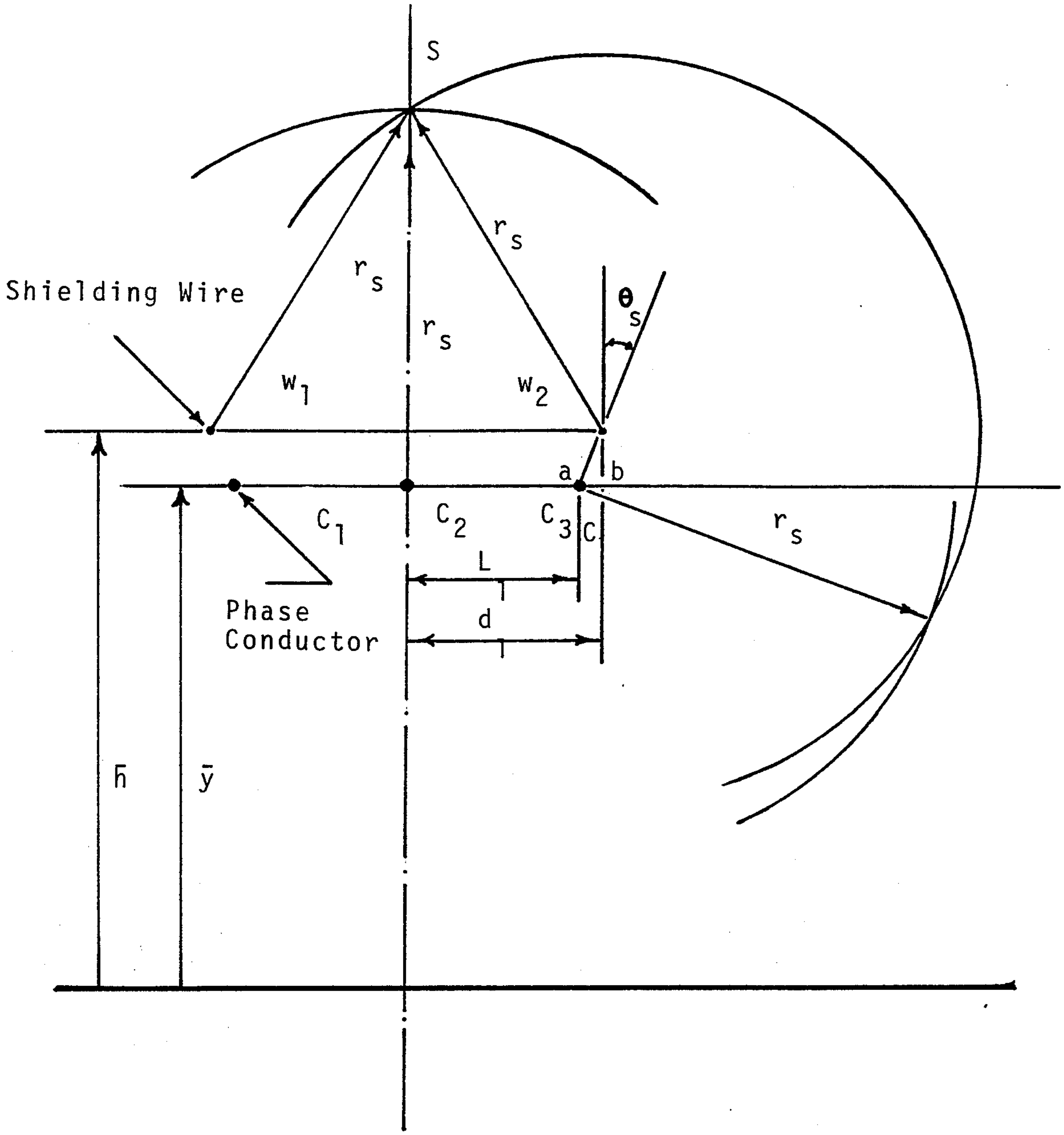

Figure 29 - Geometry of Effective Shielding of Centre phase Conductor.

$W_2 \quad [(x - d_1), (y - b)]$, with radius r_s, is

$$r_s^2 = (x - d_1)^2 + (y - b)^2 \tag{79}$$

To achieving shielding of the centre phase, the two exposure arcs should intersect at point S (o, r_s). Thus

$$d_1^2 + b^2 = 2xd_1 + 2yb \tag{80}$$

at point s. Hence

$$d_1^2 + b^2 = 2r_s b$$

$$r_s^2 - 2r_s b + b^2 = r_s^2 - d_1^2 \tag{81}$$

in the normalized form. That is, in per unit of the strike distance r_s, Equation 81 becomes

$$1 - \frac{2b}{r_s} + \frac{b^2}{r_s^2} = 1 - \left[\frac{d_1}{r_s}\right]^2$$

$$\left(1 - \frac{b}{r_s}\right)^2 = 1 - \left[\frac{d_1}{r_s}\right]^2$$

$$1 - \frac{b}{r_s} = \pm \sqrt{1 - \left[\frac{d_1}{r_s}\right]^2}$$

$$\frac{b}{r_s} = 1 \mp \sqrt{1 - \left[\frac{d_1}{r_s}\right]^2} \tag{82}$$

for minimum height b, of the shielding wire above the phase conductor. Therefore,

$$\frac{b}{r_s} = 1 - \sqrt{1 - \left[\frac{d_1}{r_s}\right]^2} \tag{83}$$

Equation 83 shows that the shielding requirements of the centre phase are independent of the phase conductors and the height of the shielding wire above the ground.

Equation 83 is plotted in Figure 30, from which it can be seen that the height b of the shielding wires becomes excessively high when the ratio d_1/r_s reaches unity, thus resulting in an uneconomical design. On the other hand, when the ratio $\frac{d_1}{r_s}$ reaches zero, for strike distance r_s approaching infinity, results in a transmission line without shielding wires. It is therefore proposed that the shielding wire spacing, d_1, be selected such that the ratio $\frac{d_1}{r_s}$ is

$$0 < \frac{d_1}{r_s} < 1 \tag{84}$$

where the strike distance r_s can be calculated from

$$r_s = 6.7(I_{oc})^{0.8} \quad \text{in meters} \tag{65}$$

and I_{oc} in K.A.

2.11 THE SHIELDING REQUIREMENTS OF THE OUTER PHASE CONDUCTORS[18]

Figure 28 clearly shows that the outer phase conductor is susceptible to lightning strokes through the exposure arc (3-5). To achieve effective shielding for the outer phase conductors, the triangle C_3W_23 is rotated clockwise so that the angle θ_1 equals angle θ_2. Thus the phase conductor exposure arc is reduced to zero (Figure 31).

It has been found that insulator flashovers occur both as a result of strokes directly to the phase conductor (the

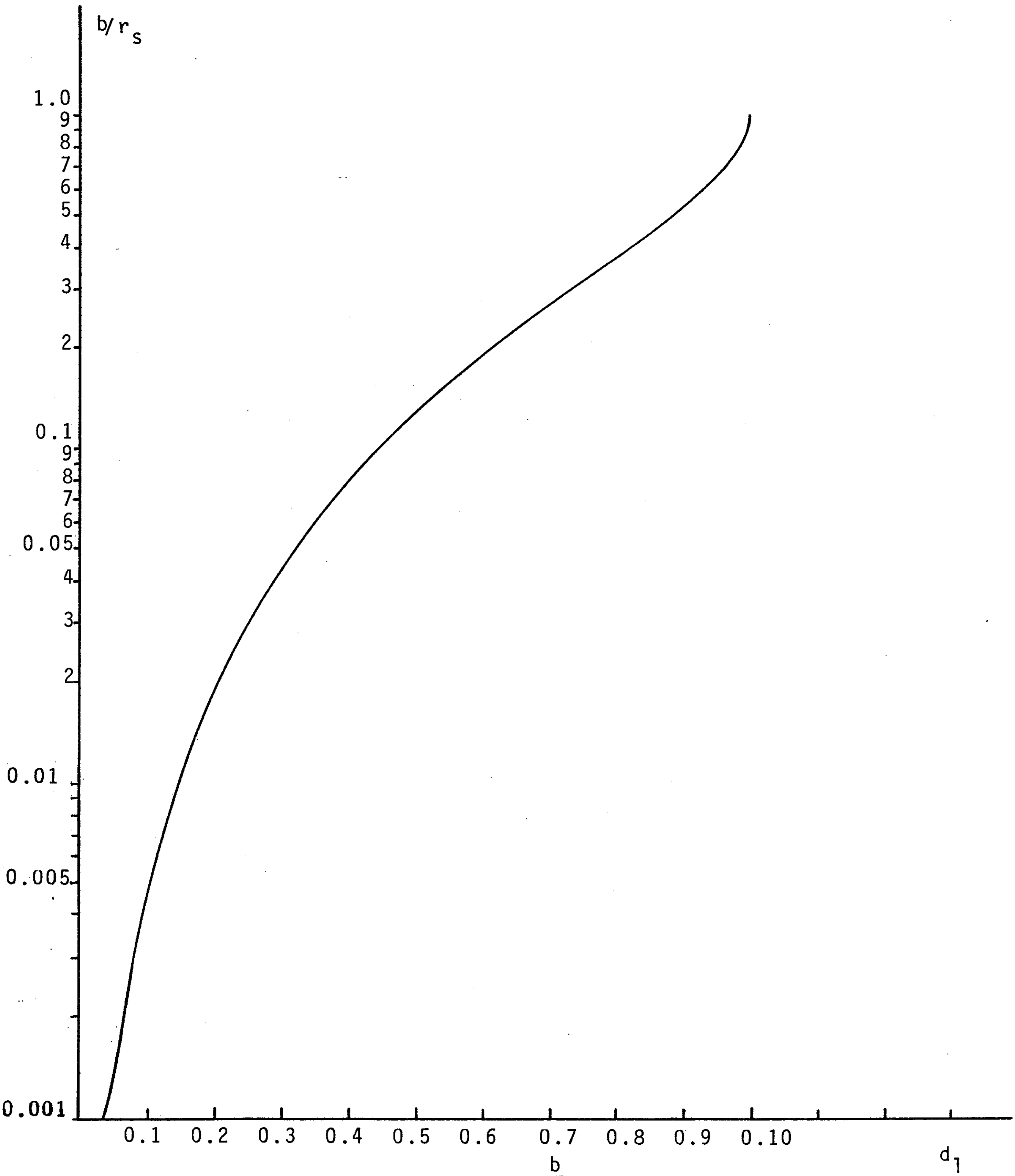

Figure 30 - Variation of the Ratio $\frac{b}{r_s}$ Versus the Ratio d_1/r_s

shielding failure mechanism) and as a result of strokes to the tower and/or shielding wire (the backflash mechanism).

The shielding failure mechanism predominates when large shielding (protective) angles are associated with high towers and low tower footing resistance to ground. The backflashover mechanism predominates when high tower footing resistance is associated with low tower heights and low insulation levels. Accordingly, the shielding angle Θ_s is reduced to a negative value, resulting in elimination of the phase conductor exposure arc Figure 31.

Again, referring to Figure 28, which shows an ineffectively shielded transmission line, the following relations may be found:

$\Theta_1 > \Theta_2$, which results in exposure arc (3-4)

$$\Theta_1 = \Theta_s + B \quad \text{and} \tag{85}$$

$$\Theta_2 = \sin^{-1}\left[1 - \bar{y}/r_s\right] \tag{86}$$

Thus, by analyzing Figure 31, for effectively shielded transmission lines the following relations are found:

$$\Theta_s = - B - \arc\sin\left(\bar{y}/r_s - 1\right) \tag{87}$$

$$B = \arc\sin\left(\frac{a}{2r_s}\right) \tag{88}$$

Equations 87 and 88 are plotted in Figure 32, from which it can be seen that the shielding angle Θ_s decreases as the ratio $\frac{\bar{y}}{r_s}$ increases. That is, for effectively shielded transmission lines, smaller shielding angles should be associated with higher towers.

2.12 PROPOSED DESIGN PROCEDURE

1. Determine the surge impedance of the phase conductor with

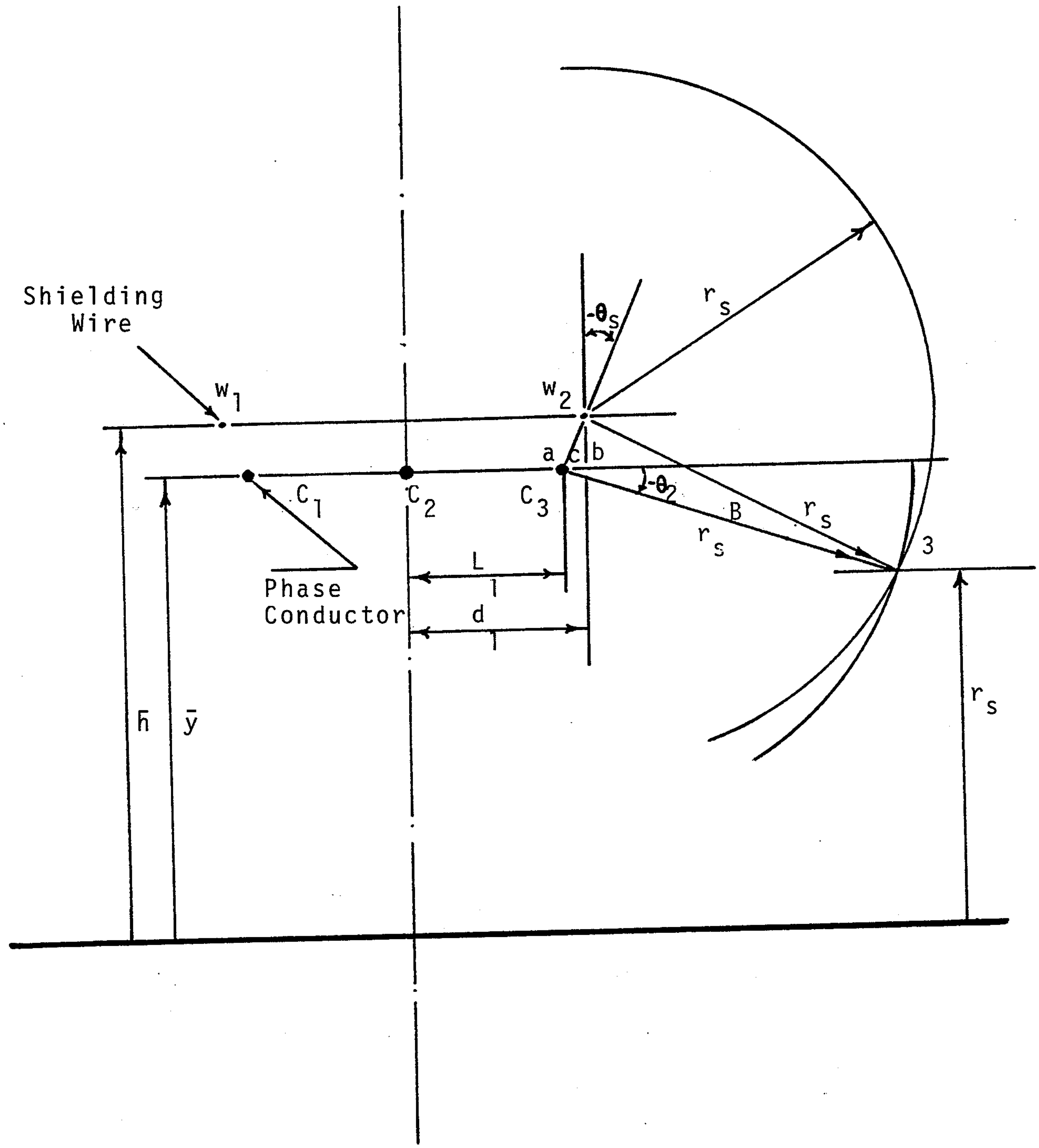

Figure 31 - Geometry of Effective Shielding of the Outer phase Conductors.[18]

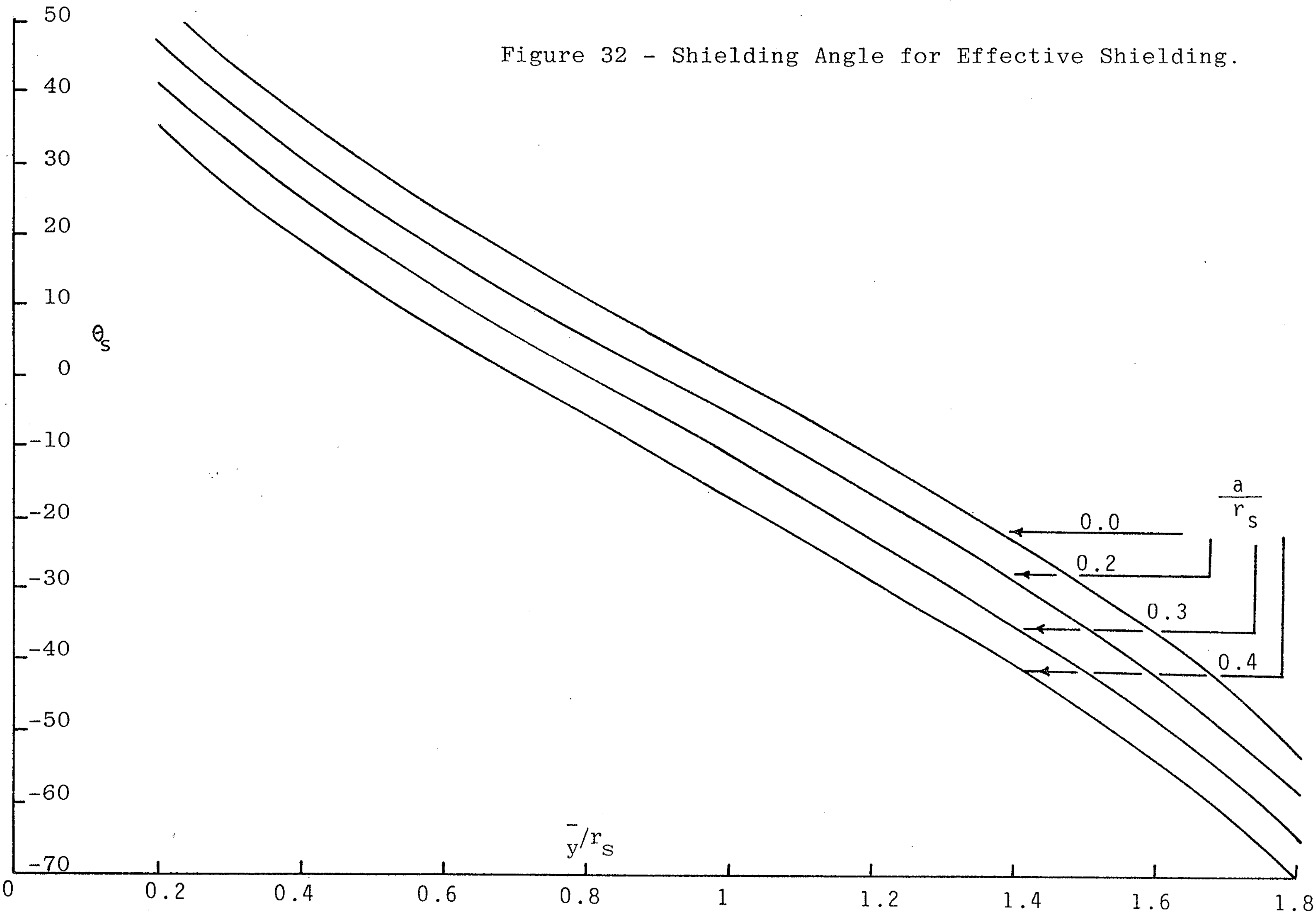

Figure 32 - Shielding Angle for Effective Shielding.

ground return, using Equation 66

$$Z = 60 \ln \frac{2\bar{y}}{r} \quad \text{Ohm} \tag{66}$$

2. Determine the critical lightning stroke current to the phase conductors, which may cause insulation flashover, where

$$I_s = \frac{BIL}{Z/2} \quad \text{in KA.}$$

3. Determine the critical prospective stroke current to zero ground resistance, I_{oc}

$$I_{oc} = 1.1\ I_s \quad \text{in KA.}$$

4. Determine the minimum strike distance at which the insulation is flashed over, according to the critical lightning stroke current This can be determined from $r_s = 6.7\ I_{oc}^{0.8}$ in meters

where I_{oc} in KA.

or from Figure 17.

5. Once the strike distance r_s is determined, the ratio $\frac{d_1}{r_s}$ can be assumed within the range proposed, that is, $0 < \frac{d_1}{r_s} < 1$.

6. From Figure 30 and by entering the value of $\frac{d_1}{r_s}$, the ratio $\frac{b}{r_s}$ and therefore the height **b** of the shielding wire with respect to the centre phase conductor can be obtained.

7. If the proposed average height of the phase conductor, $\bar{y}$, is known, then the ratio $\frac{\bar{y}}{r_s}$ can be determined.

8. The ratio $\frac{a}{2r_s}$ can be assumed to locate the proper curve in

Figure 32. Then, by entering the value $\frac{\bar{y}}{r_s}$ into the same figure, the shielding angle Θ_s can be obtained.

9. Step number 8 will determine the location of the outer phase conductor with respect to the shielding wires, so as to achieve effectively shielded transmission lines. Also, it will determine the phase-to-phase spacings. However, if the obtained spacings and heights do not satisfy the safety requirements, then the ratios d_1/r_s and $a/2r_s$ would be repeated using different values.

10. Other mechanical requirements such as phase conductor swing, ice loading, etc., should be taken into consideration in determining the clearance requirements.

CHAPTER III

TRANSMISSION LINE PROTECTION BY MEANS OF GROUNDING SYSTEMS

As previously indicated, the lightning mechanism has been classified as:

a) Direct stroke to phase conductors, resulting in shielding failure;

b) stroke to tower or shielding wire, resulting in backflash-over; and

c) stroke to nearby the transmission line, resulting in indirect stroke to the transmission system.

In this chapter the second mechanism, namely the back-flashover mechanism, will be investigated in connection with the grounding system of the transmission line. Also, it will be shown how the grounding system plays a key role in improving protection against lightning.

3.1 GROUNDING

The lightning performance of a transmission system is highly influenced by the grounding system. Furnishing an economically feasible and technically acceptable grounding system will substantially improve the lightning performance of the transmission system.

3.2 METHODS FOR REDUCING TOWER FOOTING RESISTANCE[23-30]

The current trend in reducing tower footing resistance is to increase the soil area in contact with the tower base. Thus, for high soil resistivity, where it is almost impossible to achieve an economical grounding resistance, it is customary to drive grounding rods into the earth, vertically or horizontally in the radial directions, as a counterpoise to the line conductors.[32] Normally, tower footing resistance is expressed as the measured 60-cycle value.[30] However, line performance during such disturbances depends on the impulse value of the tower footing resistance.[3,30]

The value of the impulse resistance depends on a number of factors, such as soil resistivity, critical breakdown gradient of the soil, magnitude of the surge current, and length and type of driven grounding rods or counterpoises. If long or continuous counterpoises are used because the soil resistivity is high, the initial impulse resistance is the surge impedance of the counterpoise, which is usually greater than the 60-cycle resistance. In soils of low or medium resistivity adequate grounding can usually be obtained by driven grounding rods. In this case, the impulse resistance is usually less than the 60-cycle value. For grounding resistance in the order of ten ohms or less, the impulse resistance is only slightly less than the 60-cycle value. Thus, in estimating the line performance, a tower footing resistance of ten ohms or less can be taken as the impulse value.

In the following section, the impulse characteristics of the grounding rods and the counterpoise will be studied.

3.3 IMPULSE CHARACTERISTICS OF GROUNDING RODS

Bellaschi[29,30] has concluded that grounding rod impulse resistance decreases as the impulse current increases. This reduction occurs because at a critical current, a voltage gradient is attained at the rod surface, causing the soil surrounding the rod to break down; this increases both the effective radius and the length of the rod. Thus, for each type of ground, there should be a critical current I_b at which the soil breakdown starts. The value of this current can be determined by plotting the ratio of the impulse resistance to the 60-cycle resistance against the natural log of impulse current. The intersection of the ratio $\frac{Rl}{Ro}$ equals one and the plotted curve gives the value of $\ln I_b$, This procedure is illustrated in Figure 33 for a grounding rod in clay soil. On these bases the critical current of different soils can be calculated.

To study the impulse characteristics of rods imbedded in different soils, the relation between the ratio of the impulse resistance to the 60-cycle resistance and the impulse current has been plotted as shown in Figures 34 and 35. These figures are based on the determined values of the critical current I_b and the equations of "Appendices A and B"[27,30]

3.4 FACTORS AFFECTING THE IMPULSE CHARACTERISTICS OF THE GROUNDING RODS.[30]

3.4.1 IMPULSE CURRENT POLARITY

Bellaschi's experiments were conducted to study the effects of the impulse polarity on the impulse resistance of grounding rods, either singly or grouped in parallel. It has been concluded that the impulse polarity does not appreciably affect the impulse

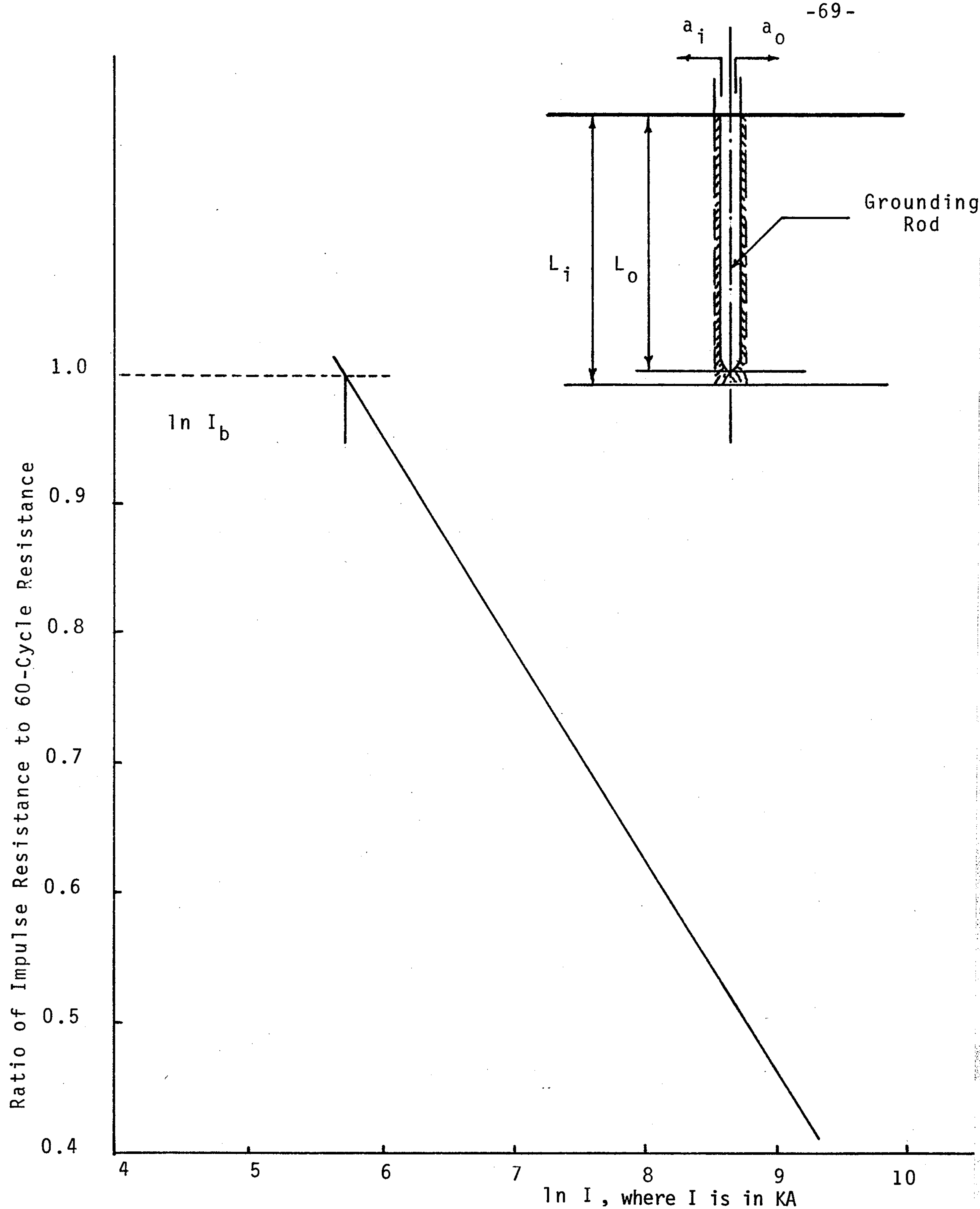

Figure 33 - Method of Determining the Impulse Characteristics of a Driven Grounding Rod.[30]

Figure 34 - Impulse Characteristics of a Grounding Rod in Clay Soil.[30]
(Reference 29)

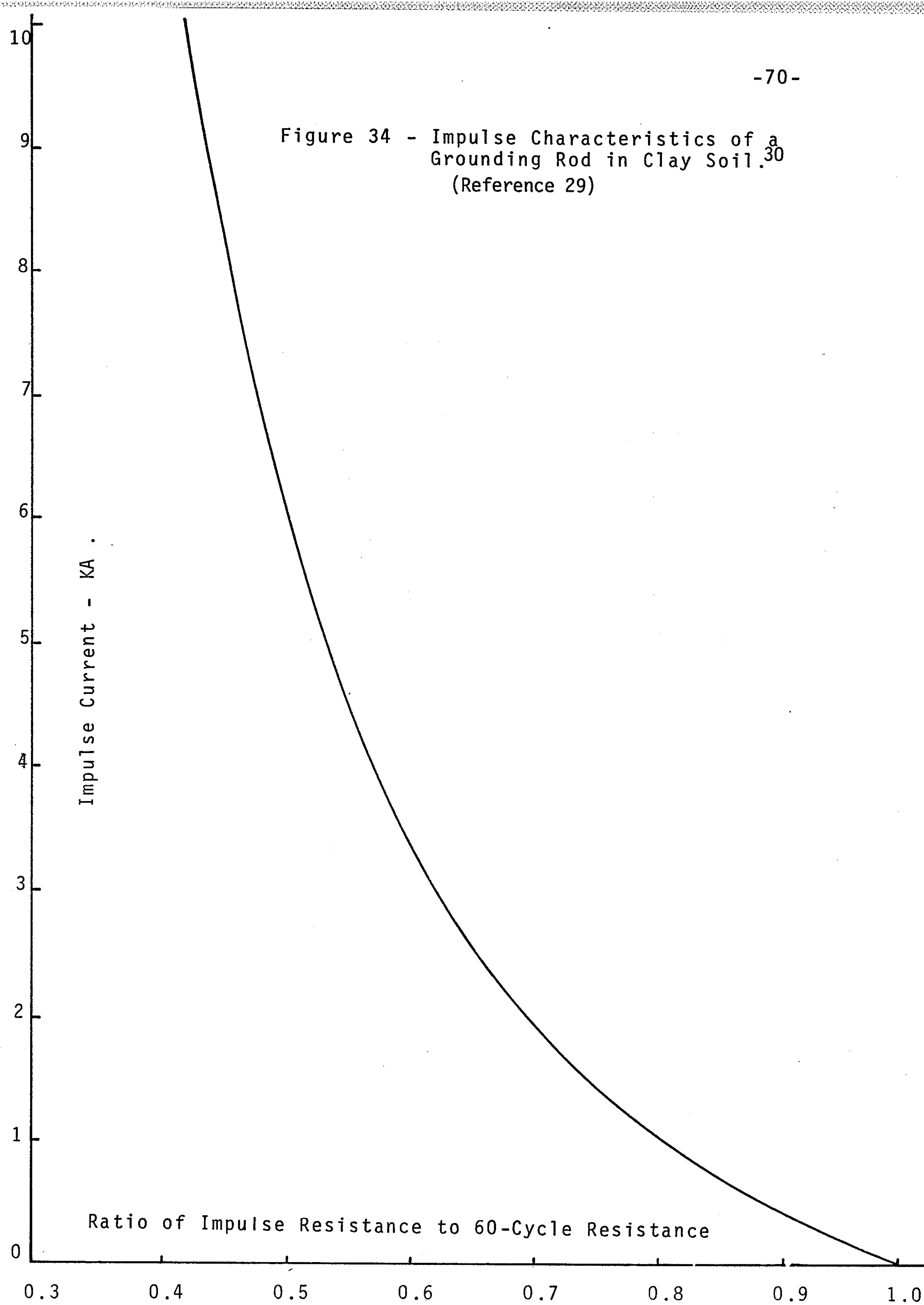

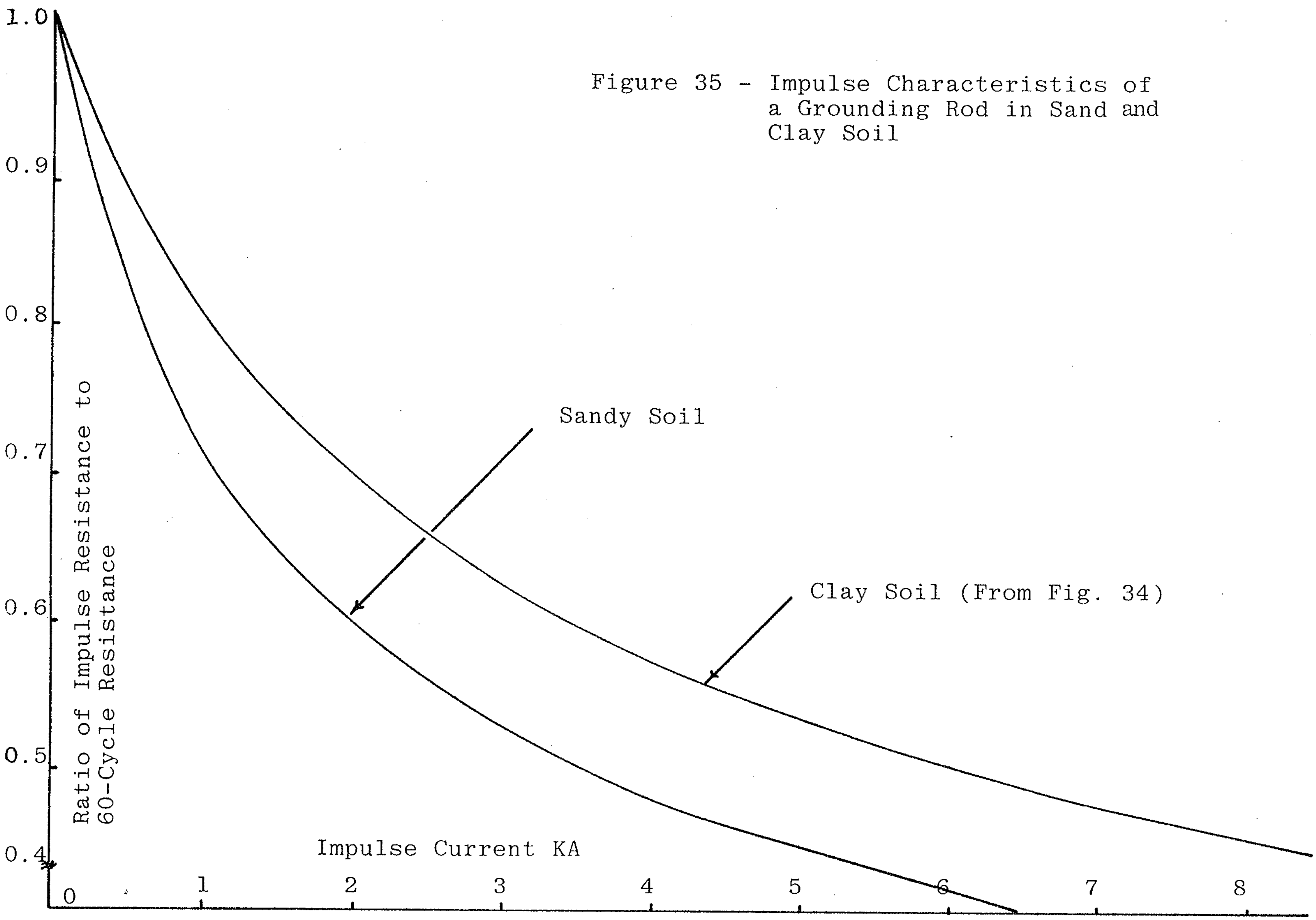

Figure 35 - Impulse Characteristics of a Grounding Rod in Sand and Clay Soil

resistance. Figure 36 shows the variation of the impulse resistance with impulse magnitudes and polarity, as recorded by Bellashi.

3.4.2 IMPULSE CURRENT

Figure 37 shows that at the start of the impulse the impulse resistance of the rod appears to be the same as the 60-cycle value, dropping with the rising current on the front and reaching a minimum at the time when the current is maximum. crest, and as the current recedes, the impulse resistance rises, apparently returning to the initial value.

3.4.3 SIZE OF GROUNDING ROD

According to B.H. Dwight,[27] the resistance to ground of a vertical grounding rod with length, ℓ, and radius, a, is

$$R = \frac{\rho}{2\pi\ell}\left(\ln\frac{4\ell}{a} - 1\right) \qquad (89)$$

Figure 38 is the plot of Equation 89, which shows the relation between the length of the grounding rod and the corresponding resistance for soil resistivity of 100 ohm meters. From the figure it can be seen that the radius of the grounding rod does not influence the resistance materially, whereas, the length is the most influential. For this reason, it is better either to use small but long rods or many small rods.

3.4.4. NUMBER AND SPACINGS OF GROUNDING RODS

Ground resistance can also be lowered by connecting driven grounding rods in parallel. If the spacing between rods is large

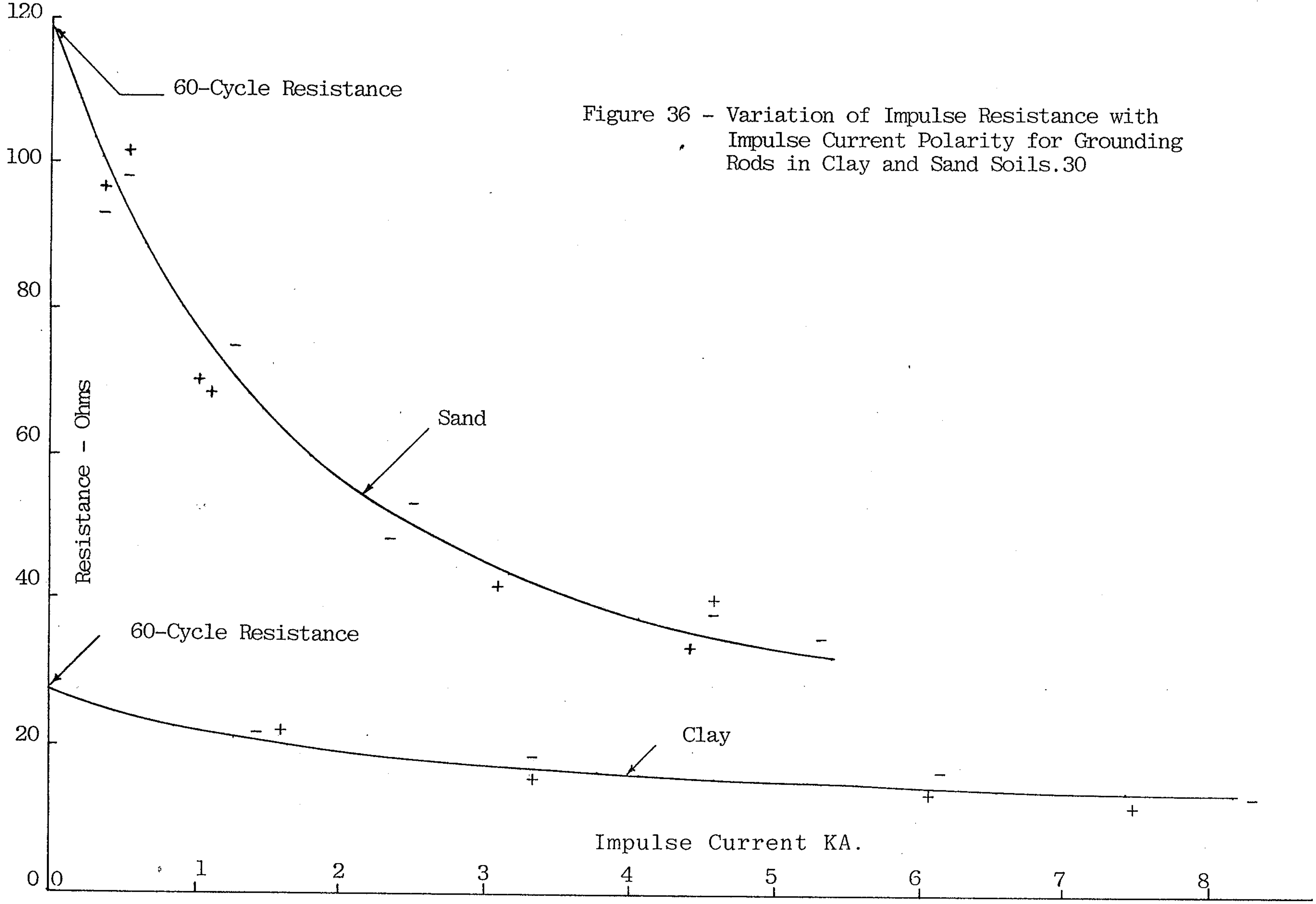

Figure 36 - Variation of Impulse Resistance with Impulse Current Polarity for Grounding Rods in Clay and Sand Soils.30

Figure 37 - Variation of Impulse Resistance During Impulse Current Discharge[30]

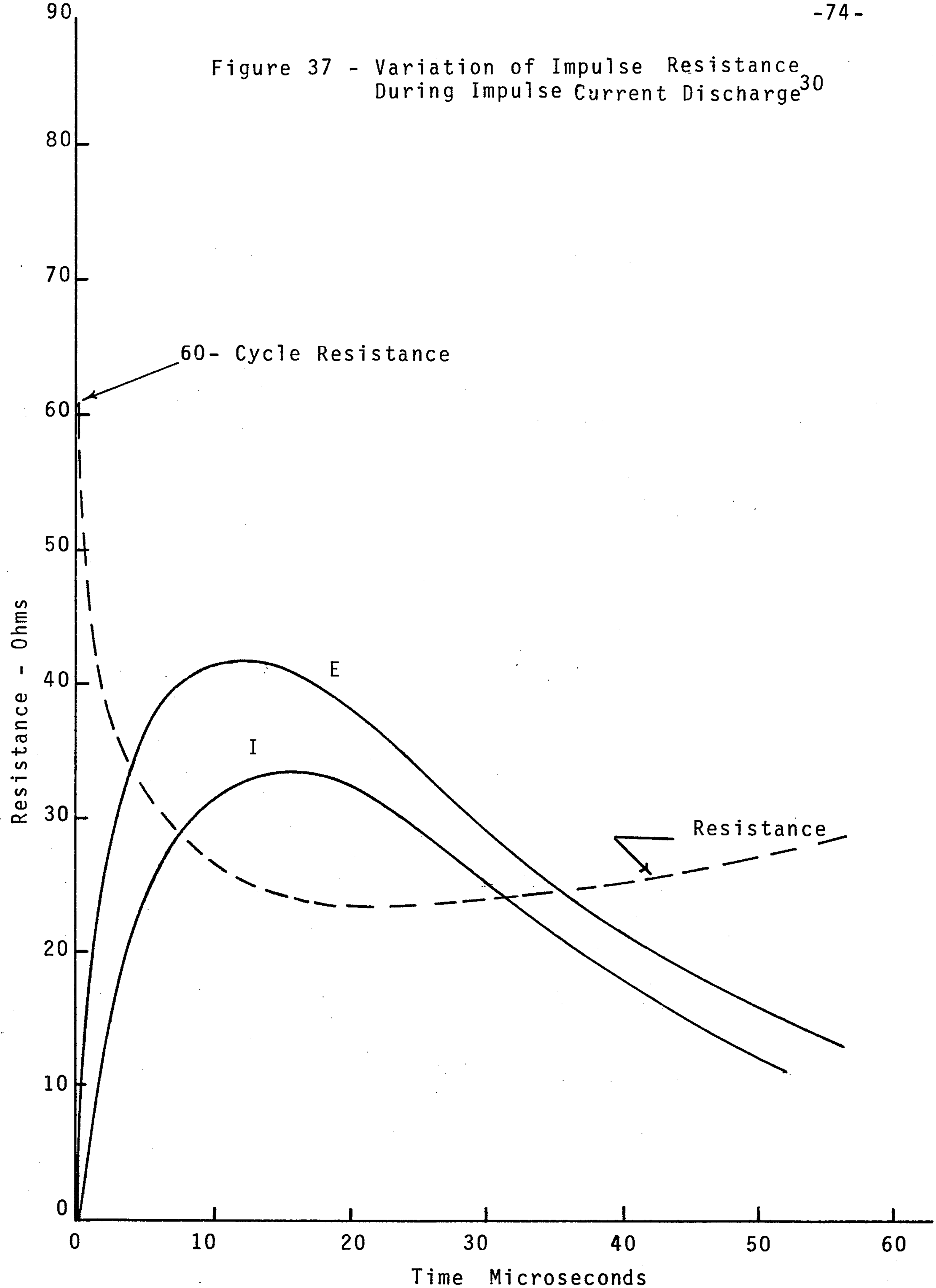

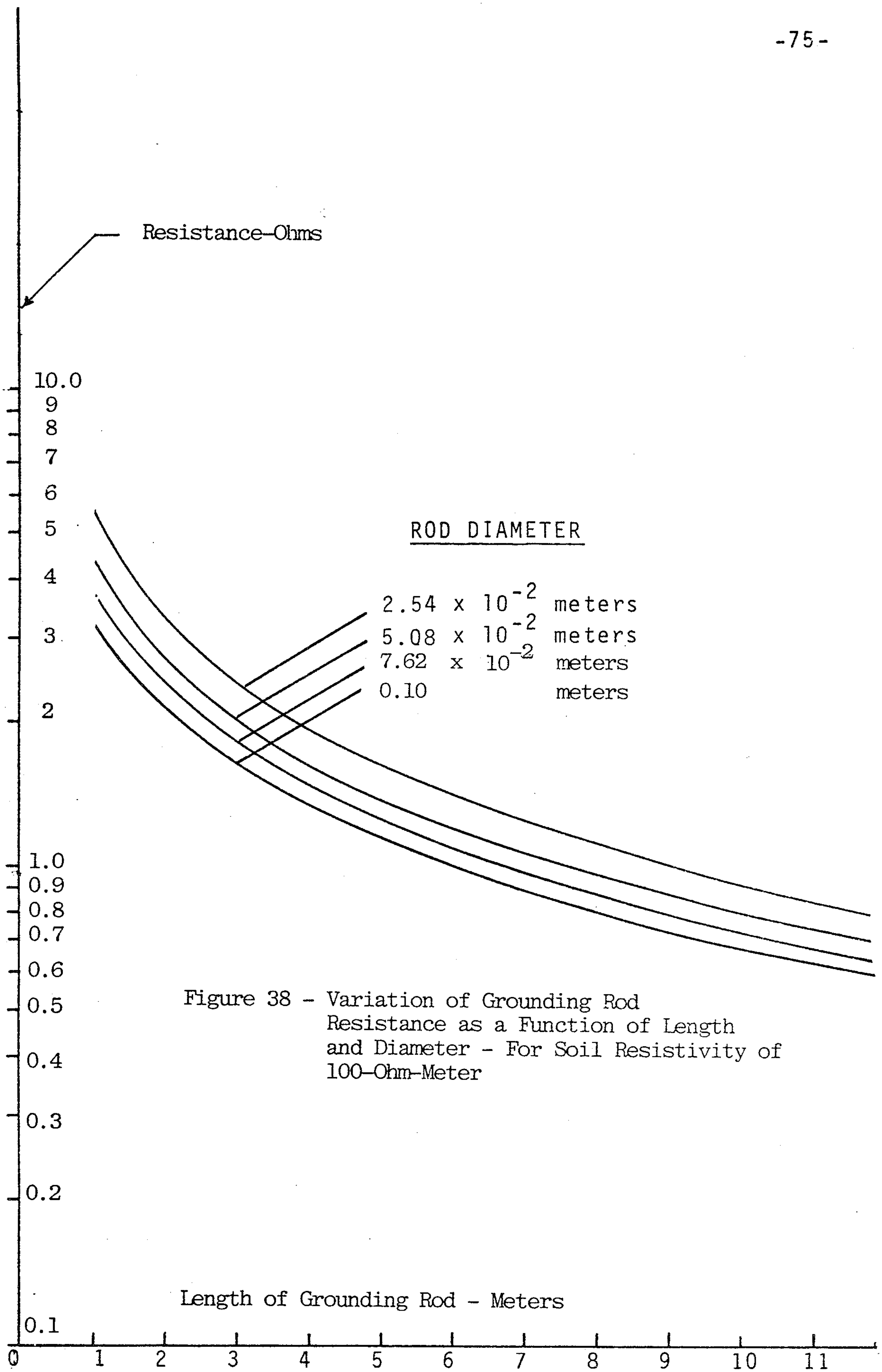

Figure 38 - Variation of Grounding Rod Resistance as a Function of Length and Diameter - For Soil Resistivity of 100-Ohm-Meter

compared to the length of the individual rods, the resistance will be reduced in proportion to the number of rods. If, however, the rods are close together, each rod will be in the intense of the electrical field of its neighbour, and the overall resistance becomes

$$R = \frac{\rho}{2\pi\ell} \ln\left(\frac{4\ell}{a}\right) \tag{90}$$

where a represents the radius of an equivalent rod. Figure 39 shows the ratio of conductivity of parallel grounding rods to that of isolated rods, as recorded by H.B. Dwight.[27]

3.4.5 SOIL RESISTIVITY

There are two properties of soil which in large measure determine the impulse characteristics of grounding rods driven into it: the resistivity, which determines the gradient for a given current density, and the critical gradient at which the soil breaks down. The influence of soil resistivity on the impulse characteristics of grounds is illustrated in Figure 40.

3.5 THE COUNTERPOISE

The counterpoise is a practical means of reducing the resistance by increasing the area of earth in contact with the grounding system. It can be connected and run parallel to, or at angles to, the line conductors. Figure 41 shows several arrangements of counterpoise connections.[3,25]

3.5.1 FACTORS AFFECTING THE COUNTERPOISE FUNCTION

Several factors must be considered in designing the counterpoise.

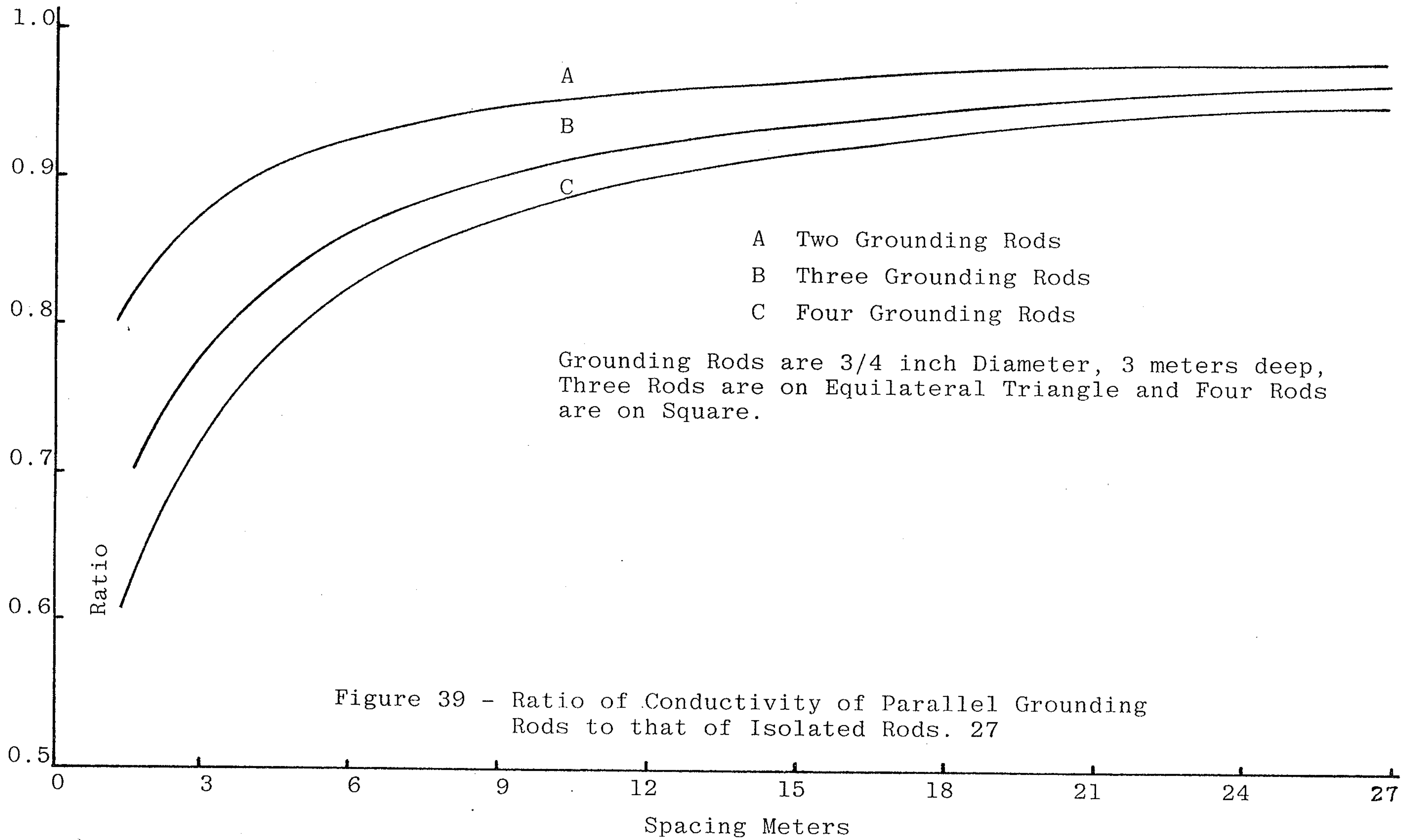

Figure 39 - Ratio of Conductivity of Parallel Grounding Rods to that of Isolated Rods. 27

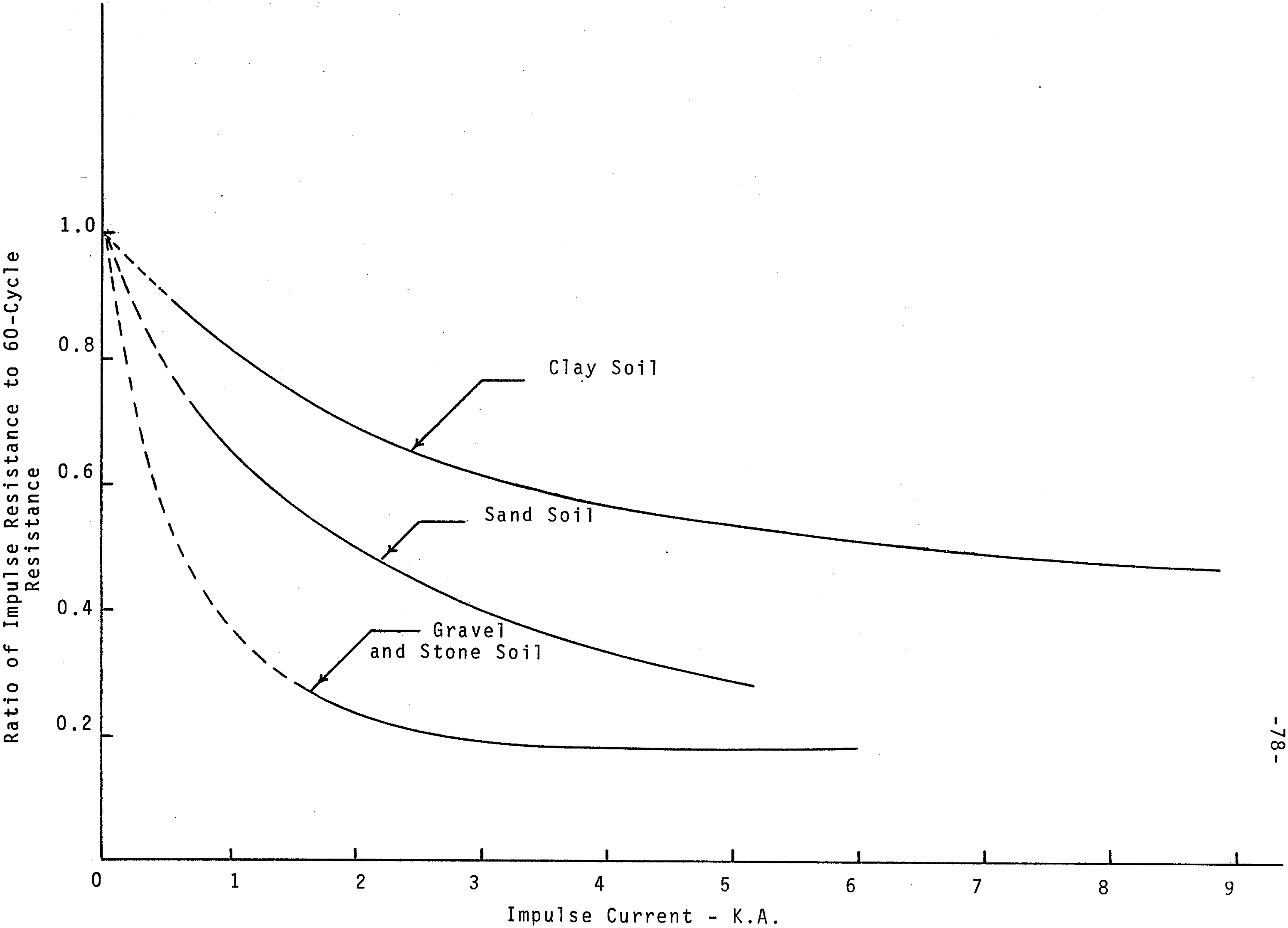

Figure 40 - Effect of Soil Resistivity on the Impulse Characteristics of Grounding Rods.[30]

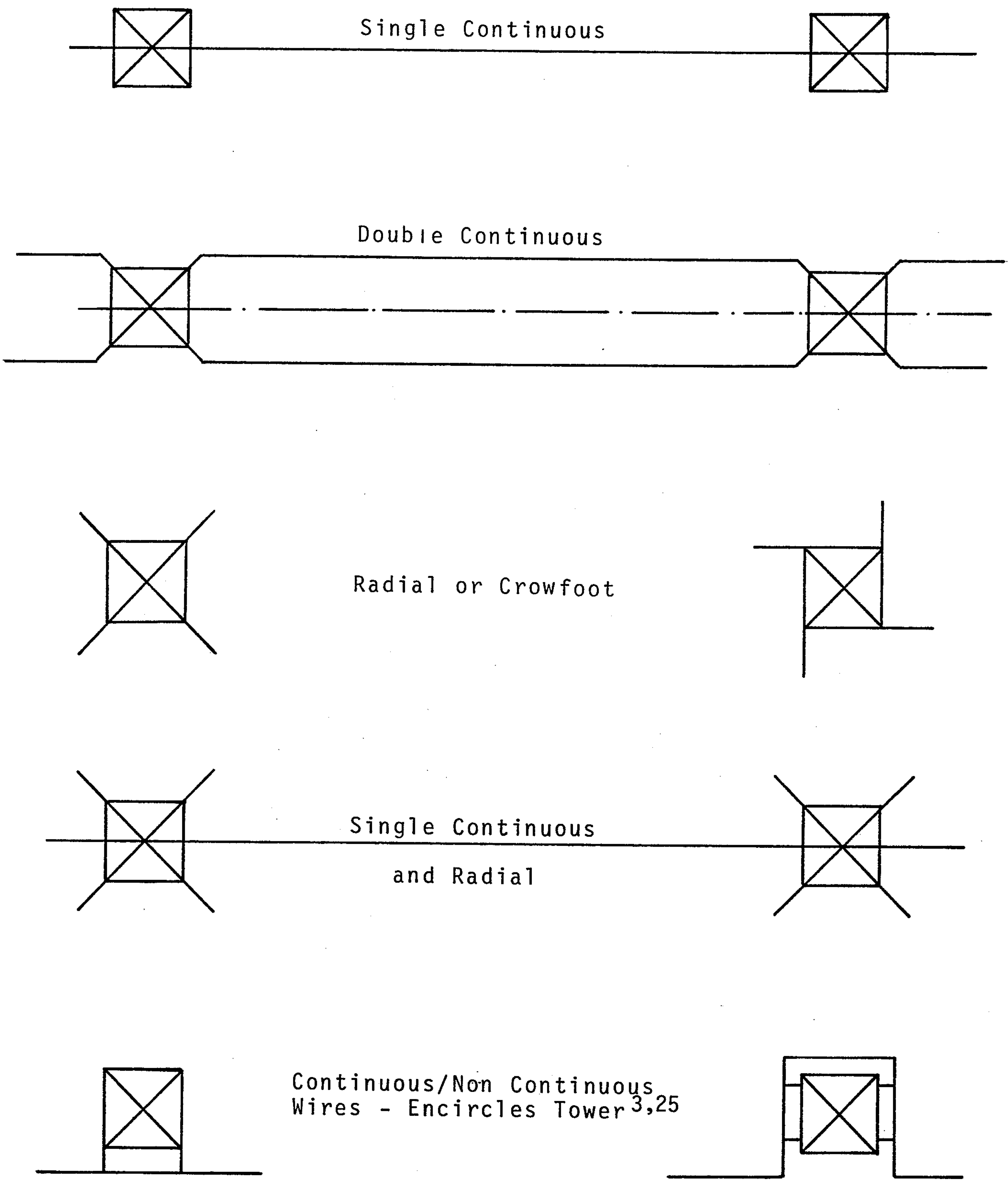

Figure 41 - Illustration of Practical Application of Counterpoise.[3,25]

A) The initial surge impedance,

B) the final leakage resistance,

C) the transition from the initial to the final impedance, and

D) the coupling with the shielding wires and line conductors.

Considering the counterpoise as a simple single conductor transmission line of length l, with constants G, L and C, negligible resistance R per unit length, and open-circuited at the far end, Bewely[6] has concluded that the impedance of such a wire is not constant, but is a varying factor which starts with initial surge impedance

$$Zc(o) = \sqrt{L/C} \tag{91}$$

and gradually subsides in an exponential fashion to the final leakage resistance

$$Zc(\infty) = \frac{1}{G\ell} \tag{92}$$

Furthermore, it has been established from the test that the surge on the counterpoise is predominantly a wave travelling at only about one-third the velocity of light. Thus, the transition from the initial value of surge impedance of the counterpoise to its final leakage resistance takes place at

$$\text{time } t = \frac{2\ell}{v} = 6 \text{ (length in thousands of feet)} \tag{93}$$

Consequently, the performance of the counterpoise is governed by the counterpoise length and to some extent by the soil resistivity.

Practically, it is desirable to utilize short pieces of counterpoise (60-90 meters length), instead of one long counterpoise. This results in a lower initial surge impedance of the counterpoise, consequently lowering the tower footing resistance Figure 42 .

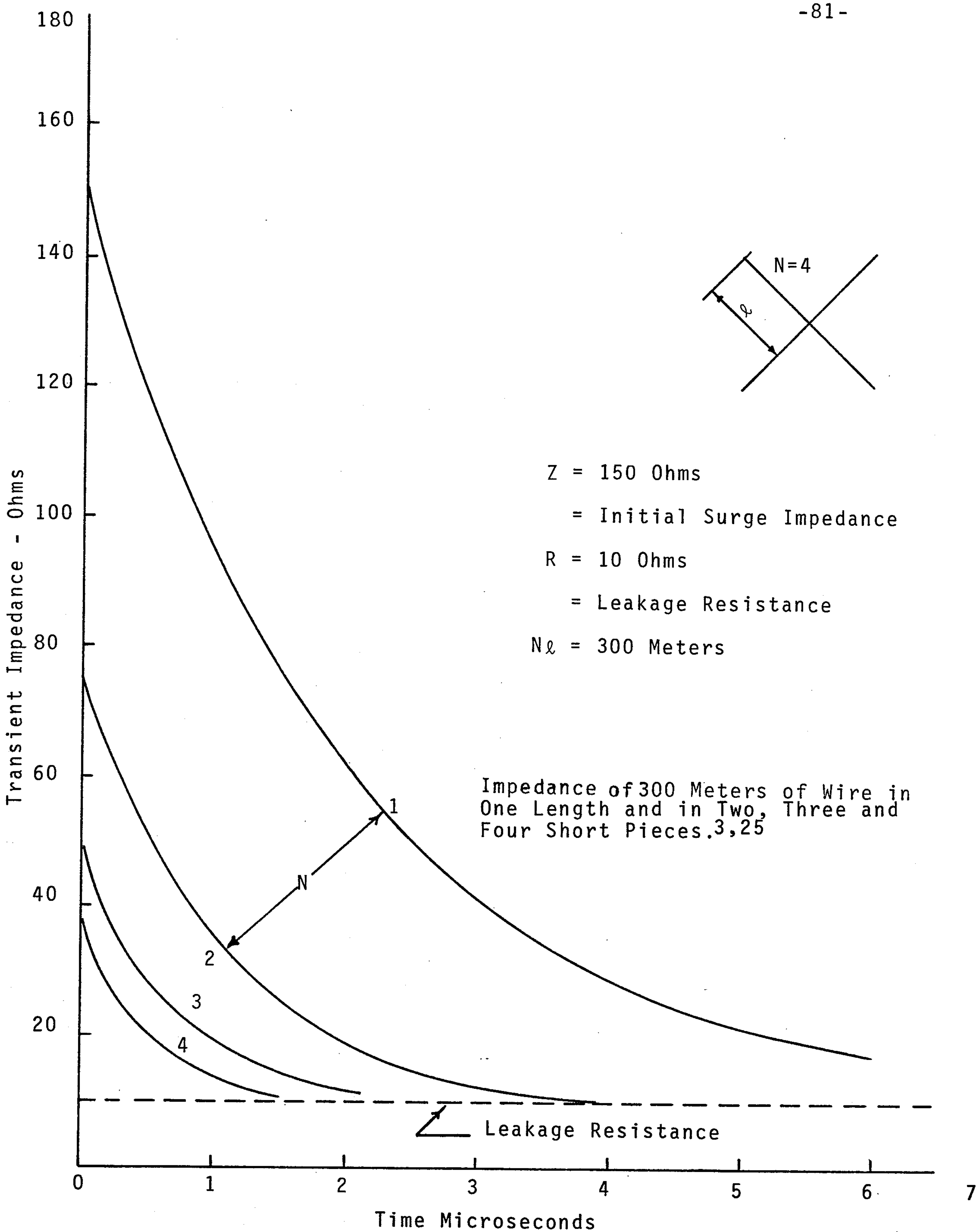

Figure 42 - Effect of the Number of Wires on Counterpoise Impedance.

The one important point in applying this rule is to assure that the leakage resistance of the counterpoise is lower than its initial surge impedance, otherwise positive reflections result, and the potential at the top of the tower increased rather than decreased.

Sunde[26] has concluded that the resistance to ground of a single wire buried in the earth is

$$R = \frac{\rho}{\pi \ell} \left[\ln\left(\frac{2\ell}{\sqrt{4ad}} \right) - 1 \right] \text{ ohms} \tag{94}$$

where

ℓ = length of wire in meters

d = burial depth of wire in meters

a = radius of wire in meters

ρ = soil resistivity in ohm-meter.

The above equation is plotted in Figure 43 for two different depths, 0.25 meters and 0.5 meters. As it can be seen from the figure, the depth factor does not materially affect the counterpoise resistance to ground.

The above discussion has shown that grounding rods and counterpoise play key roles in reducing tower footing resistance. This reduction is important in minimizing the transmission line backflashover events and consequently improving the lightning performance of the transmission system.

Thus far, illustration of the tower footing resistance reduction has been presented. The following section deals with the backflashover mechanism of the transmission system and how it can be minimized by a proper grounding system.

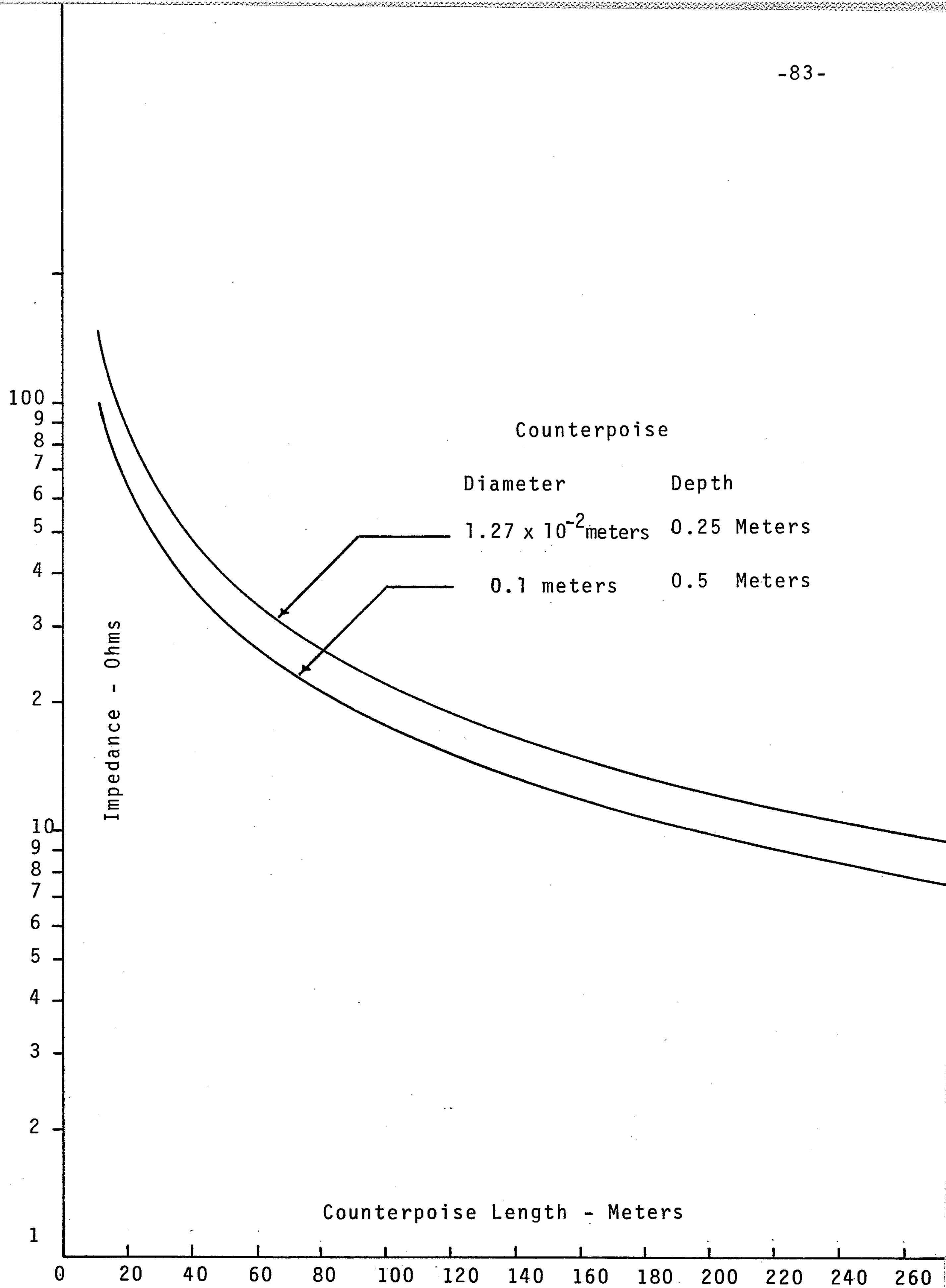

Figure 43 - Impedance of Counterpoise as a Function of Length, Diameter and Depth.[24]

3.6 BACKFLASHOVER

If tower grounding is inadequate, strokes which the shielding wire intercepts may produce sufficient voltage to flashover insulators, resulting in transmission line outage. According to Bewley,[6] if any tower or shielding wire(s) of a transmission system is hit by a lightning stroke, the incident wave will be reflected and refracted as shown in Figure 44. However, if the tower surge impedance is neglected, and the grounding system is considered an effective impedance, the relationship between the reflected and refracted waves is

$$e_1' = \frac{-\ Z_{11}}{2R + Z_{11}} \qquad e_1 = ae_1 \tag{95}$$

and

$$e_1'' = e_1 + e_1' = \frac{2R \cdot e_1}{2R + Z_{11}} = be_1 \tag{96}$$

$$e_1 + e_1' = e_1''$$

where (97)

e_1 = the initial wave on the shielding wire

e_1' = the reflected wave on the shielding wire,

e_1'' = the refracted wave on the shielding wire,

Z_{11} = Self Surge impedance of the shielding wire or the equivalent shielding wires, and

R = tower footing resistance.

Waves arriving back at the first stricken tower from the reflection points are further reflected as

$$e_1' = \frac{2ZR - Z_{11}\ (R+Z)}{2ZR + Z_{11}\ (R+Z)} \qquad e_1 \tag{98}$$

$$e_1' = \propto e_1 \tag{99}$$

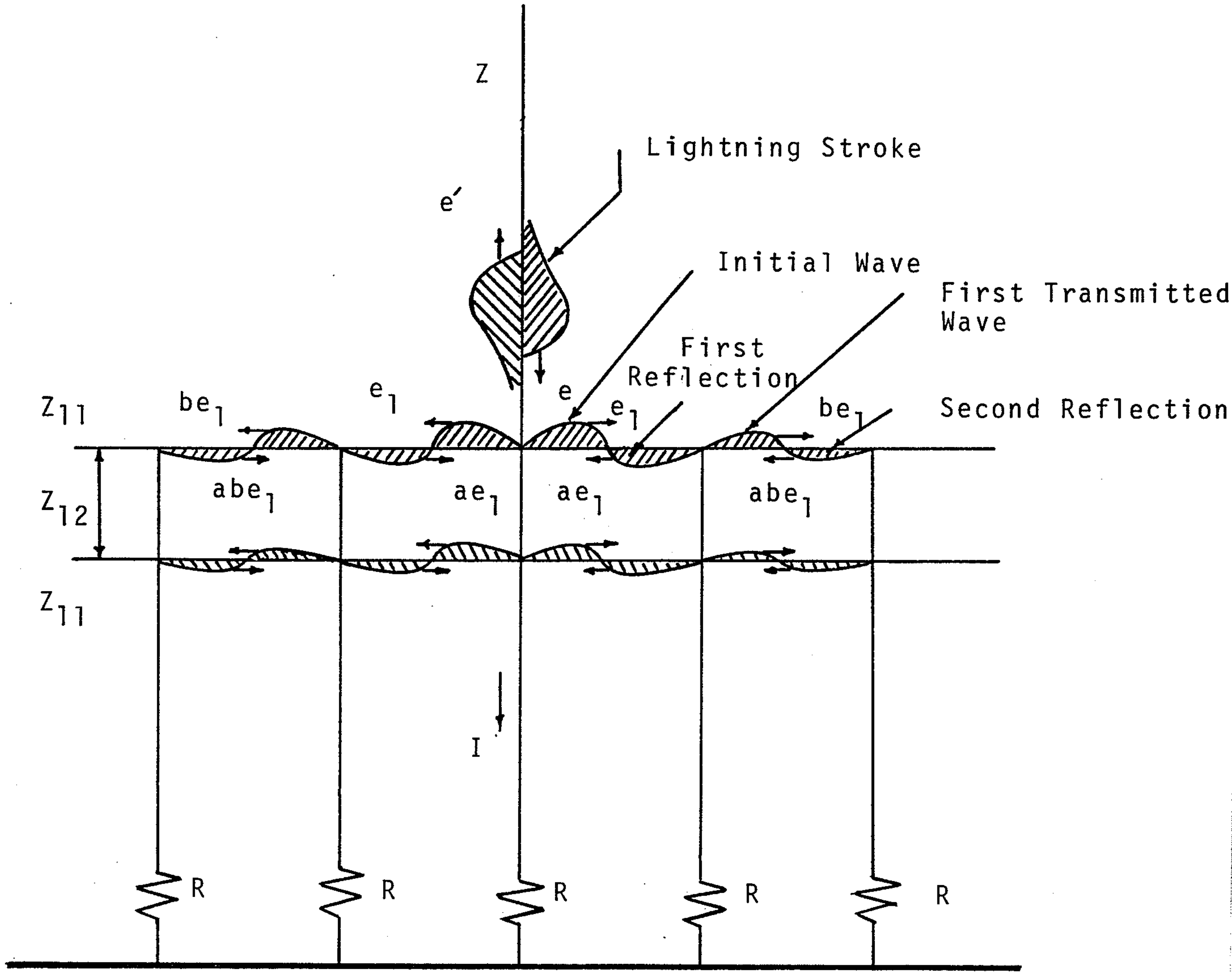

Figure 44 - Illustration of Reflected and Refracted Waves Travelling on the Shielding Wires and Phase Conductors.[6]

Equation 98 follows from equation 95 upon superimposing the two waves reaching tower 1 simultaneously from both right and left, regarding R and Z in parallel where Z represents the stroke surge impedance. Also, equation 98 can be considered a result of assuming the lightning stroke surge impedance is 2Z and the first tower footing resistance is 2R with the transmission line extending in one direction only from tower 1.

Furthermore, the potential wave passing from the lightning stroke to the shielding wire is e_1. When this wave reaches tower 2, wave ae_1 is reflected back and wave be_1 is passed on. This phenomenon of wave reflection and refraction takes place at all towers except tower 1, where the reflection coefficient α is determined by Equation 98.

When the reflection and refraction coefficients are known, a lattice diagram showing the potential at any tower at any time can be constructed (Figure 45). The same procedure can be applied to the phase conductors and a similar lattice diagram can be constructed (Figure 46) where the reflected and refracted waves relations are:

$$e_2 + e_2' = e_2'' \qquad (100)$$

$$e_2' = \frac{-Z_{12}}{2R + Z_{11}} e_1 = ce_1 \qquad (101)$$

$$e_2'' = e_2 - \frac{Z_{12}}{2R + Z_{11}} e_1 \qquad (102)$$

Equations 101 and 102 give the reflected and refracted waves at all towers except tower 1, where the reflected wave is only

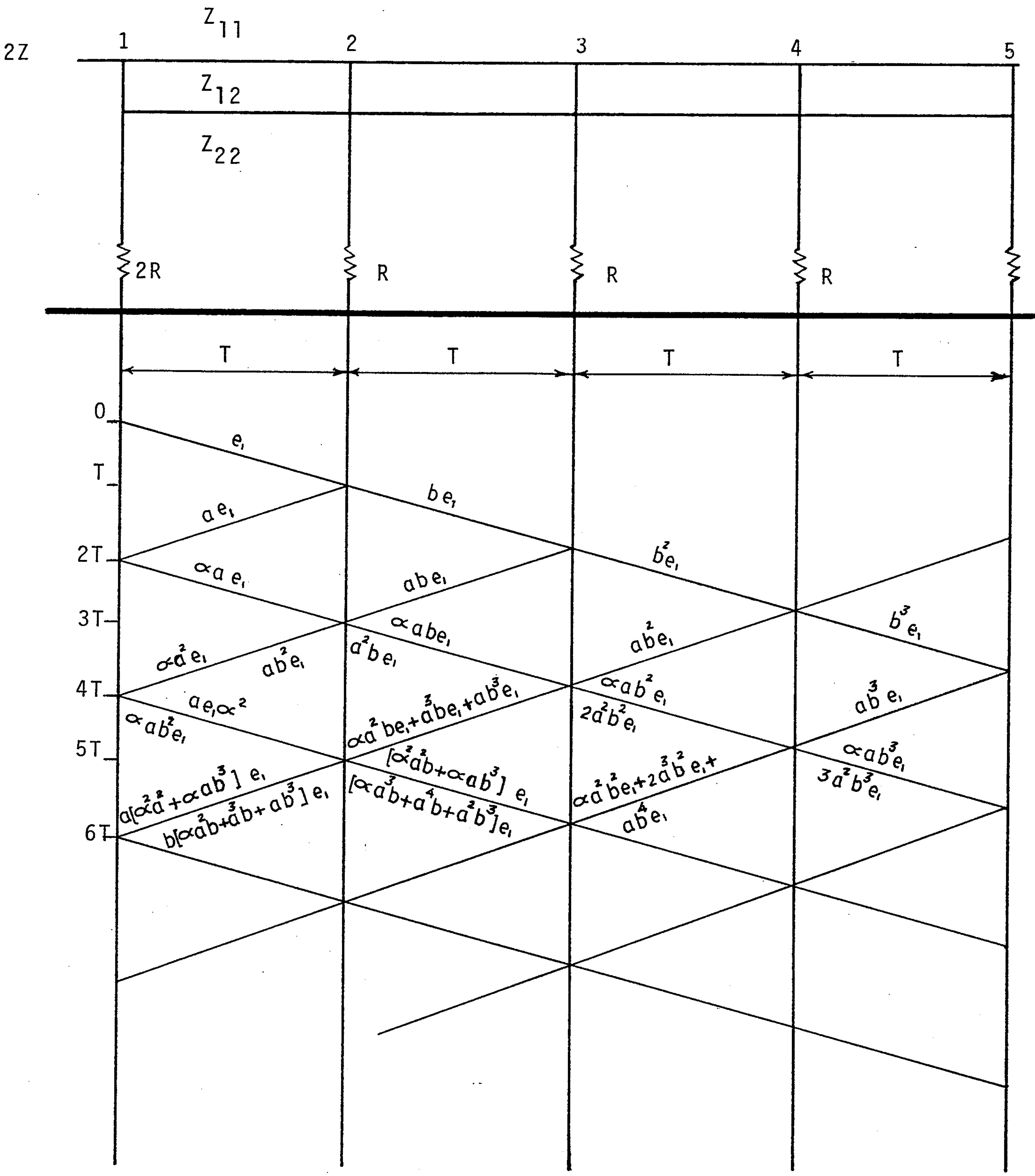

Figure 45 - Lattice Diagram of Voltage Wave Travelling on the Shielding Wires[6]

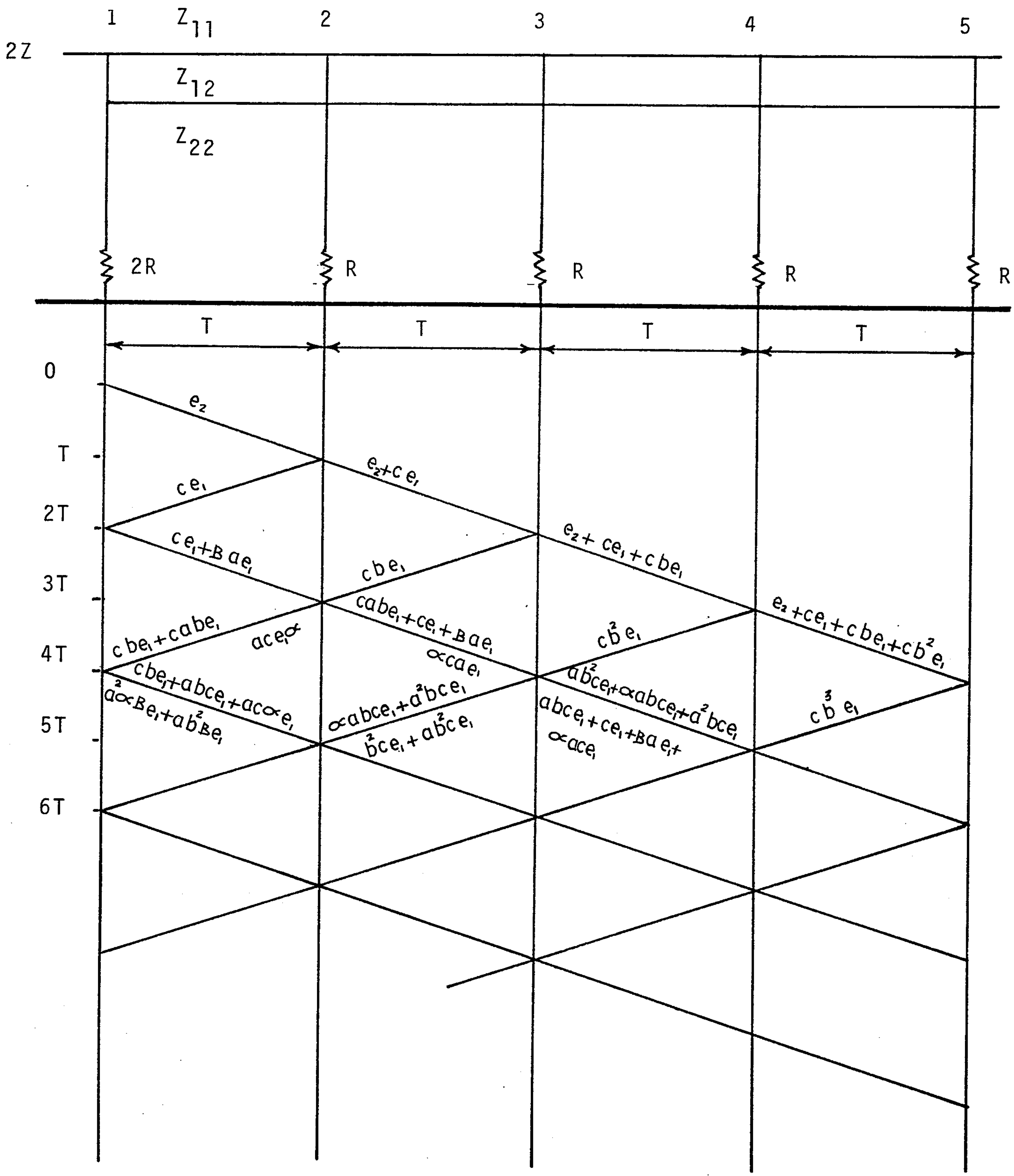

Figure 46 - Lattice Diagram of Voltage Wave Travelling on the Phase Conductors[6]

$$e_2' = e_2 - \frac{2Z_{12}\ (R+Z)}{2ZR + Z_{11}\ (Z+R)}\ e_1 \tag{103}$$

$$e_2' = e_2 - B\ e_1 \tag{104}$$

where $B = \dfrac{-\ 2Z_{12}\ (R+Z)}{2ZR + Z_{11}\ (Z+R)}$ (105)

Equations 95 to 105 have been taken from reference 6.

From the lattice diagrams for the shielding wire and phase conductor, the voltages as a function of time at any tower at any moment can be calculated.

The voltages of the shielding wire are as follows:

$$E_1 = e_1(t) + (a + \alpha a).e_1(t-2T) + (1+\alpha)\left[(\alpha a^2 + ab^2)\right] .e_1(t-4T) \tag{106}$$

$$E_2 = be_1(t-T) + \left[ab + a^2b + \alpha ab\right]\ e_1\ (t-3T) \tag{107}$$

$$E_3 = b^2e_1(t-2T) + \left[ab^2 + 2a^2b^2 + \alpha ab^2\right]\ e_1(t-4T) \tag{108}$$

and

$$E_4 = b^3e_1\ (t-3T) \tag{109}$$

Similarly, the voltages on the phase conductor are

$$E_1 = e_2(t) + \left[2C+Ba\right]\ e_1(t-2T) + \left[2bc + 2abc + 2\alpha ac + \alpha Ba^2 + Bab^2\right]\ e_1(t-4T) \tag{110}$$

$$E_2 = e_2(t-T) + ce_1(t-T) + \left[c + Ba + bc + abc + \alpha ac\right]\ e_1(t-3T) \tag{111}$$

$$E_3 = e_2(t-2T) + (c+bc)\ e_1\ (t-2T) + \left[b^2c + ab^2c + \alpha abc + a^2bc + abc + c + Ba + \alpha ac\right]\ e_1(t-4T) \tag{112}$$

and

$$E_4 = e_2(t-3T) + (c + bc + b^2c)\ .\ e_1(t-3T) \tag{113}$$

From the above equations and by considering the signs of the reflected and refracted waves, it can be seen that the voltage waves travelling on the shielding wires and phase conductors are considerably reduced by the effects of the grounding resistance of the transmission system. This conclusion can be drawn from Figures 47, 48 and 49, which show the relation between the potentials on the shielding wires and phase conductors and across the insulator as a function of tower footing resistance for several towers, as recorded from reference 6. It is thus evident that low tower footing resistance has the following beneficial results:

1. Reduced potentials on the shielding wire,
2. reduced potentials on the phase conductors,
3. reduced potentials across insulator strings, which minimizes backflashover events,
4. limitation of the disturbance to a few spans, and
5. short duration of dangerous voltages.

Figure 47 - Variation of Shielding Wire Potential With Tower Footing Resistance.[6]

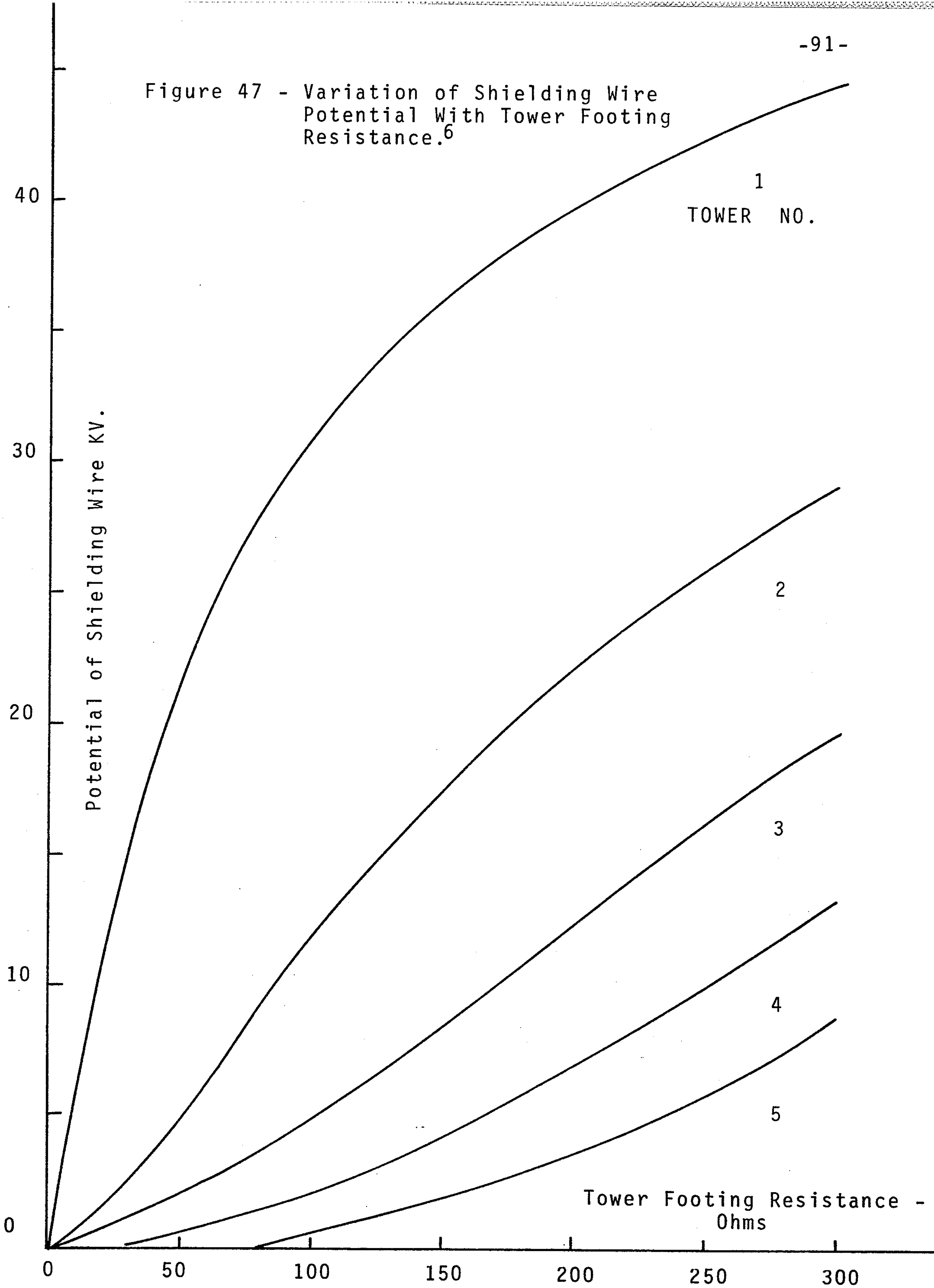

Figure 48 - Variation of Phase Conductor Potential With Tower Footing Resistance[6]

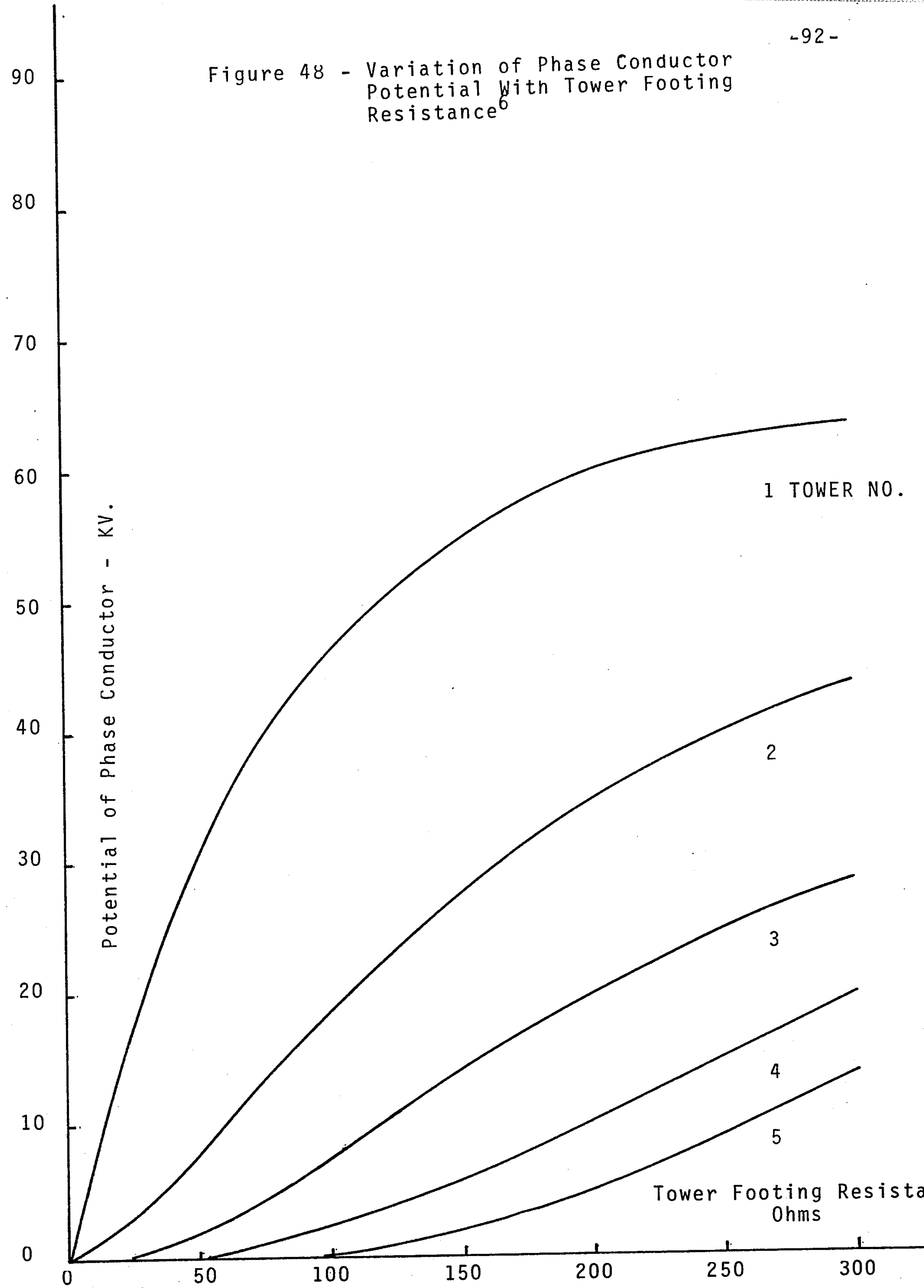

Figure 49 - Variation of the Potential Across Insulator String With Tower Footing Resistance[6]

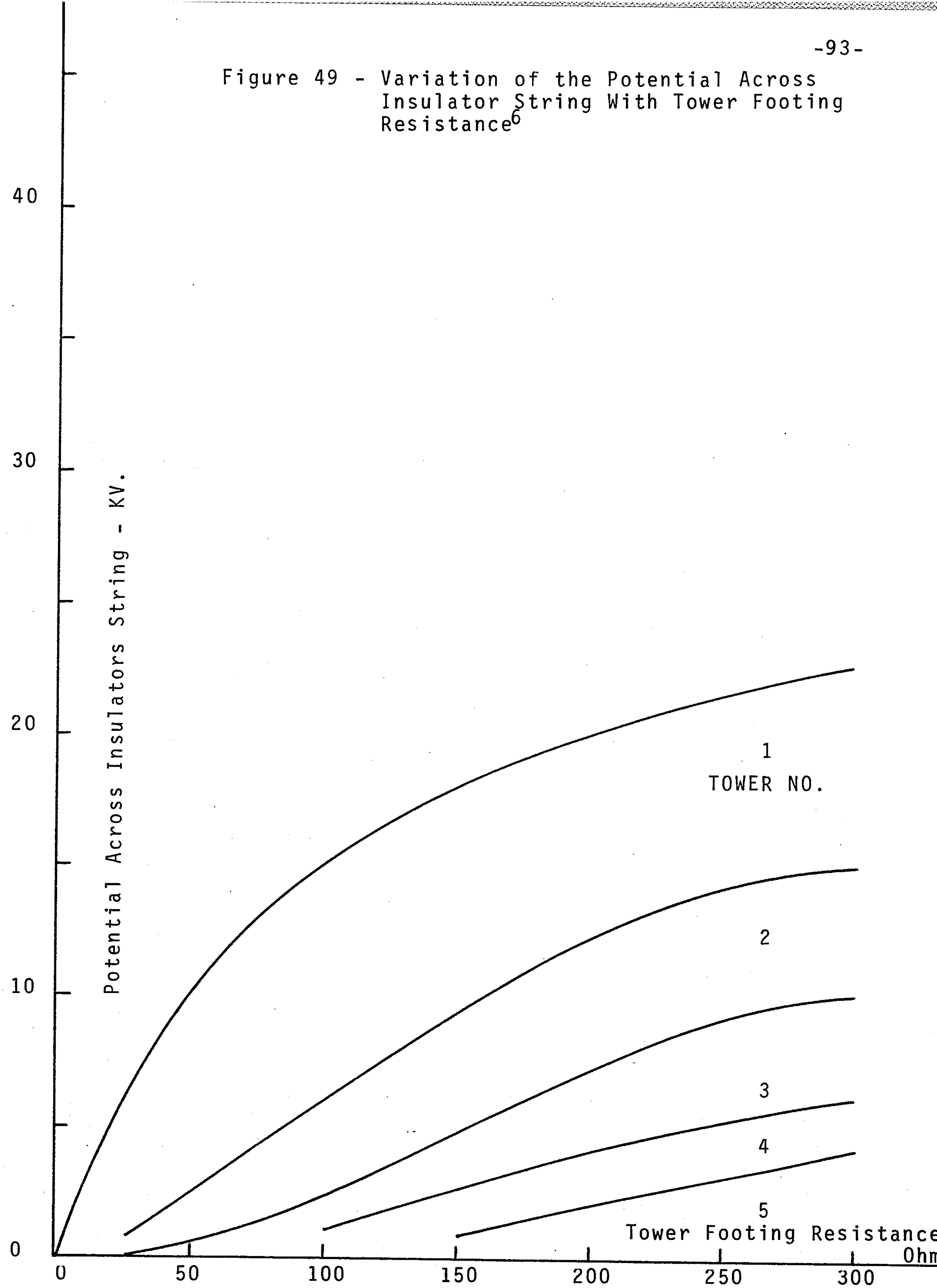

CHAPTER IV

SOIL RESISTIVITY INVESTIGATION

In the preceding chapter tower footing resistance has been reduced by utilizing grounding rods and/or counterpoise systems. In order to accomplish proper grounding, an investigation of the soil resistivity and the factors contributing to its variation should be undertaken.

4.1 FACTORS AFFECTING SOIL RESISTIVITY[28]

4.1.1 SOIL COMPOSITION

Because soil resistivity depends on the soil type, it varies with depth and with distance from a specific spot. Thus, investigation of soil resistivity along the route line should include at least a determination of the general soil composition, often to a reasonable depth by means of borings. Table I illustrates the average soil resistivity values according to soil type. These values of soil resistivity may be used if actual measurements of soil resistivity for a definite spot are not taken.

24
TABLE I

TYPE OF GROUND	RESISTIVITY IN OHM-METER
General Average	100
Sea Water	0.01 - 1.0
Swampy Ground	10 - 100
Dry Earth	1000
Pure Slate	10^7
Sandstone	10^8

For purposes of simplicity, soil resistivity is assumed to be homogeneous and the fault current uniformly distributed.

4.1.2 THE EFFECTS OF MOISTURE CONTENT AND TEMPERATURE ON SOIL RESISTIVITY

It has been found that soil resistivity is greatly influenced by the soil moisture content and by temperature. As can be seen from Figure 50, the higher the moisture content, the smaller the resistivity that can be obtained. It is also known that soil resistivity is much lower below the water level than above it. In frozen soil, as in the surface layer in winter, the resistivity is practically high. This is due to the fact that below $0^{o}C$ water in the soil begins[28] to freeze, introducing a tremendous increase in the temperature coefficient (negative value), such that as the temperature lowers, the resistivity rises enormously. At $20^{o}C$, the change in resistivity is about five percent per degree. Figure 51 shows the effects of temperature variation on the resistance of clay soil with 18.6 percent moisture content.

4.2 THE EFFECTS OF FAULT CURRENT[28]

Before proceeding with the topic of soil resistivity measurement, the penetration of the stroke current to earth and its effects will be investigated.

It was earlier assumed that soil is homogeneous and the penetrated current is uniformly distributed. Thus, for overhead lines, a ground-fault current initiated by the breakdown of an

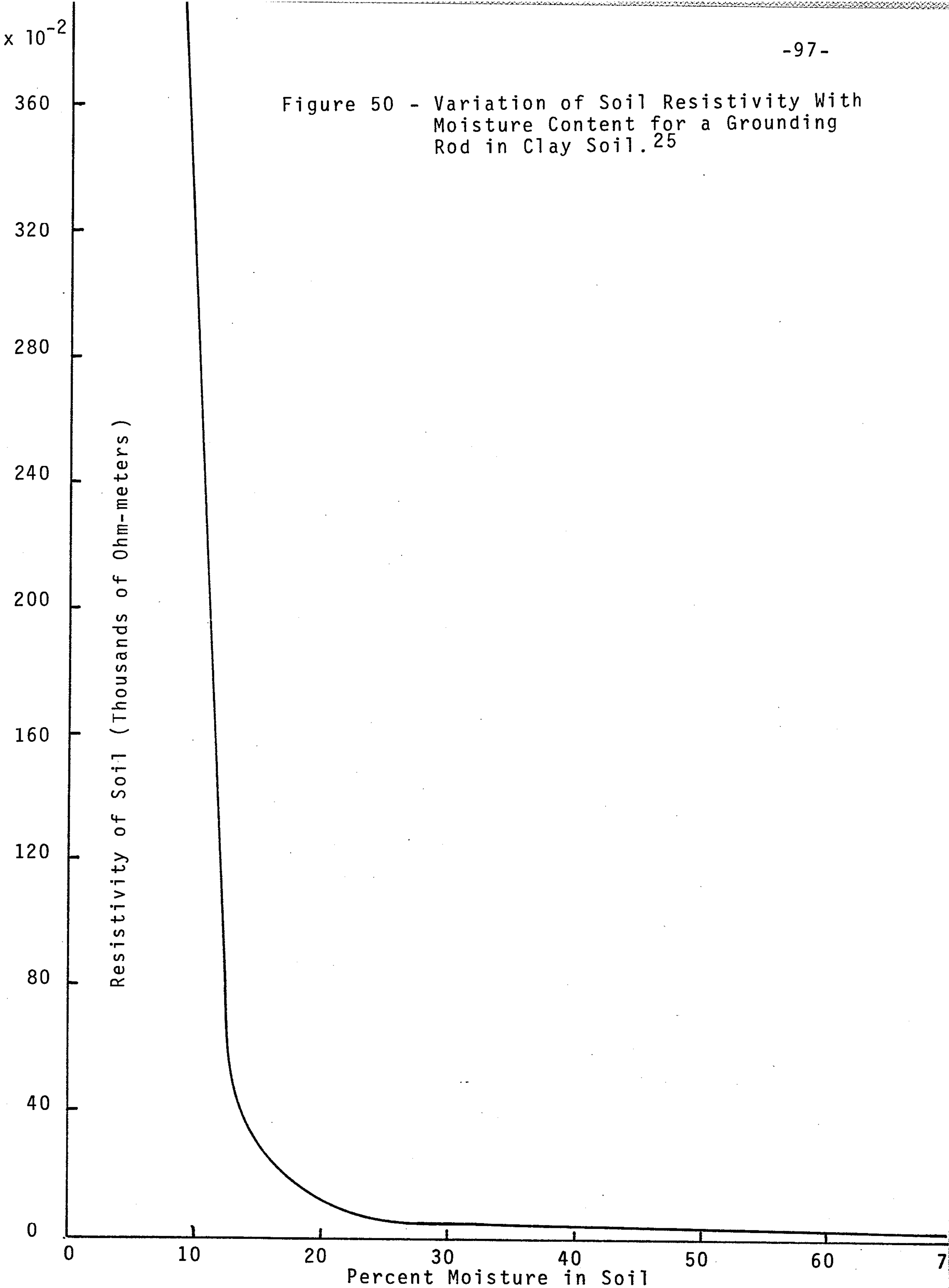

Figure 50 - Variation of Soil Resistivity With Moisture Content for a Grounding Rod in Clay Soil.[25]

Figure 51 - Variation of Soil Resistivity With Temperature for a Clay Soil Containing 18.6 Percent Moisture[25]

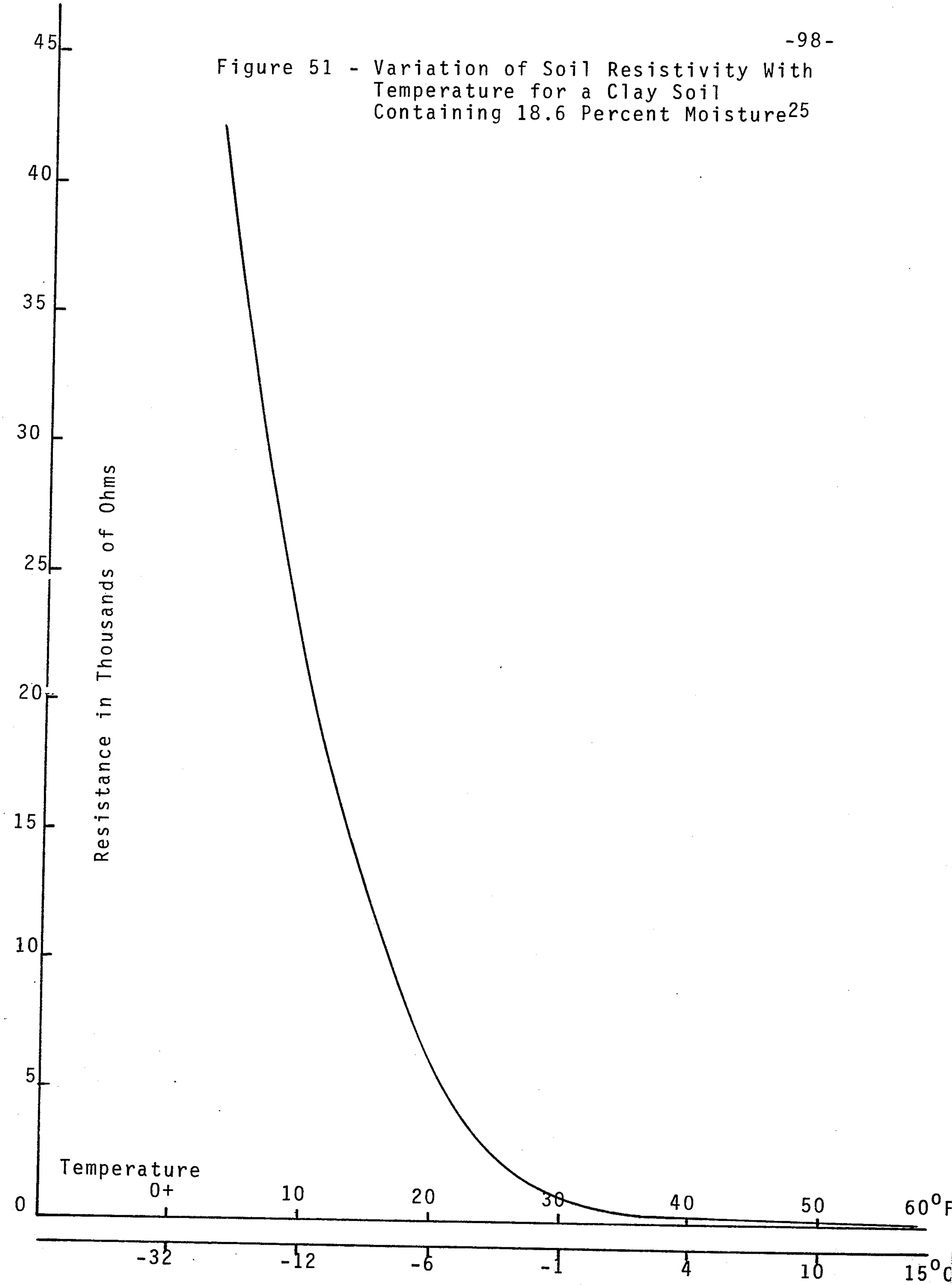

insulator, due to the lightning stroke, enters the earth through the footing of the tower, Figure 52a. In the proximity of the faulty tower, the stroke current spreads in all directions radially[28]. Due to the resistivity ρ of the soil, and according to ohm's law, this current produces a substantial electric field strength ε , the change of which with distance x is shown in Figure 52b.

Assuming homogeneous soil and uniform current flowing radially from the tower footing, every hemispherical surface (e.g. the tower base) in the ground near the centre carries the same current of density J. This earth current, for any distance x from the centre is

$$I = 2\pi x^2 J$$

Therefore, the current density $J = \dfrac{I}{2\pi x^2}$ (114)

and according to ohm's law this current produces an electric field strength $\varepsilon = \rho J = \dfrac{\rho I}{2\pi x^2}$ (115)

The voltage, as a line integral of the field strength from the hemispherical surface of radius B to a distance x, is therefore

$$E = \int_B^x \varepsilon \, dx = \frac{\rho I}{2\pi} \int_B^x \frac{dx}{x^2} = \frac{\rho I}{2\pi} \left[\frac{1}{B} - \frac{1}{x}\right] \qquad (116)$$

This relation is shown in Figure 52b. The total voltage between the hemispherical surface and a far distant point with $x = \infty$ is

$$E = \frac{\rho I}{2\pi B} \qquad (117)$$

and therefore the resistance experienced by the streamlines of

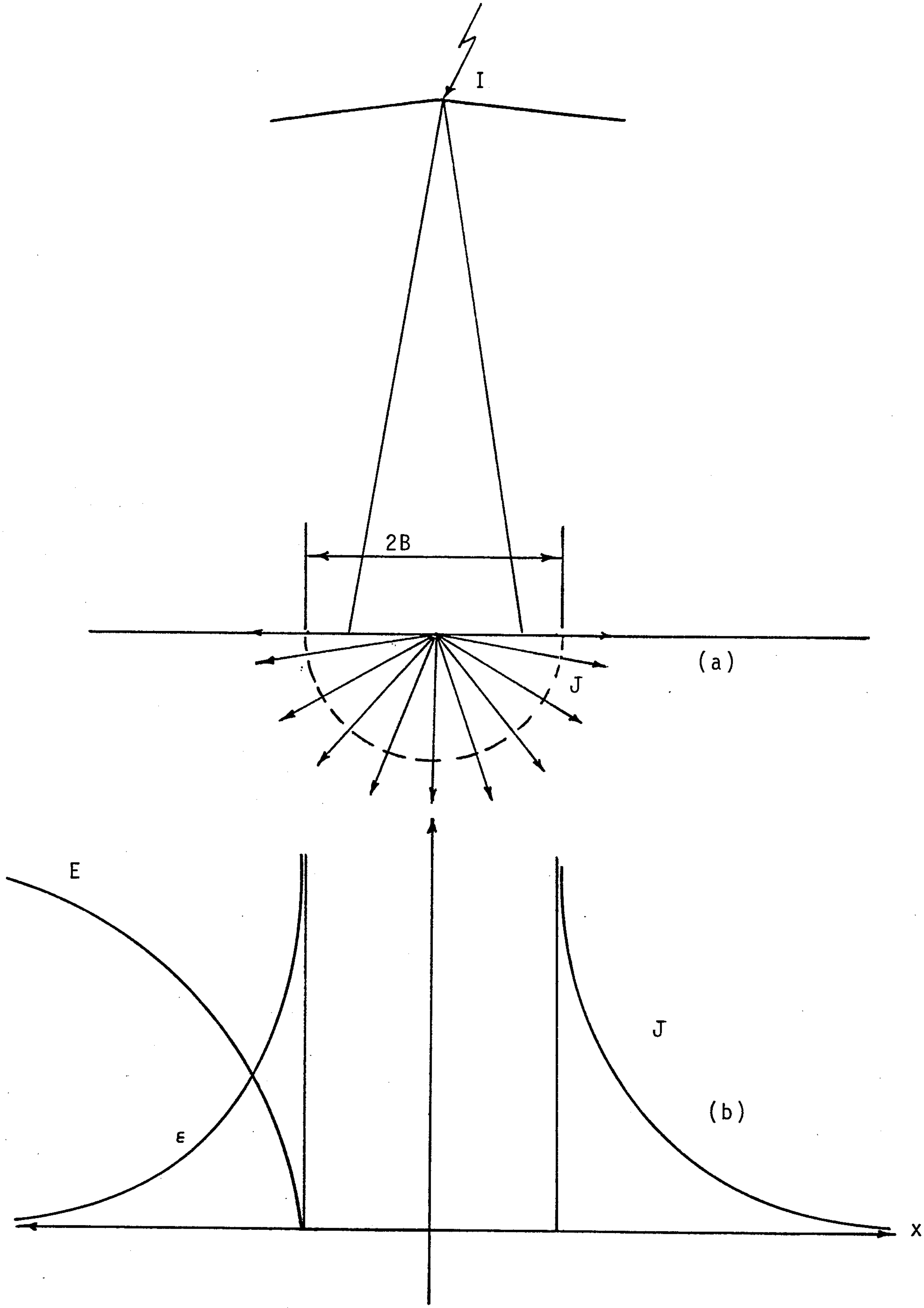

Figure 52 - Fault Current Penetration Through Earth and the Associated Voltage and Voltage Gradient.[28]

current diverging from the hemisphere is

$$R = \frac{E}{I} = \frac{\rho}{2\pi B} \tag{118}$$

Now that the penetration of the fault current to earth has been examined, the measurement of soil resistivity will be illustrated.

4.3. MEASURING SOIL RESISTIVITY[28]

The fundamental method of measuring ground resistance is shown in Figure 53. Current is circulated between the ground being tested and an auxiliary ground. Preferably, the auxiliary ground should be located at a distance which is large compared to the dimensions of the ground under test, since it is not desirable to have interaction of the ground current distributions at the two electrodes. That is, a voltage E will be independent of the distance x between the main and auxiliary electrodes only if x is much greater than both B and b. Thus, by applying Equation 116 to both systems of current distribution of Figure 53 around the hemispheres of radii B and b, superposition gives the voltage between the two electrodes. Therefore, the total voltage E between the two electrodes is

$$E = \frac{\rho I}{2\pi}\left[\frac{1}{B} + \frac{1}{b} - \frac{2}{x}\right] \tag{119}$$

and the total resistance of the ground is

$$R = \frac{E}{I} = \frac{\rho}{2\pi}\left[\frac{1}{B} + \frac{1}{b} - \frac{2}{x}\right] \tag{120}$$

the resistivity ρ can be determined by Equation 120 if the dimensions are known and if ρ is assumed constant over the

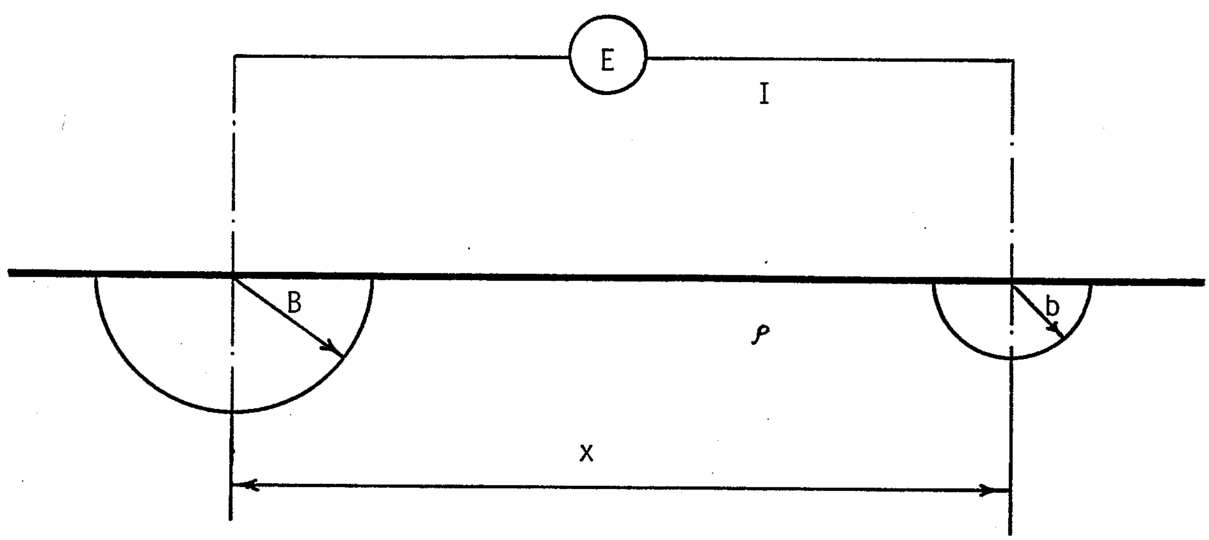

Figure 53 - Soil Resistivity Measurement.[28]

measured ground.

If ρ is not constant, the resistivity around the smaller electrodes can nevertheless be measured, if its radius is much smaller than B and x, so that not only the term 2/x, but also the term $\frac{1}{B}$ can be neglected. This gives the resistivity as

$$\rho = 2 \pi b E/I \tag{121}$$

as determined only by the voltage, the current, and the linear dimensions of b. However, if no specific measurements of soil resistivity for a definite spot of the ground are made, the values of Table I can be used as average resistivities over the underground.

CONCLUSION

In this study, the electric and geometric concepts necessary to analyze the shielding performance of transmission lines have been studied.

1. The investigation of lightning phenomena leads to better understanding of the shielding failure problem. This results in better utilization of the shielding wires above the phase conductors.

2. Applying the angular distribution function of the stroke approach angle, which is based on reference (14), this results in correct and accurate estimations of the shielding failure rates of the transmission systems, rather than assuming vertical direction for all strokes.

3. The optimum height of the shielding wires above the phase conductors, and the concept of negative shielding angles necessary for effective shielding have been studied, and the results are presented in useful curves.

4. The development of the electrogeometric model of the transmission line is based on the electric and geometric quantities of a large number of towers having lightning-proof performance.

5. A simple design procedure for effectively shielded transmission line has been presented, with the results shown in practical curves.

6. The proper location of the shielding wires above the phase conductors is studied. This leads to the following results:

(a) the taller the tower, the smaller the shielding angle needed for effective shielding;

(b) a negative shielding angle is necessary for eliminating the phase conductor exposure arcs. Thus shielding failure can be avoided.

7. It has become clear that the backflashover event is a contributing factor in insulation flashover. A study of this event leads to the following result: the backflashover predominates when high tower footing resistance is associated with low tower heights and low insulation levels.

8. Analyses of the grounding systems along the route line are of great importance in establishing integrated protection schemes.

9. Investigation of soil resistivity, and soil resistivity measurements are essential for establishing the proper grounding scheme.

10. A study of several methods for reducing tower footing resistance results in the following:

(a) For high soil resistivity, short pieces (60-90 meters) of counterpoise wire arranged in radial or crowfoot patterns result in a marked reduction of tower footing resistance. Consequently, backflashover events are materially reduced.

(b) Grounding rods of small size and with greater length are found effective in reducing tower footing resistance in soils of medium or low resistivity.

11. The shielding technique, which employed for the shielding of an ac EHV transmission systems could be applied equally to an ac high voltage (HV) systems, as well.

REFERENCES

1. Wagner,C.F., McCann, G.D. and G.L. MacLane, Jr., "Shielding of Transmission Lines", Transactions AIEE, Vol. 60, pp. 313-328, 1941.

2. AIEE Committee Report, "A Method of Estimating the Lightning Performance of Transmission Lines", Transaction AIEE, Vol. 69, Part II, pp. 1187-1196, 1950.

3. Wagner, C.F. and J.M. Clayton, "Lightning Phenomena", Electric Transmission and Distribution Reference Book, Westinghouse Electric Corp., East Pittsburg, Pennsylvania, Fourth Edition, pp. 542-577, 1950.

4. Young, F.S., Clayton, J.M. and A.R. Hileman, "Shielding of Transmission Lines", Transaction IEEE Supplement, Vol. S82, pp. 132-154, 1963.

5. Wagner, C.F. and A.R. Hileman, "The Lightning Stroke - II" Transaction AIEE, Vol. 80, Part III, pp. 622-642, 1961.

6. Bewley, L.V., Travelling Waves on Transmission Systems. Book, Dover Publications, N.Y., 1963.

7. Wagner, C.F., "The Lightning Stroke as Related to Transmission Line Performance". Electrical Engineering, Vol. 82, No. 5, pp. 339-347, 1963.

8. Hoel, P.G., "Introduction to Mathematical Statics". John Wiley and Sons, Inc., New York, 1962.

9. Schonland, B.F.J., Atmospheric Electricity, Book, Methuen and Co., London, England, 1932.

10. Schonland, B.F.J. and H. Collens, "Progressive Lightning". Proceeding of Royal Society, Vol. 143A, pp. 654-673, 1934.

11. Hagenguth, J.H., "Photographic Study of Lightning", Transaction, AIEE, Vol. 66, pp. 577-585, 1947.

12. Schonland, B.F.J., Malan, D.J. and H. Collens, "Progressive Lightning II". Proceedings of the Royal Society, Vol. 152A, pp. 595-625, 1935.

13. Weber, E., "Electromagnetic Fields", Vol. 1, John Wiley and Sons Inc., New York, 1950.

14. Whitehead, E.R. and H.R. Armstrong, "Field and Analytical Studies of Transmission Line Shielding", Transaction IEEE, Vol. 87, No. 1, pp. 270-281, 1968.

15. Gordon, W. Brown and E.R. Whitehead, "Field and Analytical Studies of Transmission Line Shielding", Transaction IEEE, Vol. 88, pp. 617-626, 1969.

16. A. Braunstein, "Lightning Strokes to Power Transmission Lines and the Shielding Effect of Ground Wires", Transaction IEEE, Vol. 89, pp. 1900-1910, 1970.

17. C.F. Wagner, A.R. Heliman, "The Lightning Stroke", Transaction AIEE, Vol. pp. 229-242, 1958.

18. E.R. Whitehead, Final Report of Edison Electric Institute, Mechanism of Lightning Flashover Research Project, EEI Publication No. 79-72-900, January, 1971.

19. D.W. Gilman and E.R. Whitehead, "The Mechanism of Lightning Flashover on H.V. and E.H.V. Transmission Line", Electra No. 27, pp. 65-96, March, 1973.

20. E.R. Whitehead, "CIGRE Survey of the Lightning Performance of E.H.V. Transmission Lines", Electra No. 33, pp. 63-89, 1974.

21. W. Diesendorf, "Insulation Co-ordination in High Voltage Electric Power System", Rensselaer Bookstore, Troy, N.Y., 1974.

22. "Lightning Performance of Typical Transmission Line", Ohio Brass Co., Mansfield, Ohio, Second Edition, 1955.

23. "Lightning Proof Transmission Lines", Edison Electric Institute, EEI, Publication No. F6, 1938.

24. "E.H.V. Transmission Line Reference Book", Edison Electric Institute, 1968.

25. W.W. Lewis, "Protection of Transmission Systems Against Lightning", N.Y., Dover Publications, Inc., Second Edition, 1965.

26. E.D. Sunde, "Surge Characteristics of Buried Bare Wire", Electrical Engineering, Vol. 89, pp. 987-991, 1940.

27. H.B. Dwight, "Calculation of Resistance to Ground", AIEE, Transaction, Vol. 55, pp. 1319-1328, 1936.

28. Rüdenberg, R., "Grounding Principles and Practice", Electrical Engineering, Vol. 64, No. 1, pp. 1-13, 1945.

29. P.L. Bellaschi, "Impulse and 60 Cycle Characteristics of Driven Grounds - I", AIEE - Transaction, Vol. 60, pp. 123-128, 1941.

30. P.L. Bellaschi, R.E. Armington, A.E. Snowden, "Impulse and 60 Cycle Characteristics of Driven Grounds - II", AIEE - Transaction, Vol. 61, pp. 349-364, 1942.

31. S.B. Griscom, "The Prestrike Theory and Other Effects in the Lightning Stroke", AIEE - Transaction, Vol. 77, pp. 918-933, 1958.

32. Rudenberg, R., "Electric Shock Waves in Power Systems", Harvard University Press, Cambridge, Mass., 1968.

33. Guide for Safety in Alternating Current Substation Grounding. AIEE No. 80, 1961.

34. Standard Mathematical Tables, "CRC, The Chemical Rubber Co., 21st Edition, 1973.

27

APPENDIX A

Method of Calculating 60-Cycle Resistance of Single and Multiple Grounding Rods

o One G.R., Length L, radius a

$$R = \frac{\rho}{2\pi L}\left[\ln\left(\frac{4L}{a} - 1\right)\right] \quad (1A)$$

o o Two G.R. $S > L$

$$R = \frac{\rho}{4\pi L}\left(\ln\frac{4L}{a} - 1\right) + \frac{\rho}{4\pi S}\left(1 - \frac{L^2}{3S^2} + \frac{2L^4}{5S^4}\right) \quad (2A)$$

o o Two G.R. $S < L$

$$R = \frac{\rho}{4\pi L}\left[\ln\frac{4L}{a} + \ln\frac{4L}{S} - 2 + \frac{S}{2L} - \frac{S^2}{16L^2} + \frac{S^4}{512L^4}\right] \quad (3A)$$

Buried Horizontal Wire 2L, depth 2S

$$R = \frac{\rho}{4\pi L}\left[\ln\frac{4L}{a} + \ln\frac{4L}{S} - 2 + \frac{S}{2L} - \frac{S^2}{16L^2} + \frac{S^4}{512L^4}\right] \quad (4A)$$

Right-Angle Turn of Wire Length of Arm L, depth S/2

$$R = \frac{\rho}{4\pi L}\left[\ln\frac{2L}{a} + \ln\frac{2L}{S} - 0.2373 + 0.2146\frac{S}{L} + 0.1035\frac{S^2}{L^2} - 0.0424\frac{S^4}{L^4}\right] \quad (5A)$$

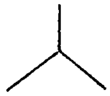

Three-Point Star, Length L, depth S/2

$$R = \frac{\rho}{6\pi L}\left[\ln\frac{2L}{a} + \ln\frac{2L}{S} + 1.071 - 0.209\frac{S}{L} + 0.238\frac{S^2}{L^2} - 0.054\frac{S^4}{L^4}\right] \qquad (6A)$$

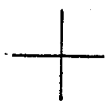

Four-Point Star, Length of Arm L, depth S/2

$$R = \frac{\rho}{8\pi L}\left[\ln\frac{2L}{a} + \ln\frac{2L}{S} + 2.912 - 1.071\frac{S}{L} + 0.645\frac{S^2}{L^2} - 0.145\frac{S^4}{L^4}\right] \qquad (7A)$$

Ring of Wire, Diameter of ring D, diameter of wire d, depth S/2

$$R = \frac{\rho}{2\pi^2 D}\left[\ln\frac{8D}{d} + \frac{4D}{S}\right] \qquad (8A)$$

APPENDIX B[30]

Method of Calculating Impulse Resistance of Single and Multiple Grounding Rods.

The basic formula used to calculate impulse resistance has the same form as that for 60-cycle resistance. Equation 1 of Appendix I is adapted to the symbols shown in the insert of Figure 33, page 69 as follows:

$$R_o = \frac{\rho_o}{2\pi L_o}\left[\ln\left(\frac{4L}{a_o}\right) - 1\right] \qquad (1B)$$

Now, considering the increase in the effective radius (a_i) of the rod, resulting from breakdown of the soil at high current,

$$R_i = \frac{\rho_o}{2\pi L_o}\left[\ln\left(\frac{4L_o}{a_i}\right) - 1\right] \qquad (2B)$$

The effective radius of the rod is determined as follows:
Since the voltage gradient along the surface of the rod is the product of the current density and soil resistivity (ρ_o), the critical value of this gradient (g_c) at which the radius (a_o) of the rod starts to increase is derived from the critical current I_b.

$$g_c = \frac{I_b\,\rho_o}{2\pi a_o L_o} \qquad (3B)$$

For current I above I_b, the gradient at the effective radius assumes critical value and is expressed by

$$g_c = \frac{I \rho_o}{2\pi a_i L_o} \tag{4B}$$

From Equations 11 and 12

$$a_i = a_o \frac{I}{I_b} \tag{5B}$$

When this value of a_i is substituted in Equation 10, the ratio of Ri to Ro becomes

$$\frac{Ri}{Ro} = \left[\ln \left(\frac{4LoIo}{a_o I} \right) - 1 \right] \div \left[\ln \left(\frac{4Lo}{a_o} \right) - 1 \right] \tag{6B}$$

Next let the rod length be increased to Li. From Equations 9 and 10, the ratio Ri to Ro is then

$$\frac{Ri}{Ro} = \frac{Lo \left[\ln \left(\frac{4Li}{a_i} \right) - 1 \right]}{Li \left[\ln \left(\frac{4Lo}{a_o} \right) - 1 \right]} \tag{7B}$$

The relation of a_i to the current can either be approximated by Equation 13, or it can be determined from

$$\frac{I}{I_b} = \frac{a_i \ Li}{a_o \ Lo} \tag{8B}$$